Study of the performance of propulsion units with nitrogen-jet thrusters for astronaut Extravehicular Activities (EVAs)

Nikolaos Monokrousos

UNIVERSITAT POLITÈCNICA DE CATALUNYA
BARCELONATECH
Escola Superior d'Enginyeries Industrial, Aeroespacial i Audiovisual de Terrassa

- This page is intentionally left blank –

UNIVERSITAT POLITÈCNICA DE CATALUNYA
BARCELONATECH
Escola Superior d'Enginyeries Industrial, Aeroespacial i Audiovisual de Terrassa

MSc. in Space and Aeronautical Engineering

Study of the performance of the propulsion units with nitrogen-jet thrusters for astronaut Extravehicular Activities (EVAs)

Master Thesis

Author: Nikolaos Monokrousos

Director: Lizandra Dalmases, Josep Oriol

Codirector: Tejedor Herran, Blanca

Submitted for the partial fulfillment

of the requirements for the Degree of

Master of Science in Space and Aeronautical Engineering

Barcelona, June 2021

Declaration of honor

I declare that,

the work in this Master Thesis is completely my own work, no part of this Master Thesis is taken from other people's work without giving them credit and all references have been clearly cited.

I understand that an infringement of this declaration leaves me subject to the foreseen disciplinary actions by The Universitat Politècnica de Catalunya – BarcelonaTECH.

Nikolaos Monokrousos		22/06/2021
Student Name:	Signature:	Date:

Title of the thesis:

"*Study of the performance of the propulsion units with nitrogen-jet thrusters for astronaut Extravehicular Activities (EVAs)*"

Abstract

The future plans of the space agencies all across the globe, mainly focus on the advance of the Extravehicular Activities (EVAs) that are orientated in the repair and maintenance of the space vehicles. This thesis presents a brief history of the space suits (EMU, Orlan-M) utilized in space applications and the propulsion units (Hand-Held Maneuvering Unit, Manned Maneuvering Unit and the Simplified Aid for Extravehicular Activity Rescue-SAFER which is currently being used for performing self-rescue maneuvers, in the case the EVA crew member becomes untethered from the orbiter) that have been used during the space activities. After introducing the space environment and the critical conditions that surround the astronaut during these activities, the fundamentals of the Cold Gas Propulsion Systems on which the function of the SAFER propulsion unit is based, are presented. The aim of this thesis is to perform a performance analysis of the SAFER propulsion unit, with the extraction of the basic space propulsion concepts, i.e. thrust, specific impulse, etc. and the verification of the produced results with the technical characteristics of the unit. The orbital dynamics applying on the astronaut during an EVA are also being studied in this thesis, starting from the scenario where the crew member becomes untethered and floats freely in the vacuum of space and at the same time, examining the case where the SAFER propulsion unit is being activated for the performance of the self-rescue maneuver, and the return of the astronaut to the orbiter.

Key words: Extravehicular Activity, Simplified Aid for Extravehicular Activity Rescue, SAFER, nitrogen-jet thrusters, spacewalking

Acknowledgments

Initially, I would like to express my gratitude to my thesis director Josep Oriol Lizandra Dalmases for his valuable guidance and support throughout the production of this thesis. Oriol offered me the chance to work under his supervision, even though his academic responsibilities were extremely demanding, managing to find some time to deal with the problems that I was facing with my thesis. He trusted me when I suggested the subject of this thesis, characteristically responding to me that throughout this process, he will be learning new things with me. It was very important to me to feel that someone trusts me, especially in such a challenging scientific area as Space Propulsion is. Together, we were able to overcome the lack of information and bibliography available regarding the nitrogen-jet thrusters of the propulsion units used during Extravehicular Activities (EVAs) and verify and produce some rather interesting results for the Extravehicular Activities. Oriol devoted an important part of his time to support my efforts and maximize the credibility of our results. Therefore, I consider myself privileged to have worked under his exemplary supervision.

Then, I would like to thank my codirector Blanca Tejedor Herrán for all the time she devoted in checking and reading everything I was writing during this thesis. Blanca has been an amazing codirector, guiding me throughout the whole process with the way a master thesis should be written, providing me with information I was completely unaware of. She thoroughly went all my texts and usage of the English language and her instructions were always to the point. I would also like to express my appreciation for all the times she intervened and literally saved my thesis and diploma, with some bureaucratic problems presented to me with the thesis registration. Her contribution to the implementation of this thesis was critical, and I am really grateful for having worked with her.

To David, Javi and Pilar, my roommates and friends, a big thank you for being there for me every day and helping me not to lose my mind, with the isolation the pandemic times yield, especially for a foreigner in a new country. The anecdotes starting with: “A Catalan, two Murcians and a Greek guy” will always be the best ones and I truly can’t wait to meet them again. The last addition in the house, Favio, will always have a special place in my heart, along with his green pony. To Jack, my British friend and fellow student in the Master, thank you for all the beers we drank in the Barceloneta and hopefully we will relive these moments. Last but not least, a big thank you to Paloma for being there for me during my last months in Terrassa. She always calmed me when I was exhausted with all the master’s workload, she taught me so many things regarding Catalonia, the fight for independency and she took me in Barcelona on Saint Jordi’s day, getting me also a book for planet Mars. Of course, traditionally, I got her a rose.

Finally, I would like to thank my parents and my brother, for all the support I had during my studies in the UPC. They convinced me to move in Catalonia, even though the master was eventually online, showing me that I should appreciate every moment of living in a completely different cultural environment than the one in Greece. Thank you for providing me with all the means to take advantage of this great opportunity of studying abroad and I hope one day I can give back to you everything you gave to me.

Nikos Monokrousos, Terrassa, 2021

Contents

Declaration of honor ..... **iii.**
Abstract ..... **iv.**
Acknowledgments ..... **v.**
List of acronyms and abbreviations ..... **ix.**
List of figures ..... **xi.**
List of tables ..... **xiii.**
List of equations ..... **xiv.**
1. Introduction ..... **1.**
1.1. Aim 1
1.2. Justification 1
1.3. Scope 3
1.4. Requirements 4
2. Literature Review ..... **6.**
2.1. Extravehicular Activities (EVAs) Space Suits 6
2.1.1. History of the Extravehicular Activities Space Suits 6
2.1.1.1. Extravehicular Mobility Unit (EMU) 9
2.1.1.2. The Orlan-M Space Suit 12
2.1.2. Theoretical Presentation of Different Propulsion Units 15
2.1.2.1. Hand-Held Maneuvering Unit (HHMU) 15
2.1.2.2. Manned Maneuvering Unit (MMU) 18
2.1.2.3. Simplified Aid for Extravehicular Activity Rescue (SAFER) 21
2.1.3. Propulsion Units Applications for Extravehicular Activities Space Suits 23
2.1.3.1. Space Application: Manned Maneuvering Unit (MMU) 23
2.1.3.2. Space Application: Simplified Aid for Extravehicular Activity Rescue (SAFER) 26
2.2. Space Environment 29
2.2.1. Introduction to Space Environment 29
2.2.1.1. Atmospheric Layers 29
2.2.1.2. Layers Characteristics 32
2.2.2. Critical Space Conditions of the Thermosphere 33

Contents

2.2.2.1. Temperature and Solar Radiation 35

2.2.2.2. Galactic Cosmic Rays 38

2.2.2.3. Gas Dynamics 40

2.2.2.4. Microgravity Environment 41

2.2.2.5. Meteoroids and Orbital Debris 43

2.2.3. Planetary Environments 44

2.2.3.1. Lunar Environment 45

2.2.3.2. Martian Environment 46

2.2.4. Extravehicular Activity (EVA) Safety Parameters 47

3. Methodology ..... 49.

3.1. Introduction to the Cold Gas Propulsion Systems 49

3.1.1. Basic Space Propulsion Concepts 49

3.1.1.1. Thrust Equation 51

3.1.1.2. Specific Impulse 52

3.1.1.3. Effective Exhaust Velocity 52

3.1.1.4. Velocity Change 53

3.1.2. Fundamentals of the Cold Gas Propulsion Systems 53

3.1.2.1. System Operation 56

3.1.2.2. System Characteristics 57

3.1.2.3. Propellant Characteristics 58

3.1.3. Design Process 59

3.1.3.1. Theoretical Performance Prediction 61

3.1.3.2. True Performance Prediction 63

3.2. Simplified Aid for Extravehicular Activity Rescue (SAFER) Propulsion Unit 66

3.2.1. Introduction to the SAFER Nitrogen-Jet Propulsion Unit 66

3.2.1.1. SAFER Flight Unit Description 67

3.2.1.2. SAFER Propulsion Module Characteristics 69

3.2.2. Maneuvering Control and Fault Detection Functions 74

3.2.2.1. Maneuvering Control Software 75

Contents

3.2.2.2. Fault Detection Function 76

3.2.3. Extravehicular Activity (EVA) Self-Rescue 77

3.2.3.1. SAFER Self-Rescue Details 78

4. Results & Discussion ..... 81.

4.1. Performance Analysis 81

4.1.1. Input Data 81

4.1.2. Performance calculations 82

4.1.2.1. Thruster performance characteristics 83

4.1.2.2. Nozzle throat characteristics 84

4.1.2.3. Propellant tanks 85

4.1.2.4. Nozzle dimensioning and geometry 85

4.1.3. Performance analysis results 85

4.1.4. Performance analysis discussion 87

4.2. Orbital Dynamics and Astronaut Repositioning 88

4.2.1. Input Data 88

4.2.2. Orbital dynamics calculations 89

4.2.2.1. Numerical solution 91

4.2.2.2. Analytical solution 92

4.2.2.3. Verification of the two solutions 94

4.2.3. Self-rescue maneuver 95

5. Conclusions ..... 97.

5.1. Summary 97

5.2. Recommendations for Future Work 97

Bibliography ..... 99.

Bibliography (Images) ..... 106.

List of acronyms and abbreviations

AAH	Automatic Attitude Hold
AMU	Astronaut Maneuvering Unit
ARES	Astromaterials Research & Exploration Sciences
CD	Converging-Diverging
CEA	Control Electronic Assembly
CGPS	Cold Gas Propulsion Systems
CSA	Canadian Space Agency
CW	Clohessy-Wiltshire
C&W	Caution & Warning
DCM	Display Control Module
EMU	Extravehicular Mobility Unit
ESA	European Space Agency
EUV	Extra Ultra Violet
EVA	Extravehicular Activity
EVR	Extravehicular Robotics
GCR	Galactic Cosmic Rays
GEO	Geostationary Orbit
GFE	Government Furnished Equipment
HCM	Hand Controller Module
HHMU	Hand-Held Maneuvering Unit
IRU	Inertial Reference Unit
ISS	International Space Station
IVA	Intravehicular Activity
JAXA	Japan Aerospace Exploration Agency
LEO	Low-Earth Orbit
MMU	Manned Maneuvering Unit

List of acronyms and abbreviations

NASA	National Aeronautics and Space Administration
NSI	NASA Standard Initiator
OS	Orbiting Station
PABF	Precision Air-Bearing Floor
PLSS	Primary Life Support System
R&D	Research & Development
SAFER	Simplified Aid for Extravehicular Activity Rescue
SOP	Secondary Oxygen Pack
SPE	Solar Particle Event
STD	Standard Temperature and Pressure
UHF	Ultra High Frequency
USAF	United States Air Force
UV	Ultra Violet
VDA	Valve Driver Assembly
WETF	Weightless Environment Training Facility

List of Figures

2.1. The “Mercury Seven” or “Original Seven” ..... 7.
2.2. Edward H. White II, the first American to step outside his spacecraft and let go ..... 8.
2.3. John W. Young, Commander of the Apollo 16 lunar landing mission ..... 9.
2.4. Extravehicular Mobility Unit (EMU) components ..... 11.
2.5. A general view of the Orlan-M suit ..... 12.
2.6. Orlan-M elements and components ..... 13.
2.7. Hand-Held Self-Maneuvering Unit to be used during extravehicular activity (EVA) on Gemini 4 .. 16.
2.8. Gemini IX-A Astronaut Maneuvering Unit ..... 17.
2.9. The Manned Maneuvering Unit (MMU) Reference Coordinate Axes ..... 19.
2.10. The Manned Maneuvering Unit (MMU) functional diagram ..... 20.
2.11. The Manned Maneuvering Unit (MMU) flown by McCandless - MMU Number 3 ..... 20.
2.12. SAFER Propulsion Module ..... 21.
2.13. Mark C. Lee test flies the SAFER device during the STS-64 mission ..... 22.
2.14. STS-41-B (STS-11) crew ..... 24.
2.15. Bruce McCandless II, the first astronaut to maneuver about in space untethered ..... 26.
2.16. STS-64 crew ..... 27.
2.17. Astronaut Mark C. Lee, crew member of the STS-64 mission, tested the new SAFER ..... 28.
2.18. Layers of Earth’s Atmosphere on a sunset view ..... 30.
2.19. Layers of Earth’s Atmosphere and space applications ..... 32.
2.20. Temperature and Pressure variations, with respect to the altitude ..... 32.
2.21. The calculated global mean vertical profile for the temperature of the neutral gases ..... 36.
2.22. The vertical distribution of the density of the major species of the thermosphere ..... 37.
2.23. Earth’s “protection” against space radiation ..... 39.
2.24. Astronauts in the middle of a spacewalk during Expedition 55 ..... 42.
2.25. Low Earth Orbit (LEO) tracked debris population ..... 43.
2.26. Lunar Surface as captured in the Apollo Missions ..... 45.
2.27. Martian Surface as captured from NASA’s Perseverance Rover ..... 45.
3.1. Generic Block Diagram for a given propulsion system ..... 50.
3.2. Typical small spacecraft in-space propulsion trade space ..... 56.
3.3. Cold Gas Propulsion System schematic ..... 57.
3.4. Typical Cold Gas Propulsion System architecture ..... 60.

Figures

3.5. Picture of the SAFER propulsion unit ..... 66.
3.6. SAFER propulsion unit deployment and stowage ..... 68.
3.7. Hand Controller Module attached to the SAFER unit ..... 68.
3.8. Representation of the SAFER unit components - IVA battery pack excluded ..... 69.
3.9. SAFER propulsion subsystem schematic ..... 70.
3.10. SAFER top assembly layout ..... 73.
3.11. SAFER Detailed Product Breakdown Structure ..... 74.
4.1. Numerical solution of the Clohessy-Wiltshire (CW) equations ..... 92.
4.2. Analytical solution of the Clohessy-Wiltshire (CW) equations ..... 93.
4.3. Verification of the Clohessy-Wiltshire (CW) solutions ..... 94.
4.4. Astronaut return back to the orbiter ..... 96.

List of Tables

2.1. Comparison between EMU and Orlan-M space suits ..... 13.
2.2. Comparative table between the 3 different propulsion units ..... 23.
3.1. Thrust and Specific Impulse (s) range of different propulsion technologies ..... 55.
3.2. Cold Gas Propulsion Systems propellants characteristics ..... 59.
3.3. SAFER propulsion unit characteristics ..... 70.
4.1. Input data of the SAFER propulsion unit ..... 82.
4.2. Performance analysis results ..... 85.
4.3. Input data for the orbital dynamics analysis ..... 59.
4.4. Initial conditions of numerical solution ..... 91.
4.5. Initial conditions of analytical solution ..... 92.

List of Equations

2.1. Kirchhoff's Law for thermal equilibrium ..... 38.
2.2. Spherical body power absorption from the Sun ..... 38.
2.3. Power emitting of a body ..... 38.
2.4. Equilibrium temperature solution ..... 38.
2.5. Local pressure scale height of a specific gas ..... 40.
3.1. Momentum equation ..... 51.
3.2. Magnitude of momentum ..... 51.
3.3. Magnitude of thrust ..... 51.
3.4. Specific impulse equation ..... 52.
3.5. Effective exhaust velocity equation ..... 52.
3.6. Velocity change equation ..... 53.
3.7. Final mass of the space suit ..... 53.
3.8. Propellant mass ..... 53.
3.9. Specific impulse for a Cold Gas Propulsion System ..... 58.
3.10. Exhaust velocity for a Cold Gas Propulsion System ..... 58.
3.11. Isentropic relations ..... 59.
3.12. Total mass of a Cold Gas Propulsion System ..... 61.
3.13. Acoustic velocity ..... 61.
3.14. Characteristic velocity ..... 61.
3.15. Thrust equation ..... 61.
3.16. Propellant mass flow rate ..... 62.
3.17. Thrust equation (alternative) ..... 62.
3.18. Specific impulse (alternative) ..... 62.
3.19. Total propellant mass ..... 62.
3.20. Total propellant tank volume ..... 62.
3.21. Expansion ratio ..... 62.
3.22. Pressure ratio ..... 62.
3.23. Throat cross-sectional area ..... 62.
3.24. Throat diameter ..... 62.
3.25. Thrust equation, bell nozzle coefficient included ..... 63.
3.26. Total propellant mass required for a Cold Gas Propulsion System ..... 64.
3.27. Ideal gas law, part 1 ..... 64.

Equations

3.28. Ideal gas law, part 2 ..... 64.
3.29. Internal energy rate of change ..... 64.
3.30. Internal energy ..... 64.
3.31. Propellant mass flow rate (alternative) ..... 64.
4.1. Vacuum thrust coefficient ..... 83.
4.2. Characteristic velocity ..... 83.
4.3. Pressure at the exit of the nozzle ..... 83.
4.4. Exhaust velocity ..... 83.
4.5. Specific impulse ..... 83.
4.6. Effective exhaust velocity ..... 83.
4.7. Tsiolkovsky equation, total velocity change ..... 83.
4.8. Theoretical thrust with nozzle coefficient ..... 83.
4.9. Throat pressure ..... 84.
4.10. Throat temperature ..... 84.
4.11. Gaseous nitrogen throat density ..... 84.
4.12. Throat velocity ..... 84.
4.13. Propellant mass flow ..... 84.
4.14. Throat cross-sectional area ..... 84.
4.15. Throat diameter ..... 84.
4.16. Reynolds number at throat ..... 84.
4.17. Discharge coefficient ..... 84.
4.18. Total time to empty the propellant tanks ..... 85.
4.19. Total propellant tank volume ..... 85.
4.20. Exit cross-sectional area ..... 85.
4.21. Exit diameter ..... 85.
4.22. Thrust calculated ..... 86.
4.23. Circular velocity ..... 90.
4.24.Angular rate ..... 90.
4.25. Propellant mass flow ..... 90.
4.26. Acceleration in x-axis ..... 90.
4.27. Acceleration in y-axis ..... 90.
4.28. Acceleration in z-axis ..... 90.
4.29. Relative position in x-axis ..... 90.

Equations

4.30. Relative position in y-axis ..... 90.
4.31. Relative position in z-axis ..... 90.
4.32. Final mass of the system ..... 95.

1. Introduction

1.1 Aim

The main objective of the thesis "Study of the performance of the propulsion units with nitrogen-jet thrusters for astronaut Extravehicular Activities (EVAs)" is to evaluate the performance parameters of the Simplified Aid for Extravehicular Activities Rescue (SAFER) propulsion unit, utilized in the current space missions and activities. The amount of thrust produced during a self-rescue maneuver, in the case the crew member becomes untethered from the orbiter (ISS, etc.), shall set the frameworks for the orbital dynamics parameters that will be studied, to describe the motions performed for the self-rescue.

1.2 Justification

Since the beginning of true spacewalking in the vacuum of space in the mid-1960s, and throughout the history and knowledge gained from each particular activity, space agencies around the globe managed to rapidly understand the importance of providing a rescue mechanism to the astronauts, in case of an emergency. Although the probability of an astronaut becoming untethered during an Extravehicular Activity (EVA) is significantly small, the human factor and the value of the human life in space activities is crucial for the agencies and industries of the space sector. No matter how accurate and effective the mission design could be, as well as the design of the extravehicular activities that shall be performed, the uncertainties that may arise while operating in outer space are decisive and of highly importance.

Over the years, 232 spacewalks have been performed at the International Space Station (ISS) alone, since its launch in November 1998, in addition to those of previous space missions (Gemini 10, Skylab 3, etc.). An astronaut propulsion unit (or astronaut maneuvering unit) allows the movement of an astronaut relative to the spacecraft, when performing an Extravehicular Activity (spacewalk). Different maneuvering units have been developed and tested, with the usage of mainly gaseous nitrogen as fuel (Hand-Held Maneuvering Unit, Manned Maneuvering Unit, SAFER, etc.), as well as hydrogen peroxide (USAF Astronaut Maneuvering Unit). However, an assessment of the behavior of the thrusters during the spacewalks should be carried out.

As space suits were evolving, adapting to the gradually increasing needs of space exploration, the maneuvering units were also integrating new features and characteristics to their functions, to meet up with

the new, higher expectations. From the Hand-Held Maneuvering Unit (HHMU) to the Manned Maneuvering Unit (MMU) and the Simplified Aid for Extravehicular Activities Rescue (SAFER), mission design, spacesuit and propulsion engineers have always been trying to improve the propulsion units utilized during spacewalks, always taking into consideration as a top priority the safety of the EVA crew member.

The goals of the implementation of an Extravehicular Activity (EVA) are primarily concentrated on the maintenance and repair of the exterior components of the orbiters (ISS, satellites, etc.). An increase in the space activities through the constantly developing space industry, shall as well yield a radical increase in EVAs around the orbiters for maintenance and repair reasons. As it will be further discussed, the researchers in the Weightless Environment Training Facility (WETF) of the NASA Johnson Space Center have actually estimated the possibility of an EVA crew member becoming untethered from the orbiter as once every 1000 EVA hours. Thus, it is of great importance to examine and understand the self-rescuing techniques and capabilities the usage of a propulsion unit provides to the astronauts performing EVAs.

This thesis studies the performance characteristics of the up-to-date SAFER propulsion unit utilized in spacewalks for the implementation of rescue maneuvers, in order to present the necessary information regarding a number of crucial parameters that characterize a propulsion unit as "adequate" for its initial scope and objectives. Based on the information provided by the technical reports of the SAFER propulsion unit, the state-of-the-art of which will be further presented in this thesis and is based on the fundamentals' analysis of the Cold Gas Propulsion Systems, the basic space propulsion concepts will be studied and verified. Finally, an introduction to the orbital dynamics applied on the body of the EVA crew member will be presented, with information regarding the performed motions yielding the activation of the propulsion unit.

Finally, throughout the conduction of the study for the performance of the propulsion units with nitrogen-jet thrusters for astronaut EVAs, a lack of information regarding the performance characteristics of the SAFER propulsion unit was observed. The amount of information available for the technical characteristics of the SAFER unit and its thrusters was rather limited, in addition to the lack of information regarding the basic propulsion concepts that arise through its utilization for self-rescue maneuvers. The necessity of this thesis is highlighted by these facts and thus, the thesis can only contribute to the further understanding of the fundamentals of the studied propulsion unit.

1.3 Scope

This thesis constitutes an analysis of the performance of the propulsion units with nitrogen-jet thrusters for astronaut Extravehicular Activities.

This project:

- Presents the history of the Extravehicular Mobility Unit (EMU) spacesuit and compares it with the Orlan-M spacesuit developed by the Russian ROSCOSMOS Space Agency
- Presents information regarding the Hand-Held Maneuvering Unit (HHMU), Manned Maneuvering Unit (MMU) and the Simplified Aid for Extravehicular Activities Rescue (SAFER) propulsion units that have been used in space missions since the Gemini space programs, as well as applications of the aforementioned units
- Introduces the space environment that surrounds the Extravehicular Activities performed by the crew members, with information regarding the atmospheric layers and conditions and the critical space conditions of the Thermosphere in which EVAs take place
- Describes the planetary environments of the Moon and Mars, in which past and future EVAs shall be performed, in addition to reporting the safety parameters that should be taken into account during an EVA
- Introduces the Cold Gas Propulsion Systems, on the fundamentals of which the SAFER propulsion unit is based, by presenting information regarding the basic space propulsion concepts, the operation and the characteristics of the Cold Gas Propulsion Systems, as well as extensive information for the selected propellant.
- Describes the design process for a Cold Gas Propulsion System such as the SAFER propulsion unit using gaseous nitrogen-jet thrusters, for the theoretical and true prediction of the performance of the thrusters
- Presents the state-of-the-art of the SAFER propulsion unit description and module characteristics, in addition to the Maneuvering Control and Fault Detection functions which distinguish it from the propulsion units utilized in previous space missions
- Presents information regarding the implementation of a self-rescue maneuver and the cases where the activation of the SAFER propulsion unit shall be necessary for the rescue of the EVA crew member

- Identifies the orbital dynamics fundamentals that apply to the orbiting EVA crew member in the case it becomes untethered
- Conducts the performance analysis of the SAFER propulsion unit with nitrogen jet thrusters for the astronaut EVAs, with an estimation of the principle space propulsion concepts

This project does not:

- Design the nozzle of the thrusters used on the Simplified Aid for Extravehicular Activities Rescue (SAFER) propulsion unit
- Conduct a performance analysis of the Hand-Held Maneuvering Unit (HHMU) and the Manned Maneuvering Unit (MMU) for astronaut EVAs, predecessors of the SAFER propulsion unit
- Perform a Computational Fluid Dynamics (CFD) analysis on the SAFER propulsion unit's thrusters
- Perform a thermodynamics analysis on the SAFER propulsion unit's thrusters
- Study the economic aspects of the SAFER propulsion unit or its activation during an Extravehicular Activity (EVA)

1.4 Requirements

During the realization of this thesis, a number of requirements have been fixed in advance, regarding the analysis of the SAFER propulsion unit and the simulations of the performance analysis and the orbital dynamics applied on the EVA crew member.

The performance analysis of the SAFER propulsion unit is:

- Based on information regarding the characteristics of the propulsion unit, extracted from the technical report of the unit, as published by the corresponding space agency.
- Considering a zero ambient pressure surrounding the EVA crew member, when the activation of the propulsion unit is necessary.

The orbital dynamics analysis applied on the EVA crew member:

- Studies the mass system of the astronaut, the EMU space suit and the SAFER propulsion unit as a rigid body, taking into account that the system responds uniformly to the forces applied. Normally,

the EMU space suit has rather specific dynamic behavior, with the arms for example corresponding differently to the forces applied on it than the head of the suit.

- Suggests a 3-minute maneuver for the self-rescue of the untethered crew member, taking into account that the total time calculated to empty the propellant tanks of the propulsion unit has been calculated to be 16 minutes.
- The position of the EVA crew member corresponds to a circular orbit and a motion on the equatorial plane. In addition, the spacecraft (ISS, etc.) is assumed to perform an exact circular motion like the crew member performing the EVA.

2. Literature Review

2.1. Extravehicular Activities (EVAs) Space Suits

2.1.1. History of the Extravehicular Activities Space Suits

True spacewalking began in the mid-1960s with the exploits of the two astronauts representing the greatest space agencies of that time, Alexei A. Leonov of the Soviet Union and Edward H. White II of the United States [1]. Since those first highly risky probings outside the orbiters, astronauts and cosmonauts have performed thousands of hours on Extravehicular Activities (EVAs), while some of them have even stepped their feet on the Moon. EVA spacesuits have been used in plenty of space missions such as servicing the Hubble Space Telescope or for satellites' retrieval.

The future space missions of all the space agencies around the world such as the return of NASA to the Moon to establish a permanent base or the surface exploration of Mars by humans, shall require extremely innovative and reliable spacesuits systems and astronauts' tools. In contrast to the -rather geologically orientated and strictly scheduled- Apollo missions, where the main tasks of the astronauts were to create a knowledge guideline for the lunar surface [2], future crewed missions to Mars will emphasize scientific exploration and observation, by gathering data and samples of great scientific importance for understanding the Red Planet better. The Extravehicular Activities' space suits that will be developed by space agencies and private corporations in the future, shall supplementary address to the knowledge gap regarding EVAs, that focuses on three main axes: 1) how varied multidisciplinary scientific objectives can be effectively integrated, 2) adaptation to new data acquired between and during Extravehicular Activities and 3) understanding integration methods for scientific experts [3].

The Mercury manned space flight program conducted by NASA introduced a full-pressure suit design of an inner gas-bladder layer of neoprene-coated fabric and an outer restraining layer of aluminized nylon. The Mercury suits were designed to serve only as a backup in case of a spacecraft cabin decompression, thus no EVAs were performed using them. Hopefully, no Mercury capsule ever decompressed during a mission, thus the suits never inflated. NASA introduced the Project Mercury astronauts to the world on April 9, 1959· the Mercury spacesuits can be seen in the following picture [2.1]:

(Fig. 2.1.: The “Mercury Seven” or “Original Seven”, (front row, left to right) Walter M. "Wally" Schirra Jr., Donald K. "Deke" Slayton, John H. Glenn Jr., M. Scott Carpenter, (back row) Alan B. Shepard Jr., Virgil I. "Gus" Grissom and L. Gordon Cooper, Jr.)

The Gemini space program followed the Mercury’s flights series, where spacesuit engineers had to overcome and adjust the new spacesuits in more advanced challenges and problems. This time, the spacesuits not only needed to serve as a pressure backup to the spacecraft cabin and for extravehicular activities, but also as escape suits, in case of an aborted launch, where the ejection seats had to be fired. In addition to modifications and adjustments performed on the materials used for the spacesuits design, the new spacesuits also featured augmented mobility in the shoulders and the arms and were more comfortable when worn during space flights up to 14 days, in unpressurized conditions.

The term “spacewalking” was introduced during the Gemini program, where the astronaut Edward White II, used a small hand-held propulsion gun to perform a maneuver in space. By pulling the trigger, the propulsion gun released jets of nitrogen that propelled him in the opposite direction. The equipment was considered the first personal maneuvering unit used in space and was the forerunner of the development of the future propulsion units developed for extravehicular activities. It also made everyone realize that EVAs were not as simple as they might have been considered, since adequate practice in maneuvers was required, in addition to technical difficulties that required improvements, such as coming up with a better method of cooling the astronaut.

During the astronaut's EVA, heat and moisture were quickly produced from the breathing process, resulting in the fogging of the inside of the helmet visor, which made it hard for the astronaut to see. The gas cooling system of the spacesuit that was used up to that time, was an area where the spacesuit engineers should make improvements, in order for the upcoming EVAs not to be strained from mechanical limitations. The photo of astronaut Edward White II, performing a maneuver can be seen below [2.2]:

(Fig. 2.2.: Edward H. White II became the first American to step outside the spacecraft and let go on June 3, 1965)

The Apollo program was rather radical, in comparison to the previous human spaceflights, due to the fact that the Apollo mission actually required astronauts to walk on the surface of the Moon. This time, apart from the improvements that had been made in the Gemini spacesuits, the new spacesuits were designed in a way to provide greater mobility in the legs and the waist, so that the astronauts could bend and pick up samples on the free space environment of the lunar surface. The spacesuits needed to be able to perform in microgravity and in the one-sixth gravity of the Moon's surface, in addition to the self-contained portable life-support system that was necessary for the astronaut's extravehicular activity while on the Moon [4].

During the Apollo program, a total of 161 hours of EVA on the Moon's surface and in microgravity in transit from the Moon to Earth, were performed by 12 astronauts. The EVA of Commander John W. Young, saluting the American flag on the Descartes region of the Moon, can be seen in the following picture [2.3]:

(Fig. 2.3.: John W. Young, Commander of the Apollo 16 lunar landing mission to the Descartes region, salutes the American flag as he jumps upward on the Moon. Behind him are the lunar module "Orion" and the lunar roving vehicle)

During the Skylab program, the necessity of human spaceflights and the human factor became apparent, since the space suited Skylab astronauts were the ones who literally saved the program. Different problems and dysfunctions appeared in the Skylab space station, a micrometeoroid shield ripped away from the station's outer surface, two of the six solar panels deployed prematurely and insufficient electrical power was provided by the remaining panels to the station. These problems were all resolved thanks to the three-astronaut crew that was assigned by NASA to repair the station, either on board the Skylab station, or by performing Extravehicular Activities. The Skylab EMU was a simplified version of the Apollo Moon suits, since the crew member performing an EVA was attached to the station by an umbilical tether which provided life-support, and thus no need for a portable system was required.

2.1.1.1. Extravehicular Mobility Unit (EMU)

The original Space Shuttle Extravehicular Mobility Unit (EMU) was developed and used from 1979 to 2002. The EMU design was upgraded in 2002, two years after the launch of the International Space Station (ISS) [5] and has been in use since that time. During the Apollo program, there were three one-time garment spacesuits available for each astronaut crew member, custom built to fit each astronaut's size, one for flight, one for training and one used as flight backup, in case a malfunction might appear. The Apollo Moonwalk EVAs were the first time astronauts experienced real freedom, because of the portable life-support system worn on their back, since up to that time, all the EVAs performed required the astronaut to

be tied to the spacecraft by a tether line, which supplied oxygen and kept crew members from drifting away. At the time NASA decided to alter its approach from launching astronauts on expendable rockets to the Space Shuttle system, with its reusable orbiter and solid rockets boosters, spacesuit engineers started developing a new type of spacesuits, a reusable Extravehicular Mobility Unit (EMU). These EMUs consist of a variety of standard-size parts to fit astronauts of different measurements and can be assembled for each mission in combinations needed to fit male or female astronauts. The design is cost effective since the suits are reusable and not custom fitted [1].

On Earth, a fully assembled EMU (the suit and all its components) weighs about 113 kilograms [1], while orbiting above Earth it has no weight at all. Combined with the SAFER module, EMU weighs about 124.6 kilograms [6]. The Extravehicular Mobility Unit (EMU) used in the Space Shuttle programs consists of 18 different items, when fully assembled, it can be considered as an anthropomorphic, flexible, customized spacecraft. The Shuttle EMU is focused on providing all the necessary means for the astronaut's short - term survival· oxygen, cooling and drinking water, food, waste collection (including carbon dioxide removal), as well as pressure, thermal and micrometeoroid protection. Finally, the communication between the astronaut performing an EVA and the crew and ground control shall remain constant and unhindered. For this reason, EMU provides electrical power and communications. Thus, EMU accommodates a variety of interchangeable systems that interconnect easily and securely in a single-handed operation, for either normal or emergency use.

The main component of the Extravehicular Mobility Unit (EMU) is the backpack on the pack of the suit which is called Primary Life Support System (PLSS). PLSS contains all the necessary equipment and consumables to support the life of the astronaut utilizing the EMU and it is being exposed in the vacuum of space during the Extravehicular Activity (EVA), while the rest of the space suit is pressurized in a nominal pressure of 4.3 psid (pound per square inch differential) [7]. The EMU contains two very important pieces of safety equipment, in case the EVA crew member is in a state of emergency: the Secondary Oxygen Pack (SOP) attached in the bottom of the PLSS, which is capable of providing the astronaut with a 30-minute supply of oxygen, and the Simplified Aid for EVA Rescue (SAFER) propulsion unit, which allows the astronaut to perform self-rescue maneuvers, in case of detachment from the spacecraft. A detailed schematic of the Extravehicular Mobility Unit and its components can be seen in the following figure [2.4]:

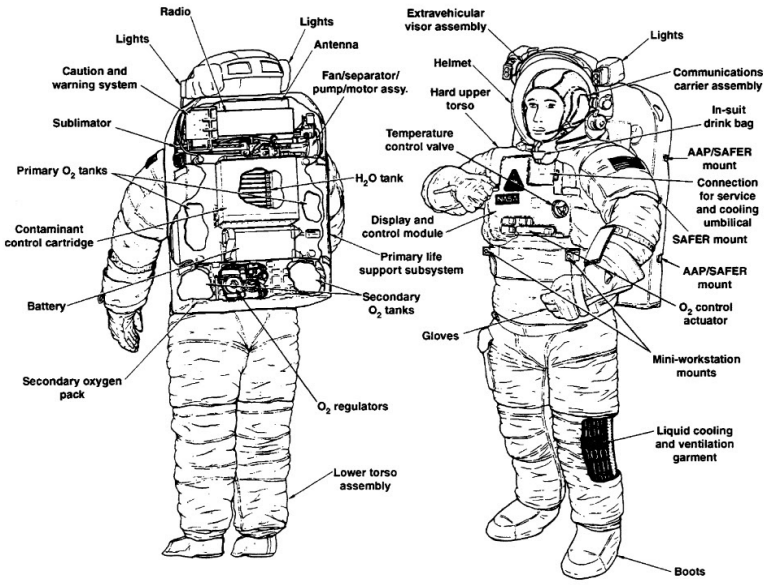

(Fig. 2.4.: Extravehicular Mobility Unit (EMU) components)

Along this line, developers decided that the design of the Shuttle spacesuits will be mainly concentrated on implementing a single function· providing the ability to perform Extravehicular Activities (EVAs). Spacesuits of previous missions and designs were able to satisfy multiple purposes· Gemini missions required protection in case an ejection was necessary during launch, or backup pressure should be provided in case of cabin pressure failure, while the Apollo missions required a microgravity environment and low gravity while walking on the moon on EVAs.

During launch and re-entry, astronauts wear a special orange-colored flight suit with helmets for protection, during the stay in the orbiter comfortable shirts and slacks or shorts are worn, while the Shuttle suits are only worn when an EVA is scheduled [1]. In addition, Shuttle astronauts have greater freedom than the Apollo lunar astronauts, due to the fact that they are performing EVAs in the microgravity environment of space. Astronauts are required to be tied to the spacecraft by a tether line also, although this time, those tethers act only as safety lines and do not provide any life-support at all. The fact that the tethers can be moved in different locations around the orbiter, along a slide wire attached to its exterior surface, allows even greater freedom for the astronauts to move.

2.1.1.2. The Orlan-M Space Suit

Considering the knowledge and experience resulting from the Extravehicular Activities of NASA missions over the years, the Russian Space Agency Roscosmos also contributed to the development of the human flight space suits, through its cosmonauts in the Mir orbiting station (OS).

More than 158 excursions have been performed from the Mir orbiting station, by Soviet and Russian cosmonauts (in addition to the occasional participation of ESA and NASA astronauts) wearing an Orlan type semi-rigid space suit during their EVAs. From 1986 to 2000, when the operation of Mir was terminated, 25 crews accumulated 362 hours and 8 minutes of operation in free space. 15 suits (2 Orlan-DM models, 10 Orlan-DMA models and 3 Orlan-M models) were used in orbit, each performing 5 to 15 EVAs, while some of them operated for more than 3 years [8]. The models Orlan-M, Orlan-MK and Orlan-MKS have been used and tested in missions on ISS, complementary to the use of EMU while performing the EVAs required during the corresponding missions. The Orlan-M space suit can be seen in the picture below [2.5]:

(Fig. 2.5.: A general view of the Orlan-M space suit)

Semi-rigid type of suits turned out to be the most appropriate for EVAs performed from orbiting stations, thus the Orlan-M model, the last version of the Orlan family, was even accepted for operation within the program of the ISS. However, the real condition of the Orlan space suits after an EVA operation could not be ultimately evaluated, since the service and maintenance of the space suit was conducted in orbit, thus no critical observations and comparisons could be made with the EMU.

The Life Support System of the Orlan-M space suit is also located in the back of the suit, like in the case of the EMU, but this time the system is located inside the pressurized volume of the suit, in a pressure of 5.7 psid. In the case of emergency, the Orlan-M space suits also carry a backpack oxygen supply bottle for the cosmonaut, and the SAFER propulsion module can also be modified and attached to the suit [7].

As it can be seen in the following figure of a general view of the Orlan-M suit (sign 15), the fixtures and elements for operation with SAFER had been introduced in the Orlan-M suit that was accepted in the ISS [2.6]:

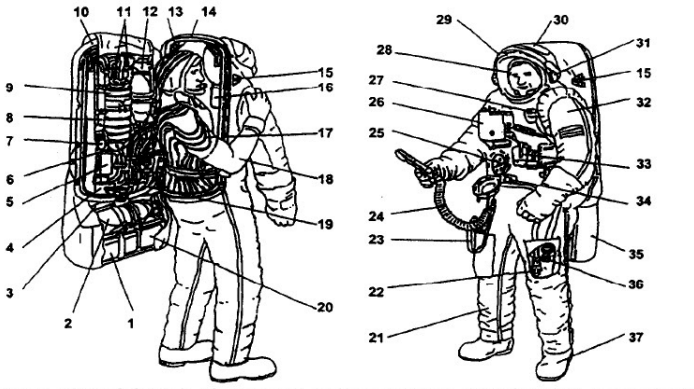

1 - battery; 2 - primary O_2 bottle; 3 - telemetry unit; 4 - moisture separator; 5 - monitoring unit; 6 - heat exchanger; 7 - filter; 8 - feedwater tank; 9 - CO_2 removal cartridge; 10 - backpack; 11 - primary and back-up fans; 12 - back-up O_2 bottle; 13 - pressure regulators; 14 - hard upper torso; 15 – SAFER attachment points; 16- drink bag; 17 - water cooling garment; 18 - underwear; 19 - primary and back-up pumps; 20 - radiostation; 21 - lower "soft" torso; 22 - electrical connector; 23 - safety tether; 24 – adjustable length safety tether; 25 - umbilical combined disconnector; 26 - electrical control panel; 27 - suit pressure gauge; 28 – headset; 29 - light visor; 30 - additional visor; 31 - lights; 32 - "soft" arm; 33 - LSS control panel; 34 - SS attachment point; 35 - removable assembly with battery, radio and telemetry equipment; 36 - connector for emergency oxygen hose; 37 – boots.

(Fig. 2.6.: Orlan-M elements and components)

Now that some of the features of the EMU and Orlan-M space suits have been described, an extensive comparison table with the characteristics of the two suits can be presented [7]:

Suit Feature	**EMU**	**Orlan-M**
Sizing	Modular: The EMU is composed of several interchangeable parts which are sized to fit the 5th percentile female to the 95th percentile male. Sizing rings in the arms and legs allow for resizing on orbit. Over 100 measurements are taken to ensure a proper fit in the gloves, upper torso, arms, lower torso and boots	One adjustable size: The Orlan is compatible for crewmembers whose height falls between 5 feet 7 inches and 6 feet 2 inches. The Orlan's size is adjustable on orbit using Velcro straps to cinch up excess lengths
Entry Method	Waist entry: The crew member puts on the EMU like clothes. There are various parts of the suit to assemble for donning. Self-donning is possible, but usually an Intravehicular (IV) crew member assists	Rear entry: The Orlan has a back door which swings open to allow the crew member to step inside the suit. Self-donning is typical

Pressure	4.3 psid nominal	5.7 psid nominal
In-suit Prebreathe An in-suit prebreathe with 100% O_2 is required to allow the body to get rid of any nitrogen left in the bloodstream which could cause decompression sickness (also known as "the bends")	If the cabin has been at 10.2 psi for at least 36 hours, a 40-minute in-suit prebreathe is required. If the cabin has been at 14.7 psi, a 4-hour in-suit prebreathe is required	30-minute nominal prebreathe (One reason for the shorter nominal prebreathe is the Orlan is pressurized to 5.7 psid. Also, the Russian Space Program accepts a higher level of nitrogen in the bloodstream. Note that neither NASA nor the Russian Space Program has ever reported a case of the bends in space.)
On orbit useful life	From the time the EMU leaves processing (Boeing), the useful life of the EMU is 180 days or 25 EVAs. At the end of its useful life, the EMU is serviced and recertified for flight	The Orlan's useful life is 4 years or 10 EVAs. At the end of its useful life it is placed in a Progress and burned up on re-entry
Displays	The EMU is equipped with Caution and Warning Software (C&W) which sends messages to the Display and Control Module (DCM) mounted to the front of the suit and warning tones to the crew member's Comm Cap. The crew member views messages and suit parameters on a 12-character LCD on the DCM	The Orlan suit is equipped with Caution and Warning (C&W) lights on the front of the suit and in the helmet which alerts the crewmember when critical suit parameters are beyond acceptable values
Communication	The EMU radio uses an Ultra High Frequency (UHF), duplex communication system. (Hardline communication is used for IV operations in the airlock.) EV crew members talk to the IV crew member or the Capcom on the ground	The Orlan radio uses an UHF, duplex communication system, EV crew members talk directly with engineers on the ground (as opposed to Capcom)
Suit Servicing	The EMU umbilical provides power, battery, recharge, suit cooling water, oxygen recharge, water recharge, and hardline communication for IV operations	The Orlan umbilical provides power, suit cooling water and prebreathe oxygen to the suit
On-orbit Maintenance	There is very little on-orbit maintenance required for the EMU because the water tanks, oxygen tanks, and battery can be recharged through the EMU umbilical Some on-orbit maintenance would include changing out the Metox canisters (the Carbon Dioxide (CO_2) scrubbing mechanism in the suit) and resizing the EMU with various sizing rings	There is a relatively large amount of on-orbit maintenance required for the Orlan's because the water tanks and oxygen tanks are completely replaced after each EVA (as opposed to being resupplied via an umbilical)
EVA Training	Task-based: U.S. EVA training currently utilizes a task-based training program. Crew members are trained to perform very specific tasks for an EVA on a specific flight. (For example: Task-based training teaches the crew members to use a specific power tool on a specific bolt, using a particular torque setting and turning it a set number of times).	Skills-based: Russian training utilizes a skills-based training program. Skills-based training teaches general concepts and generic skills which apply to numerous tasks and a variety of EVAs. (For example: Skills-based training would teach the crew member general concepts, about a power tool, how to use it, what its capabilities are, and when it

	Although task-based training has been effective in the shuttle program, the ISS EVA training will become more skills-based in the future	should be used. Skills-based training does not necessarily go into the details of flight specific tasks)

(Table 2.1.: Comparison between EMU and Orlan-M space suits)

2.1.2. Theoretical Presentation of Different Propulsion Units

Throughout the history of the Extravehicular Activities' space suits, space agencies managed to rapidly understand the importance of providing a rescue mechanism to the astronauts, in case of an emergency. No matter how accurate and effective the mission design could be, as well as the design of the extravehicular activities that shall be performed, the uncertainties that may arise while operating in outer space are decisive and of highly importance.

As space suits were evolving, adapting to the gradually increasing needs of space exploration, the maneuvering units were also integrating new features and characteristics to their functions, to meet up with the new, high expectations. In this section, a theoretical presentation of different propulsion units shall be made, providing information regarding the modules and their contribution to the up-to-date maneuvering unit used in the current space missions.

2.1.2.1. Hand-Held Maneuvering Unit (HHMU)

As mentioned above, during the first American EVA on the Gemini program, Edward White II experimented with a personal propulsion device, the Hand-Held Maneuvering Unit (HHMU).

HHMU was a three-jet maneuvering gun, consisting of two jets located at the end of rods and aimed back (so that by activating them, White would move forward) and a third jet aimed forward, operating as a braking force. Due to the corresponding mission requirements, HHMU was stored inside the spacecraft cabin, not allowing the design of it based on a hazardous propellant gas, in case of a leakage. Thus, two small built-in tanks at 27579.08 kilopascals, released 0.32 kilograms of compressed gaseous oxygen, producing the propulsive force of the HHMU [9]. It is an integral unit that contains its own high pressure metering valves and nozzles required to produce controlled thrust. Also, a camera is mounted on the front

of the unit. The key to using HHMU was in the fact that the gun should have been held near the center of mass of the astronaut, aiming in the direction in which he wanted to move, thus being able to propel himself forward. The third jet (center jet) aiming in the opposite direction, would break that movement when fired.

The operation of the HHMU was based on the flow of the gaseous oxygen through the system. After the propellant was released from the two built-in tanks, it was led to a "shutoff and fill" valve, through a manifold. By opening the valve, the propellant entered the pressure regulator, which reduced its pressure to 827.37 kilopascals, allowing it to enter the handle of the HHMU and end to two valves, after passing through a filter. The valve at the forward-end part of the unit redirected the gas through a rotating joint to two arms and to the tractor nozzles, while the valve at the back of the handle allowed the gas to flow through the trigger guard to the pusher nozzle [9]. As the gas flow to the nozzle was increased, HHMU could provide a thrust from 0 to 0.91 kilograms. Finally, the amount of the compressed gaseous oxygen in the two tanks, provided a velocity change (ΔV) of 1.83 (m/s) [9]. HHMU was stored separated in two sections: a hand assembly one and the high pressure section. By connecting a coupling at the regulator and inserting a pin beside the pusher nozzle, the two sections could be connected.

In order to produce the desired motion, the Hand-Held Maneuvering Unit needed to be held as close as possible to the center of mass of the astronaut, making it extremely difficult for the motion to be performed without interferences. Due to the bulkiness of the spacesuit, determining the center of mass of the astronaut was difficult and thus, White was mainly relying on guessing and his experience. In addition, achieving precise motions was rather difficult and physically exhausting, when trying to position the astronaut during an extravehicular activity. The HHMU tested on the Gemini 4 flight had dimensions of 43.18 centimeters length, 25.4 centimeters width and 7.62 centimeters depth [10], folded, and is presented in the following picture [2.7]:

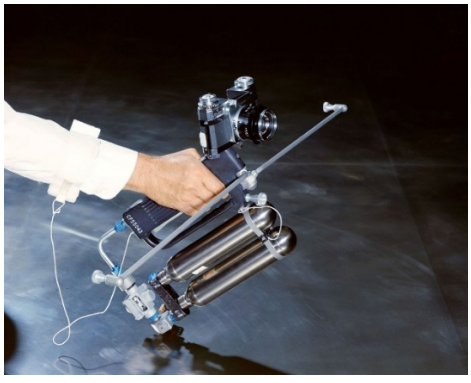

(Fig. 2.7.: Hand-Held Self-Maneuvering Unit (HHMU) on Gemini 4 flight)

On the Gemini 9 (IX-A) mission, a backpack maneuvering unit was introduced and carried for the first time, although communications dysfunctions with the unit and helmet fogging due to the heavy breathing from trying to deploy the control arms, prevented astronaut Gene Cernan from testing it. The propulsion unit consisted of 12 hydrogen peroxide reaction jets to allow three axis movement via hand controls which extended from the unit. The unit was then scheduled to fly on Gemini 12, but NASA decided the risk and unknowns associated with the unit did not warrant the effort involved [11]. The Astronaut Maneuvering Unit of Gemini 9 mission can be seen in the following picture [2.8]:

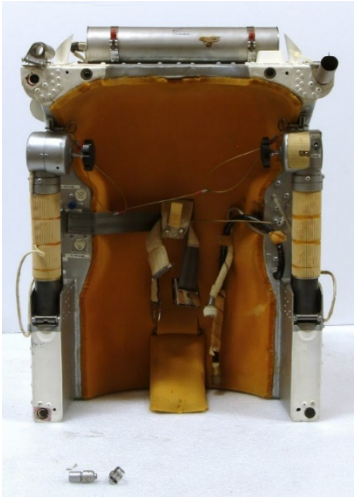

(Fig. 2.8.: Gemini IX-A Astronaut Maneuvering Unit)

Another version of the Astronaut Maneuvering Unit was introduced in the second and third manned Skylab missions, although it was only tested inside the spacecraft. A total of 14 hours testing this more advanced device than HHMU showed that it is adequate and capable of being used during future Extravehicular activities.

AMU had the shape of a large hiker's backpack, while a replaceable tank of compressed nitrogen gas was built inside the frame. 14 nozzles were arranged in a way to produce six degrees of freedom in movement to the astronauts (top-bottom, front-back and right-left), while 11 additional nozzles provided the ability to move and position more precisely than the HHMU of the Gemini program. The AMU could move forward, back, up, down and side to side, in addition to rolling, pitching and yawing. The unit surrounded the astronaut, eliminating HHMU's disadvantage of guessing the center of mass of the astronaut before activating the thruster, as well as offering the astronaut the ability to move closely along the surface of a curved or irregularly-shaped object like the outer surface of the spacecraft or a satellite, without making contact with it.

When deciding to operate the small thrusters, propulsive jets of nitrogen gas were released from the various nozzles located around the unit, allowing the astronauts to perform their desirable action.

2.1.2.2. Manned Maneuvering Unit (MMU)

During the early Space Shuttle flights, the development of the AMU led to a more advanced maneuvering unit, the Manned Maneuvering Unit (MMU). MMU was used on three Shuttle missions in the mid-1980s, was designed to fit over the life-support system backpack of the Shuttle EMU and was operated by a single space-suited astronaut. It was designed in a way to operate in the extreme temperatures and the microgravity environment of outer space that the astronaut would have to encounter during an Extravehicular activity. MMU operations were according to constraints and guidelines provided by previous Space Shuttle mission rules, the design philosophy of the MMU propulsion engineers as well as from the flight experience gained from the Skylab M509 maneuvering system [12].

The MMU had dimensions of approximately 127 centimeters height, 83 centimeters width and 69 centimeters depth. The controller arms of the maneuvering unit were folded for storage, but were unfolded, when an astronaut backed into the unit and snapped the life-support system into place. Fully deployed, the arms increased the depth of the MMU to 122 centimeters, with an adjustment of 13 centimeters for astronauts with different arm length. With a fully propellant load, MMU had a mass of 110 kilograms and it was small enough to be moved within complex structures.

The characteristics of the MMU can be given for two different types of recharge: 1) recharge of the unit through the Orbiter supply, in the Flight Support Station (FSS), or 2) initial ground charge, prior to a mission. The main focus shall be on the Orbiter supply, where 11.8 kilograms of gaseous nitrogen (GN2) at a pressure of 20684.27 kilopascals, enough for a six-hour EVA (depending on the amount of maneuvering), were contained in two aluminum tanks. On an initial ground fully charge, the propellant tanks contain 18.14 kilograms of GN2, at 31026.41kilopascals and 21.11 °C. The propellant recharge of both tanks can be completed in less than 10 minutes and the rate of the propellant consumption varies with the type of maneuvers performed by the astronaut (velocities, trajectories, etc.) [12]. The MMU cold gas propulsion system is considered non-contaminating, while the EMU Life-Support System rejects approximately 0.45 kilograms of water vapor to space, per hour. However, for specific payload operations, the MMU's level and type of contamination is considered acceptable. Under normal conditions, each aluminum tank fed one system of thrusters. 24 nozzles were sorted in teams of three, each on the eight

corners of the MMU, aiming along three axes perpendicular to each other and permitting six degrees of freedom of movement. Each of the 24 dry nitrogen gas thrusters produces 0.64 kilograms of thrust. The delta velocity available from the Orbiter recharge is typically 24.38 to 30.48 meters per second [12].

Regarding the safety that MMU provides, the propulsion unit is considered a "fail-safe" system, which technically means that in case of a single failure, the astronaut can still return safely to the spacecraft. The propulsion engineers of the unit managed to separate the 24 thrusters into two independent systems of 12 thrusters each, which also allow six-degree-of freedom control, in case the other system fails. The control electronics assembly system of the unit is also capable of conveying commands to each cluster of 12 thrusters, in case of a failure appears. Finally, another feature of the "fail-safe" behavior of the system is the fact that it allows the astronaut to activate an Automatic Attitude Hold (AAH) mode, in case of an emergency, or, in the case where the astronaut needs to use both of his hands while performing the Extravehicular Activity tasks. AAH is able to perform for attitude maintenance in any or all of the axes of rotation.

At the ends of the MMU's two arms, to hand controllers were located for the astronaut to manipulate and operate the propulsion system· the left-hand controller produced acceleration without rotation for moving up-down, left-right and forward-back, while the right controller produced rotational acceleration for roll, pitch, yaw. Combining the two controllers, complex movements could be performed in the unit, while after achieving the desired orientation, an automatic attitude-hold function could be activated, allowing the astronaut to use both of his hands for work. The center of the mass of the astronaut/EMU/MMU system, as well as the reference coordinate axis can be seen in the following figure [2.9]:

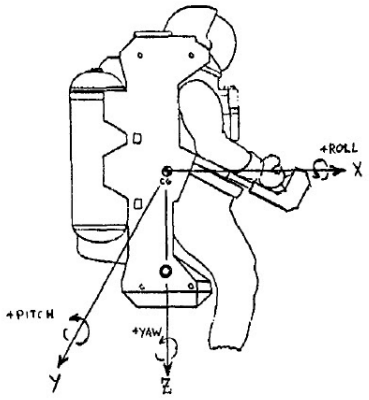

(Fig. 2.9.: The Manned Maneuvering Unit (MMU) Reference Coordinate Axes)

The provisions along the propulsion unit to attach equipment or cargo during an EVA, also allowed the astronaut's hand to remain free during the operations, while the fold of the arms permitted the crewmember to approach the worksite in a closer distance. During an EVA, the only interaction between the spacecraft and the astronaut/EMU/MMU system can be implemented through the voice communications link which is included in the EMU. Finally, during MMU maneuvers, the astronaut can estimate the relative velocity and distance only using visual cues, while the continuous assessment of the power consumption and the nitrogen fuel levels is performed in the displays of the Display and Control Module (DCM). The functional diagram of the MMU can be seen in the following figure [2.9]:

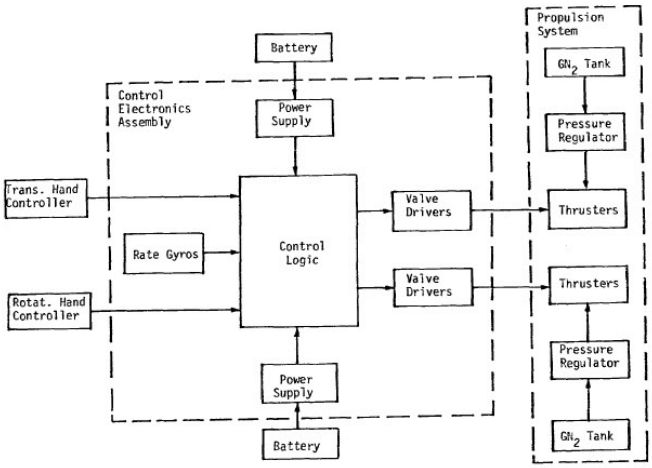

(Fig. 2.10.: The Manned Maneuvering Unit (MMU) functional diagram)

The full structure of the MMU (basic structure, the propulsion subsystem, two-hand controllers and a control electronics assembly (CEA)), as worn by the astronaut Bruce McCandless II, is shown in the following picture [2.10]:

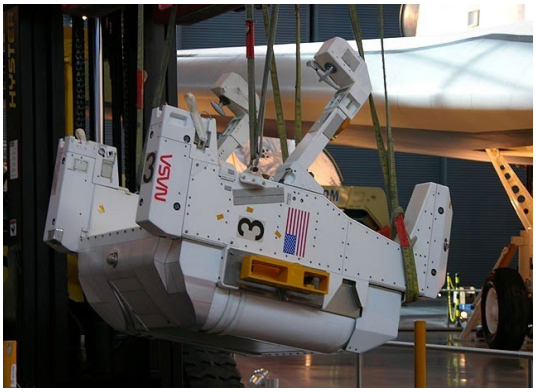

(Fig. 2.11.: The Manned Maneuvering Unit (MMU) flown by McCandless - MMU Number 3)

2.1.2.3. Simplified Aid for Extravehicular Activity Rescue (SAFER)

The EMU as it was designed, did not have a maneuvering capability, which is something that was added by fitting a gas jet-propelled Simplified Aid for Extravehicular Activity Rescue (SAFER), over the Shuttle's EMU's Primary Life-Support System (PLSS). The mass of the propulsion unit has been estimated to be 38.56 kilograms. The Shuttle EMU is pressurized to 29.6 kilopascals. It has been found that a suit pressure of 24.13 kilopascals (sea level - 101 kilopascals) would suffice enough if the person who is wearing it breathes pure oxygen [1].

SAFER is in essence a scaled down version of the MMU and it serves as a self-rescue device for use on the International Space Station. In the event of an astronaut becoming separated from the station while performing an EVA and a Shuttle is not available to retrieve the crew member, the propulsive power of SAFER could return the astronaut to the station structure.

Gaseous nitrogen is expelled through the 24 nozzles that are located in different orientations around the device. Four cylindrical tanks, each charged to 22407.96 kilopascals, hold a total of 1.4 kilograms of the propellant, providing a total velocity change (Δv) of 3.05 meters per second. Each of the 24 nozzles provides a thrust of 0.4 kg [13]. A SAFER propulsion module sketch can be seen in the following figure [2.11]:

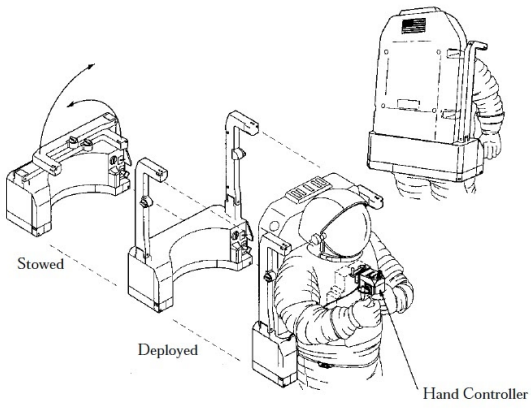

(Fig. 2.12.: SAFER Propulsion Module)

In the bottom of SAFER, a control module consisting of a display and joystick are located, while during operation, the astronaut moves the control module on the front part of the suit for easy access. In addition, an autopilot system (Automatic Attitude Hold) can be activated for a limited period of time, to keep the astronaut at the same orientation and free the hands for work, while six degrees of freedom maneuvering

are allowed. The nitrogen recharging of the SAFER Jetpack was implemented in orbit from the Shuttle's nitrogen system and it was stored in the crew cabin during launch and landing. Finally, a 28-volt battery pack required for the functioning of SAFER can be replaced in orbit [14]. During the STS-64 mission, astronaut Mark C. Lee tested successfully the SAFER module, on a landmark extravehicular activity [2.12]:

(Fig. 2.13.: Mark C. Lee test flies the Simplified Aid for Extravehicular activity Rescue (SAFER) device during the STS-64 mission)

As mentioned before, the Simplified Aid for EVA Rescue (SAFER) was developed for usage on the ISS and Shuttle/Mir EVAs. It provides a second level of fault tolerance in case of an unintentional separation of the crew member from the station, in addition to the first lever of fault tolerance which is the safety tethers [15]. The necessity of SAFER's utilization can be seen by the fact that the station is not able to rendezvous with the separated crew member, in contrast to the Shuttle EVAs. Most of the components comprising the safety tether system that the astronauts are attached to are considered structural members of the spacecraft, thus the possibility of a failure happening is considered insignificant. However, since the tether system could fail due to a human error, something that has happened once in the past, NASA considers the specific threat existing.

A summarized, comparative table among the 3 different propulsion units presented, can be seen in the following table:

	Hand-Held Maneuvering Unit (HHMU)	Manned Maneuvering Unit (MMU)	Simplified Aid for EVA Rescue (SAFER)
First EVA used	Gemini 4 mission	STS-41-B mission	STS-64 mission
Number of Propellant Tanks	2	2	4
Propellant	Oxygen (O2)	Gaseous N2 (GN2)	Gaseous N2 (GN2)
Propellant Pressure (kPa)	27579.03	20684.27 (max)	22407.96
Propellant Mass (kg)	0.32	11.8	1.4
Unit Mass (kg) (No propellant)	3.08	110	38.56
Number of Jets / Nozzles	2+1	24	24
Thrust / nozzle (kg)	0.91 (max)	0.64	0.4
Velocity Change ΔV (m/s)	1.83	24.38 - 30.48	3.05
Degrees of freedom	2 (back and forth)	6 (3 translation, 3 rotation)	6
Automatic Attitude Hold (AAH)	No	Yes	Yes
Shape	Three-jet maneuvering gun	Fit over LSS backpack	Fit over PLSS backpack

(Table 2.2.: Comparative table between the 3 different propulsion units)

A further, in-depth analysis of the Simplified Aid for EVA Rescue (SAFER) propulsion unit shall be presented in the forthcoming chapters of this thesis.

2.1.3. Propulsion Units Applications for Extravehicular Activities Space Suits

Extravehicular activity (EVA), in addition to the Extravehicular Robotics (EVR), are the primary means of the assembly and maintenance of the International Space Station (ISS). The Russian Space Agency (Roscosmos) is responsible for the EVAs on the Russian portion of the ISS, while every activity of the other part of ISS is managed by the United States (NASA), Canada (CSA), Europe (ESA) and Japan (JAXA). An EVA consists of three phases: the transition of the crew and the hardware required for the activity's fulfillment to the corresponding worksite, the arrangement and the restraints' installation on the worksite and finally, the implementation of the EVA task [15].

In contrast to the U.S. (as well as the rest of the space agencies) EVAs which rely on ground training in task resolution, the Russian EVA relies more on the familiarization of the Russian crew members with the specific tasks when on orbit. Most Russian EVAs have been performed on long-term space stations, as compared to the U.S. EVAs which have been performed on time constrained Shuttle or Apollo missions.

2.1.3.1. Space Application: Manned Maneuvering Unit (MMU)

During the race to the Moon that was taking place between the space agencies of the Soviet Union and the United States, a mission known as STS-41-B was a landmark for the application of propulsion units in the

space suits that were being used during space missions. STS-41-B mission's results were different from the previous missions' ones, since the deployment of the two communications satellites never reached the premeditated geosynchronous orbits due to booster rocket malfunctions, while the EVAs performed were rather a huge success.

On February 7 (5h 55m), and again on February 9 1984 (6h 17m), astronaut Bruce McCandless II, who had been working with MMUs and EVAs' development and training for years, in addition to the mission specialist Robert L. Stewart, strapped themselves into the MMUs of their EMUs and performed the first untethered walk in space [16]. The propellant was enough to provide more than six hours of EVA. Inside the shuttle, the crew members, who were fully aware of their roles and actions in case of an emergency, were constantly monitoring and controlling the two astronauts who were moving approximately 92 meters away from the Shuttle, and back, multiple times during the EVAs. Both the astronauts and the shuttle, were travelling at the time with speeds reaching nearly 29000 kilometers per hour. The crew of the STS-41-B mission can be seen in the following picture [2.13]:

(Fig. 2.14.: STS-41-B (STS-11) crew included (seated left to right) Vance D. Brand, commander; and Robert L. Gibson, pilot. Standing left to right are mission specialists Robert L. Stewart, Ronald E. McNair, and Bruce McCandless)

On the 7th of February 1984, the 5th day of STS-41-B space mission, the first EVA using the MMU would be performed. Before initiating the EVA that would be critical for the testing of the MMU, astronaut Bruce McCandless II spent almost 90 minutes checking and putting on the propulsion unit, before testing it inside the payload bay, maneuvering around equipment. Seemingly, performing tests before going out untethered in the vacuum of space turned out to be crucial, since Bruce McCandless perceived that when forward movement was applied in attitude hold mode, the backpack was shaking from its original position [17].

Three different venturings were performed during that EVA, all of them ending with the astronaut returning to the payload bay· a 45 meters, a 96 meters and finally a 99 meters distancing from the shuttle. Intravehicular support informed the EVA crewmember to return back to the payload bay as soon as possible, due to the fact that the tracking lights of the MMU were insufficient for tracking the crewmember if he distanced himself too much during the orbital night. Robert L. Stewart strayed 93 meters away from the Challenger during his EVA, in a MMU test lasting 65 minutes.

Both EVAs evidenced a higher nitrogen propellant consumption than that estimated during the simulations on Earth. On the 9th of February, 7th day of the mission, the two astronauts ventured outside again. This time, the EVA was completed with a Shuttle maneuvering to rescue the crewmember. Although the failure was not relevant to the function of the MMU, NASA decided to characterize this unexpected run of events as a test of the Shuttle's ability to rescue an astronaut in case of an MMU failure.

According to the commander of STS-41-B Vance D. Brand, the key to performing untethered EVAs was to not let the EVA crewmembers move too far from the shuttle. Although the Shuttle had the capability to chase and perform designated maneuvers to rendezvous with the two astronauts, in addition to the contribution of the activation of the nitrogen-propelled Manned Maneuvering Unit (MMU) to bring them back to safety, orbital mechanics could have taken over and lead to unenviable results. STS-41-B mission´s EVA was an astonishing success and produced one of the most well-known space pictures ever taken [2.14]:

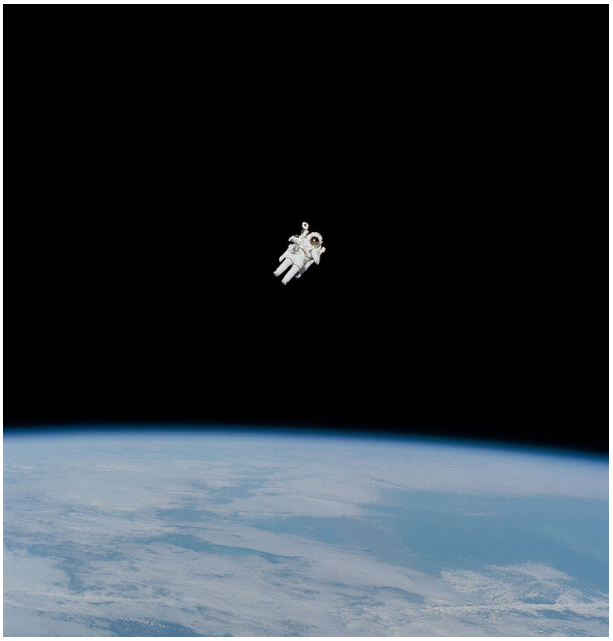

(Fig. 2.15.: STS-41-B mission astronaut Bruce McCandless II, the first astronaut to maneuver about in space untethered)

2.1.3.2. Space Application: Simplified Aid for Extravehicular Activity Rescue (SAFER)

Almost ten years after the testing of the Manned Maneuvering Unit (MMU) by the astronaut Bruce McCandless II and the mission specialist Robert L. Stewart, the new Simplified Aid for Extravehicular Activity Rescue (SAFER) backpack was introduced during EVAs. Mission Specialists Marc C. Lee and Carl J. Meade completed the 28th EVA of the Space Shuttle Program on September 16. During a 6h 15m EVA, they tested the SAFER backpack, a small, self-contained, propulsive backpack that can provide a free-flying astronaut control and mobility, designed for use in case a crew member becomes untethered while conducting an EVA. The unit provides the astronaut with a wide range of self-test capabilities. Four specific test demonstrations were conducted during the 28th EVA by the two crew members of the Discovery spacecraft [17], all of them untethered from the shuttle. The crew of the STS-64 mission can be seen in the following picture [2.15]:

(Fig. 2.16.: STS-64 crew included Richard N. Richards, commander (center front); L. Blaine Hammond Jr., pilot (front left); and Susan J. Helms, mission specialist (front right). On the back row, from left to right, are Mark C. Lee, Jerry M. Linenger, and Carl J. Meade, all mission specialists)

In the first demonstration, the EVA member performed several short single-axis translational and rotational sequences, in order to familiarize himself with the propulsion device. On the first part, the propulsion unit's automatic attitude hold mode was activated, while on the second the mode was off. The sequence was completed with the crewmember documenting the percentage of nitrogen used before and after a maneuver performed in a square trajectory inside the shuttle payload bay, to compare the results with the theoretical that were estimated in simulations.

After the finish of the first demonstration, the EVA proceeded with the engineering evaluation of the device, for later use from the crew members and the ground control. To produce and collect data for the evaluation, the crew member performed several maneuvers, like a one-second thrust forward, a five-second coasting, a one-second braking thrust, as well as the same type of commands for rotations.

In the third demonstration, a self-rescue sequence was performed. The EVA crewmember rotated the SAFER space walker numerous times, yielding the unit's attitude control system activation to stop the rotation and the return of it to the end of the arm. During the demonstration, the astronaut was standing in the food restraint, at the end of the shuttle's mechanical arm.

In the fourth and final test of the 28th EVA, the precision translated that would be useful for future space missions and applications was demonstrated, through a flight qualities evaluation. During this sequence,

the EVA crewmember flew a predefined trajectory that followed the bent mechanical arm as seen in the picture below [2.16]:

(Fig. 2.17.: Astronaut Mark C. Lee, crew member of the STS-64 mission, tested the new SAFER backpack in the first untethered U.S. EVA in 10 years, launched on September 9, 1994, aboard the Space Shuttle Orbiter Discovery)

It should be noted that, between each of the demonstrations performed during the EVA, SAFER jetpack was being recharged from the Discovery's nitrogen supply, through a recharge station located in the forward section of the cargo bay. The 28-volt battery pack was also changed, before Marc C. Lee handed the SAFER unit to Carl J. Meade. Every spacewalking tool that was scheduled to be tested during the 28th EVA were also tested while the SAFER jetpack was activated.

2.2. Space Environment

2.2.1. Introduction to Space Environment

Where space begins and ends, as well as what conditions appear in the environment of space are fundamental questions that always inflated human's fantasy to discover. Different definitions have been given regarding where space begins, for a human who is standing somewhere on Earth. One of them states that space begins at an altitude of about 130 kilometers, which is where an object (satellite, etc.) is put in orbit and remains in orbit for a small period of time, until the thin air molecules of the upper atmosphere drag it back to Earth. Another definition, used by NASA and the U.S. Air Force states that space begins at the altitude of 92.6 kilometers, where although you don't have to go into orbit, one can be awarded with the Astronaut Wings Plaque [18]. The determination of where space begins is not only a matter of physical properties, but of international politics as well.

To begin with, the chemical composition of the atmosphere of Earth can be identified as followed [19]:

- 78% Nitrogen (N_2)
- 21% Oxygen (O_2)
- 1% Argon (Ar), carbon dioxide (CO_2) and small percentage of water vapor
- Different small-sized particles (both solids and liquids), called "aerosols"

Although the atmosphere is mostly rich in oxygen and nitrogen at the level of the sea, the amount of carbon dioxide and ozone increases, with respect to an increase at the altitude. The environmental conditions of the atmosphere of Earth on the standard sea-level are: pressure of 1 atmosphere (or 101.3 kilopascals), temperature of 17 °C and air density of 1.22 (kg/m^3) [20].

2.2.1.1. Atmospheric Layers

A picture of the layered structure of the atmosphere of Earth taken from the International Space Station, can be seen below [2.17]:

(Fig. 2.18.: Layers of Earth's Atmosphere on a sunset view (Credit: Image Science & Analysis Laboratory, NASA Johnson Space Center)

In order to identify the space environment where an Extravehicular Activity takes place, Earth's atmospheric layers should be defined, in which the trajectories of the -up to date- manned orbiters are maintained. Earth's atmosphere has a series of layers, each with its own exact characteristics. This vertical structure of the Earth's atmosphere is categorized by regions, based on the vertical structure of the temperature profile. Starting from ground level and moving upward, the atmospheric layers are: the troposphere, stratosphere, mesosphere, thermosphere and finally the outer boundary of the atmosphere, exosphere, which leads to the outer, interplanetary space [21]. The mentioned layers are explained more specifically as follows [22]:

- **Troposphere**: troposphere is the lowest layer of the atmosphere, as it extends 8 to 14.5 kilometers above the level of the sea. Most of the Earth's weather phenomena take place inside the troposphere, due to the fact that 99% of the water vapor in the atmosphere can be found in the troposphere. It is the densest part of the atmosphere and as you move up, temperature gets colder and the pressure of the air drops.
- **Stratosphere**: stratosphere starts just above the troposphere and extends to 50 kilometers above the ground. Inside the stratosphere, the ozone layer can be found, which is responsible for absorbing and scattering the harmful -for the humans- solar ultraviolet radiation. The stratospheric air lacks the turbulence of its lower layer, which is why commercial passenger jets fly in the lower part of the stratosphere, to secure a more stable flight. In addition, the lack of turbulence and upward air currents, makes the stratosphere warmer as you move up.
- **Mesosphere**: after the stratosphere, the mesosphere starts and extends to 85 kilometers above the ground. The Mesosphere gets colder as you move away from the stratosphere, while the coldest temperatures that have been recorded in the atmosphere of Earth can be found on the top of this

layer (-90 °C). The air is too thin, the pressure at the bottom of the layer is below 1% of that at the sea level and it reduces until the end of the layer. Finally, the mesosphere is the layer of the atmosphere in which meteors burn up, before colliding with the Earth.

- **Thermosphere**: The thermosphere starts above the mesosphere and reaches 600 kilometers above the ground. Regarding the temperatures of this layer, they reach hundreds -or even thousands- degrees (from 500 °C up to more than 2,000 °C), due to absorption of the high-energy X-rays and the ultraviolet radiation from the Sun. The air in the thermosphere is so thin that the conditions inside it are more similar to those of outer space, than to other parts of the Earth's atmosphere. Satellites and spacecrafts that are sent in space maintain their orbits inside the thermosphere· the International Space Station (ISS) follows a nearly circular orbit in the center of the thermosphere with a minimum mean altitude of 330 kilometers and a maximum of 410 kilometers, forming a 51.6° inclination with the equator of Earth [23]. The impressive phenomena of the Aurora, the Northern and the Southern Lights also occur inside this layer.
- **Exosphere**: the upper limit of the atmosphere of Earth, which extends up to 10,000 above the ground is called exosphere. The conditions applied in the exosphere are also more similar to those of outer space, since the air is extremely thin and is constantly leaked into it. There have been various approaches regarding where the atmosphere ends and where interplanetary space begins, with estimations ranging the attitude from 100,000 to 190,000 kilometers above the ground.
- **Ionosphere**: finally, even though the ionosphere is not considered a distinct layer, it overlaps parts of the mesosphere and thermosphere, and thus it should be mentioned when analyzing the layers that comprise the atmosphere of Earth. The ionosphere is a layer which contains plentiful electrons, ionized atoms and molecules (separations which have been caused due to the high-energy radiation from the Sun) and starts from about 48 kilometers above the ground and reaches the edge of space at about 965 kilometers. Based on the contextual solar conditions, the ionosphere either shrinks or grows, and can also be divided into further sub-regions (D, E and F1 and F2), based on the wavelength of the absorbed solar radiation. The reason why the ionosphere is considered such an important layer of the atmosphere of Earth, is that not only it's the connection link between the interactions between Sun and Earth, but also, since it is the layer that allows the radio communications to be implemented.

2.2.1.2. Layers Characteristics

The layers of Earth's atmosphere, in addition to applications performed in each one of them, as well as the different sub-regions of the ionosphere (depending on the density of the electrons), can be seen in the following figure [2.18]:

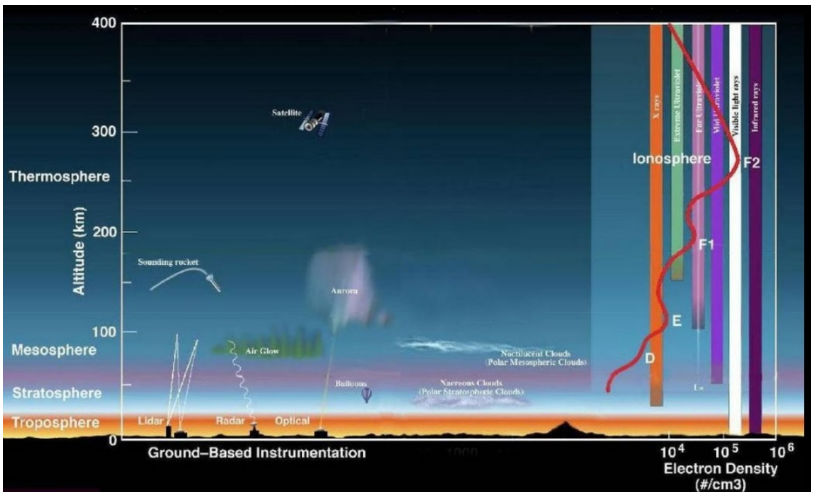

(Fig. 2.19.: Layers of Earth's Atmosphere and space applications)

The temperature gradients and the pressure variations, with respect to an altitude increase, can be seen in the following figure [2.19]:

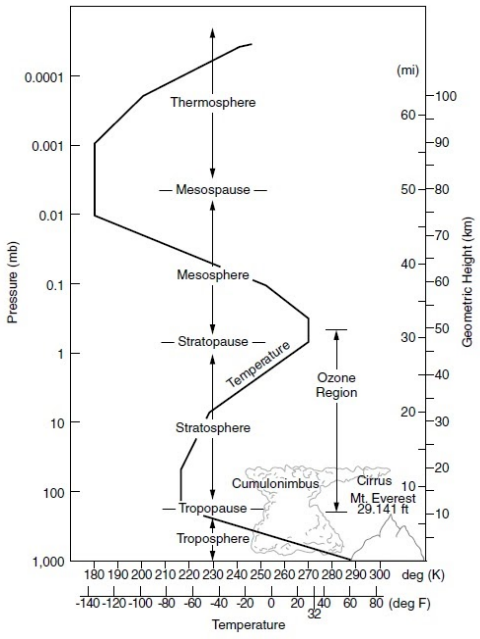

(Fig. 2.20.: Temperature and Pressure variations, with respect to the altitude)

Since satellites and spacecrafts (like the ISS) maintain their orbits inside the thermosphere (up to 600 kilometers above the ground), it is assumed that every Extravehicular Activity (EVA) takes place under the environmental conditions of the thermosphere layer. In addition, the critical space environments that may affect the function and performance of the propulsion units of the Extravehicular Mobility Units (EMU) that will be studied and presented later in this chapter, will be those of the thermosphere. As mentioned above, the air density of the thermosphere is so low, that is considered and treated in different scientific analyses as "outer space", while one of the most common approaches regarding where space begins, also indicates the altitude of 100 kilometers (somewhat higher than the mesopause at the bottom of the thermosphere) as a starting point [24].

Note: Different approaches to the atmospheric layers locate the extension of each layer at different altitudes, making it complicated and disorientating to understand the environmental conditions in which an Extravehicular Activity is implemented. In this thesis, the atmospheric layers definitions are based on the material obtained from the University Corporation for Atmospheric Research Center for Science Education (UCAR SciEd) [22], which is in line with the definitions provided by the National Aeronautics and Space Administration (NASA) [21]. The thermosphere reaches up to 600 kilometers above the ground surface, thus every Extravehicular Activity performed outside an orbiter, is implemented under the thermospheric conditions.

However, the very much acknowledged Dava J. Newman, former Deputy Administrator of NASA, the book of whom "Interactive Aerospace Engineering and Design" [20] also contributes to the "Chapter 3. Space Environment" of this thesis, places the Exosphere at an altitude of 300 kilometers, considering the orbits of different spacecrafts and satellites to be maintained under exospheric conditions. The analysis of the natural and chemical phenomena that takes place in each altitude remains the same, regardless of the naming of each atmospheric layer.

2.2.2. Critical Space Conditions of the Thermosphere

Every applicable critical space environment shall be identified and every potential condition that might arise during the complicity of the human factor in it shall be predicted, before initiating a human space exploration mission or activity. The scope of this section is to provide a sampling of the critical environments of the thermosphere that an astronaut crew member encounters during an Extravehicular

Activity, and not to define every aspect of the space environment that might potentially affect specific aspects of the mission.

Space endeavors and human space exploration activities contain a great risk to be implemented, thus a successful outcome requires highly effective management, planning and organization before performing any actions. During these endeavors, different risks can arise from different elements of the space environment, whose behavior can be considered unpredictable and hazardous. The main challenge for the scientists and engineers designing the space missions at a whole or the spacesuits that are used during the Extravehicular Activities, is to ensure that the human body shall adapt perfectly to the extreme conditions that the astronaut will encounter, so that their physical and mental situation remains stable and safe. Throughout human evolution, the human body has evolved based on the protective, oxygen-filled atmosphere of Earth surrounding it, experiencing the normal gravity of 1 G. Thus, not only it is of highly importance to figure out ways to transport these critical conditions for the human's body prosperity in space, but also it needs to be done in an optimal way, with respect to the complexity and the cost of the problem.

As stated before, inside the thermosphere temperature increases rapidly as you move to the higher layer, exosphere. The ionosphere, which overlaps with the thermosphere, can be defined as an ionized plasma which interacts with the neutral gases of the thermosphere dynamically and electrodynamically. In addition, both layers absorb Ultraviolet (UV) Radiation deriving from the Sun, while in the Polar Regions, when solar winds are affected by the magnetic field of Earth, aurora processes are generated in the thermosphere and the ionosphere. Due to the overlapping of the two layers, they are also both affected by dynamic processes deriving from the lower atmosphere, such as tides, gravity and planetary waves.

A plethora of physical and chemical processes take place in the thermosphere and thus, it is really important to study and understand them when designing a space mission or activity, especially in the case the human factor is concerned. For example, the collisions of the atoms and molecules with the spacecrafts or the satellites in orbit, create a small drag force that contributes in the dynamic behavior of the orbiters, causing mild decreases in the altitude and eventually a potential re-entry in the atmosphere of Earth [25]. Other processes regarding the temperature, the solar radiation and the galactic cosmic rays that affect space activities, in addition to the dynamics of the gases and the microgravity environment that surround those activities shall be presented in the following subsections. Finally, the dangers arising from the impact probability with orbital debris and meteoroids shall also be introduced.

2.2.2.1. Temperature and Solar Radiation

The extreme temperatures a human body or the space equipment has to encounter during a space endeavor or an Extravehicular Activity, make it necessary to provide not only shielding and insulation against them, but also cooling and heating rejection mechanisms. Regarding the surrounding gas temperatures during a space activity, there are two main factors that influence and determine the variations of temperatures inside the thermosphere:

- the absorption of solar extreme ultraviolet (EUV) radiation (at wavelengths lower than 103 nanometers), which causes the ionization and dissociation of the gases in the thermosphere and leads to the creation of the thin ionized plasma, the ionosphere
- the absorption of solar ultraviolet (UV) radiation (wavelengths ranging from 130 to 175 nanometers), which separates molecular oxygen and nitrogen into their corresponding atomic species and changes the atmospheric behavior of the thermosphere, from a molecular atmosphere at an altitude of 85 kilometers to an atomic atmosphere at the altitude of near 500 kilometers

The different neutral gases that exist in the thermosphere are 33% heated by the absorbed EUV and UV radiation, while the rest of the 67% is either emitted to the exosphere, or absorbed in the lower atmosphere. At the end of the mesosphere-start of the thermosphere (about 90 kilometers), chemical energy transportation phenomena also take place, contributing to the heating of the thermospheric neutral gases [25].

In contrast to the heating mechanisms of the thermosphere, cooling mechanisms due to the long-wave (infrared) emissions of different molecules (NO, CO2 and O) also appear in the thermosphere, although they are not adequate to counterweight the heating from the Sun and balance the radiative equilibrium. Two cooling mechanisms are developed in the thermosphere [25]:

- **downward thermal conduction**: happens above about 120 kilometers and signifies an increase of the temperature based on the altitude in which you study. Downward thermal conduction creates a positive temperature gradient as the altitude increases in the lower part of the thermosphere. Due to the thinner atmosphere of the upper part of the thermosphere, the molecular thermal conduction coefficient exceeds the local heating rate, leading to an isothermal (with respect to the altitude) behavior of the temperature and a value called “exospheric temperature”
- **downward eddy heat conduction**: happens in the area surrounding the mesopause, where the infrared cooling reaches a point of magnitude where it can emit the overabundant energy to space.

(Note: The mesopause is the limit point between the mesosphere and the thermosphere, where the minimum temperature is referred [26]).

Temperature varies significantly in the thermosphere, since the Extreme Ultraviolet (EUV) and the Ultraviolet (UV) radiations that are absorbed by the Sun, vary significantly as well. The thermal, compositional and dynamic behavior of the thermosphere and ionosphere depend on the solar cycle (~11 years) and on lower time-scale solar phenomena that diversify the amount of radiation absorbed by the two overlapping layers. At altitudes higher than 100 kilometers, there are ten heating and five cooling processes that characterize the neutral gases heating rate, the description of which is out of the scope of this thesis, but can be found in the available bibliography [25]. What is important to present is the global mean vertical temperature profile of the neutral gases in the thermosphere, since the Extravehicular Mobility Unit (EMU) that an astronaut is wearing during an Extravehicular Activity, interacts and it is affected by the neutral gas molecules that surround it and cover the thermosphere [2.20]:

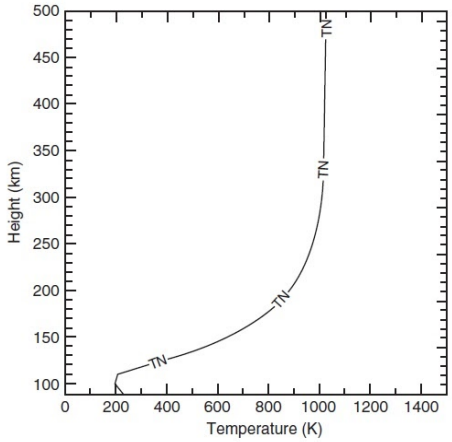

(Fig. 2.21.: The calculated global mean vertical profile for the temperature of the neutral gases, at solar medium conditions (F10.7=150))

As it can be seen in the figure above, the temperature of the neutral gases in the thermosphere increases with respect to the height. Up to 200 kilometers, the temperature profile of the neutral gases appears to have a linear behavior, while as the altitude increases, the curve stabilizes at a temperature of 1000 K (726.85 °C). The density profile (particles per cubic centimeter) of some of the major chemical elements of the thermosphere, can be seen in the following figure [2.20]:

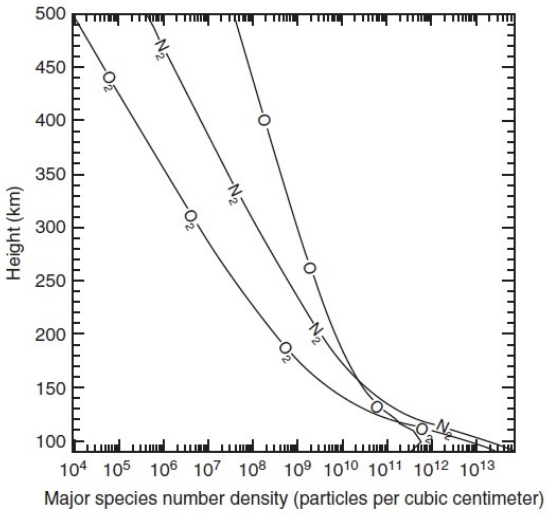

(Fig. 2.22.: The vertical distribution of the density of the major species of the thermosphere, O, O2 and N2, also at solar medium conditions (F10.7=150))

The atomic oxygen (monatomic oxygen, O), the behavior of which is of highly importance due to the material degradation that it can cause to the spacecraft and the spacesuits while on EVAs, has a number density that decreases logarithmically, as the altitude increases. In other words, the higher the spacecraft orbits, the lower the particles of O, O2 and N2 per cubic centimeter.

It should be noted that the term “solar medium conditions” refers to those periods during the 11-year Solar cycle, where the solar activity and sunspots are of medium amount, thus in neither the solar minimum (beginning of the solar cycle), nor the solar maximum (middle of the solar cycle) [27]. The F10.7 (mean daily flux at radio wavelength of 10.7 centimeters (2800 MHz)) index, indicator of the amount of global activity, is considered adequate and effective, to characterize the results of the gases examined [28]. Regarding the results of the two figures shown above and their dependency on the solar conditions, it should also be mentioned that sunspot cycle 25 (i.e. the next decade) has been estimated to be similar or borderline more extreme than the current sunspot cycle, which can potentially differentiate the above-mentioned results [29].

Regarding the interaction of an astronaut performing an Extravehicular Activity with the surrounding environment in the vacuum of space, heat transform can exclusively occur by radiation, given that the body is in a state of thermal equilibrium. Kirchhoff’s Law of thermal radiation determines that a body in thermal equilibrium shall absorb from the universe surrounding it the same amount of energy that it has the capability of radiating. Thus, the two factors that determine an astronaut’s temperature are the energy

exchange and balance at the specific time examined, which are highly dependent on the solar absorption coefficient α. A brief introduction to the mathematical aspect of the equilibrium temperature of a body, which can also be applied in the case of an Extravehicular Activity, will now be presented [20].

As stated before, taking into consideration Kirchhoff's Law for thermal equilibrium, the amount of power absorbed from the outer universe, is equal to the amount of energy emitted from the body:

$$P_{absorbed} = P_{emmited} \quad \text{(Eq. 2.1.)}$$

The amount of power a spherical body absorbs from the Sun can be found as:

$$P_{absorbed} = (a)(\frac{P_S}{4\pi d^2})(\pi r^2) \quad \text{(Eq. 2.2.)}$$

where, α is the solar absorption coefficient, P_s is the total power emitted by the sun and equal to P_s = 4.18×1026 (W), d is the distance of the body from the Sun and r the radius of the examined body.

The amount of power a body is capable of emitting can be found as:

$$P_{emitted} = (\varepsilon\sigma T^4)(4\pi r^2) \quad \text{(Eq. 2.3.)}$$

where, ε is the body's emissivity, σ is the Stefan-Boltzmann constant equal to σ = 5.67×10^{-19} ($Wm^{-2}K^{-4}$), T is the equilibrium temperature and r again, the radius of the examined body.

The combination of the two equations presented above, leads to the solution of the equilibrium temperature for any body at a given distance d from the Sun, as:

$$T = 0.707T_S(\frac{\alpha}{\varepsilon})^{\frac{1}{4}}(\frac{R_S}{d})^{\frac{1}{2}} \quad \text{(Eq. 2.4.)}$$

where, T_s is the mean temperature of the Sun and R_s its radius, yielding a direct dependency of the equilibrium temperature not only from the distance d of the body from the Sun, but from the value of α/ε as well.

2.2.2.2. Galactic Cosmic Rays

Space radiation is one of the most dangerous aspects of human space activities and space missions in general. There are three different types of space radiation· the trapped particles in the magnetosphere of

Earth, the particles shot into space during solar flares (Solar Particle Events, SPE) and the galactic cosmic rays (GCR), which will be briefly presented in this section. The reason why space radiation atoms are so hazardous, is that since the electrons of the atoms have been separated and the atom travels with speeds similar to the speed of light, only the high-energetic nucleus of the atom ultimately remains.

One of the greatest life-threatening dangers an astronaut has to encounter while performing an Extravehicular Activity (EVA) but also in every space activity, especially outside the atmosphere and magnetosphere of Earth, is the presence of GCR. Galactic cosmic rays derive from galactic and/or extragalactic sources and are principally composed of protons, heavy ions and highly energetic α particles.

A potential collision between a high energy GCR particle and a piece of space equipment, can be devastating for the latter, since great damage shall be caused in the electronic components of the equipment. In addition, astronauts' exposure in space radiation increases the risk for radiation sickness, while increasing the possibility of experiencing cancer, side-effects in the central nervous system and other extremely hazardous diseases [30].

Even though GCR ions cause ionization to the atoms they pass through and can practically penetrate a typical spacecraft or even easier the skin of an astronaut, the protection of the atmosphere and the magnetosphere of Earth offer for low-altitude and low-inclination orbits, render GCR into a manageable factor. The Van Allen belts, which will not be further presented in this thesis, also offer protection for human space activity in Low Earth Orbits (LEO) below 1,400 kilometers, since they "trap" GCR particles or ions deriving from solar flares [20]. The protection atmosphere and the geomagnetic field of Earth offer, can be represented in the following figure [2.21]:

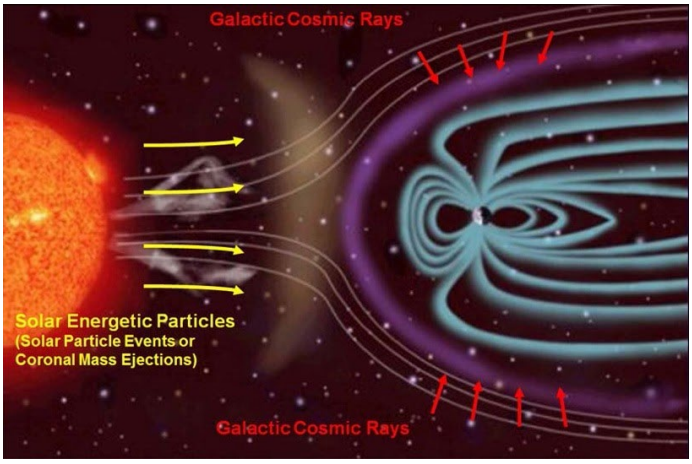

(Fig. 2.23.: Earth's "protection" against space radiation)

Finally, the amount of radiation an astronaut receives depends on three main factors [30]:

- **Altitude**: the higher a spacecraft moves from the surface of the ground, the weaker the protection offered from the atmosphere and the magnetosphere of the Earth, against the ionizing particles. In addition, as the distance from Earth increases, the trapped radiation belts a spacecraft might have to overpass are more frequent
- **Solar Cycle**: as it was mentioned before, there are specific periods of the 11-year solar cycle that present numerous solar flares, responsible for the solar radiation particles
- **Individual's Human Body Vulnerability**: the decisive factor that makes a human body more vulnerable to radiation than another one, is an area that scientists and researchers are still trying to determine and analyze

2.2.2.3. Gas Dynamics

One of the characteristics of the thermosphere, regarding the dynamics of the specific layer, is the development of three forces which do not appear in the lower thermosphere, and thus need to be considered in the analysis of the critical space environment an Extravehicular Activity takes place: the viscous force, the pressure forces due to the variations in the composition or the mean molecular mass, and finally, the ion drag force. Epigrammatically [25]:

- The viscous forces appearing in the upper part of the atmosphere are so strong that at an altitude of 300 kilometers and above, the winds have a uniform behavior. This phenomenon derives from the exponential increase of the kinematic molecular viscosity (even several orders of magnitude) with respect to the altitude. The vertical gradients of the velocity of the winds reduce so much, leading to uniform winds, eliminating any turbulent phenomenon that may arise
- Above the altitude of 160 kilometers, the uniform mixture of the atmospheric gases no longer exists and each gas behaves in a state of diffusive equilibrium. In order to calculate the local pressure scale height of each gas, the law of ideal gases can be applied as:

$$H_i = \frac{RT}{M_i g_0} \qquad \text{(Eq. 2.5.)}$$

where H_i is the scale height, R=8.314 ($JK^{-1}mol^{-1}$) the gas constant, T the absolute temperature, M_i the appropriate molecular mass of the gas and g_0 the gravitational acceleration. The variations of the thermospheric composition or the mean molecular mass, creating the pressure forces are not

included in the scope of this thesis, however further analysis of this area is referred to in the available bibliography [31].

- The ion drag force is a force originating from the collisions occurring between the neutral particles that float in the thermosphere, with the charged particles of the overlapping ionosphere. The ion drag terms and coefficients result from the frictional force originating from the ion-neutral collisions, due to the created acceleration of the particles. The frequency of the collisions depends on different factors such as the geomagnetic field lines in which the ions appear, the electric fields, the altitude and the potential development of neutral wind flowings, as well as the time of the day in which the phenomena take place (during the day: large ionization and ion drag forces, wind flows from area of high temperature-pressure to those of lower, during the night: decrease of the ions' and electrons' density, larger winds due to the reduced ion drag).

During the on-ground analysis of the space environmental conditions surrounding the implementation of an Extravehicular Activity, space agencies need to take into account a plethora of interactions that take place in the thermosphere. In order to accurately and adequately model or simulate the thermospheric conditions, one shall consider the interactions of the layer with the overlapping ionosphere, the interactions between the layer and the magnetosphere and lower atmosphere of the Earth, concerning energy and momentum inputs and finally, different highly complicated plasma dynamics and electrodynamic interactions that take place in the examined system. The use of ideal static models with a fixed lower boundary is therefore suggested.

2.2.2.4. Microgravity Environment

In the worst case scenario where an astronaut becomes untethered from the orbiter during an Extravehicular Activity and starts floating in outer space, the main environmental effect that takes place is microgravity. The necessity of activating the propulsion unit at that point, in the case where the orbiter does not have the ability to rendezvous with the astronaut, becomes crucial for the astronaut's rescue. Microgravity is the feeling of weightlessness an astronaut encounters while performing an EVA or while remaining inside the orbiter, implementing the mission's experiments or other survival procedures. An astronaut performing an EVA in microgravity, can be seen in the following picture [2.22]:

(Fig. 2.24.: Astronauts in the middle of a spacewalk during Expedition 55. Source: NASA)

There is a great misconception that there is zero gravity on spacecrafts or in outer space. The fact is that gravity can be found everywhere in space, in different magnitudes· the moon orbits the Earth, Earth orbits the Sun and the Sun lies inside the galaxy of the Milky Way, all because of gravity. It has been estimated that in Low Earth Orbits (LEO), only the radial component of the gravitational acceleration is being applied on the orbiters, and that with a value of 90% of the corresponding value applied on the environment of Earth ($g_0 = 9.81\ ms^{-2}$) [32]. Thus, the gravitational pull decreases, as the distance between the interacting objects increases.

The microgravity phenomenon will be briefly introduced and discussed in this section, since the scope of the thesis does not require further insight in this specific aspect of the environment in which Extravehicular Activities are performed.

The answer to the question why astronauts float inside the orbiter or while performing an Extravehicular Activity tethered to the orbiter, is that in the vacuum of space, the gravitational force applied to all the objects (regardless of their masses), causes them to fall at the same rate. There are two motions the orbiters (like the International Space Station) perform during their orbit· regarding the ISS, the gravity of Earth is attracting the orbiter towards its surface, while the orbiter is also moving at an orbital velocity of approximately 7.6-7.7 (km/s) (around 27,500 km/h) [33]. This specific orbital velocity has been estimated to be the velocity that the free-falling orbiter's curve best compromises with the way Earth's surface curves. The role of the centrifugal force is crucial to identify microgravity, since it is the necessary force to keep an object moving in a curved path, away from the center of motion. Thus, the orbiters keep falling towards Earth, but never really collide with it [34].

2.2.2.5. Meteoroids and Orbital Debris

Orbital debris can be considered as any human-made particle that has been in space since the launch of Sputnik-1 in 1957. During human spaceflights and Extravehicular Activities (EVAs), the danger of a mission or activity failure due to a potential collision with space debris should always be taken into consideration.

Nowadays, orbital debris is detected using ground-based radars and optical measurements. In Low-Earth Orbits (LEO), during experiment observations radars can detect objects above 2 millimeters, while during routine space surveillance, above 5 centimeters. In Geostationary Orbits (GEO), telescopes during experiment observations are able to detect debris as small as 15 centimeters, while during routine space surveillance, of the size of 1 meter. Finally, in-situ detectors and retrieved surface material can provide really important information regarding small-sized debris [35].

The most serious factors generating orbital debris are the explosion and collision fragments, contributing to a 39.9% of the traceable debris population, in 2005. Many different fragments have been recorded, due to explosions or collisions, propulsion system explosions, electrical system failures (battery explosions mostly), accidental collisions between spacecrafts and mission's objects, as well as other causes that have yet to be determined. Furthermore, debris irrelevant to fragmentation events can be resulted from solid rocket motor firings, which generate dust and slag particles. The following figure is computer generated and represents orbital debris objects that are currently being tracked by the Astromaterials Research & Exploration Science (ARES) of the NASA Orbital Debris Program Office. In this illustration, almost 95% of the objects are debris orbiting in Low Earth Orbits (LEO), i.e., not functional satellites [2.23]:

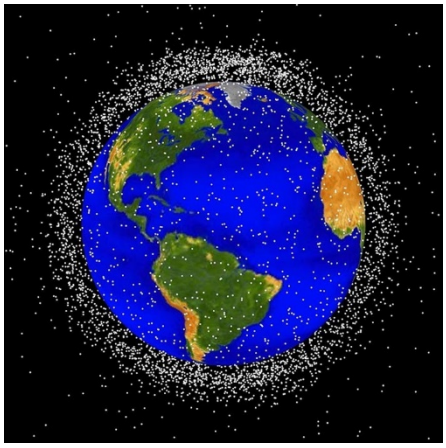

(Fig. 2.25.: Low Earth Orbit (LEO) tracked debris population)

Throughout 50 years since the beginning of space activities, 40,000 tons of meteoroids reach the atmosphere of Earth every year and contribute to the population of 27,000 tons of orbital debris that have been accumulated from human activities. Meteoroid collisions are not only less likely to occur, due to the smaller diameters of the particles comprising the meteoroids, in comparison with those of the orbital debris, but also there are more possibilities to identify meteoroids using human equipment. In space missions design and analysis, the meteoroid environment is considered more stable and easily predictable than the highly dynamic orbital debris environment.

The orbitals debris impact probability, as well as the meteoroid impact probability, can both be approached with the same statistical methodology. Both populations can be adequately represented using the kinetic gas theory laws. By identifying the number of collisions and approaching the collision probability with a Poisson distribution, one can finally estimate the probability of one or more impacts. The statistical analysis of the collision probabilities is out of the scope of this thesis, however further insight on this scientific area is referred to in the available bibliography [35].

2.2.3. Planetary Environments

So far, Extravehicular Activities (EVAs) have only been performed in the vacuum of space, outside of orbiters for maintaining or scientific experimental reasons and on the lunar surface of the Moon, with the Apollo 17 Mission being the last human exploration mission to perform such an activity. The landing site chosen for the Apollo 17 mission was the Taurus-Littrow highlands and valley area, where three EVAs-moonwalks were performed of total duration 22 hours and 4 minutes, by Commander Eugene Cernan. In addition, Command Module Pilot Ronald Evans also performed a trans-earth (from the moon, towards Earth) EVA, 5 days after Commander Cernan [36].

Ever since, no EVA has been performed on a planetary environment, with the Artemis program and more specifically Artemis III space mission marking the beginning of lunar exploration in 2024, after almost 50 years. Currently, NASA is preparing to perform a minimum of two moonwalks in the lunar surface endeavor of Artemis III, while the target is to implement four planned EVAs, in addition to one more unplanned activity, in such an event. NASA orientates on focusing on moonwalks on days 1, 2, 4 and 5, with day 3 being for the crew to rest and perform experiments inside the ascent vehicle and finally day 5 to be dedicated to cleaning up the site and securing tools and moonwalk instruments for potential future EVAs [37].

2.2.3.1. Lunar Environment

Next, a brief introduction to the lunar environmental conditions and consideration shall be presented. The temperatures that can be observed in the lunar surface vary depending on the examined location and the daylight cycle. For example, the surface temperatures near the lunar equator may increase 280 °C at a period of time between the lunar dawn and noon. Near the poles of the Moon, in the craters who have no contact with the light of the Sun and are always shadowed, temperatures of -233 °C have been observed. The dayside temperatures reach a maximum value of 122.86 °C, while during the 2 weekend long lunar night, temperature drops down to -157.15 °C [38].

Regarding the atmosphere of the Moon, the atmosphere is so thin that gases are leaked to outer space. The most important gases that can be found in the lunar atmosphere Neon (20Ne), Helium (He), Hydrogen (H2) and Argon (40Ar), while a plethora of particles from solar winds, comets and meteorites collided on the ground can be also traced [38]. To fully understand the thinness of the atmosphere of the Moon, the atmospheric density of the Earth's atmosphere is approximately 14 orders of magnitude more dense than that of the Moon. An interesting fact that can be found in the available bibliography characteristically states that "six Apollo landings delivered six times as much gas to the lunar surface as there is in the ambient atmosphere" [39]. A representative picture of the lunar surface can be seen below [2.24]:

(Fig. 2.26.: Lunar Surface as captured in the Apollo Missions)

2.2.3.2. Martian Environment

Although the road to Mars has not yet been set and the lunar endeavor of the Artemis Space Program will be a gateway for reaching the "Red Planet", a small introduction to its environment and characteristics can be made. Mars is considered one of the inner Earth-like planets of our galaxy (Mercury, Venus and Mars) and thus it is believed to have formed without an extensive atmosphere. The paradigm of Earth shows that when a plethora of uncombined oxygen exists in a planet, the atmosphere can evolve significantly over time, a fact that favors the presence or development of forms of life [37]. In addition to the fact that the orbits of the two planets create small "launch windows" where a spacecraft can launch from Earth to Mars and vice versa, Mars has been selected as the planet for the future human spaceflight expeditions [40].

Some useful environmental conditions that affect an Extravehicular Activity (EVA) performed on the Martian surface will now be presented. The typical surface pressure of Mars is approximately 0.01 of the Earth's atmosphere, while the mean temperature of Mars is 55 °C, ranging from -133 °C during the Martian winter, to 25 °C on the equator during the Martian summer. The chemical composition of the atmosphere of Mars mainly includes 95.3% of carbon dioxide (CO_2), 2.7% of nitrogen (N_2), 1.6% of argon (Ar) and 0.13% of oxygen (O_2) with the remaining 0.27% consisting of different traces of gas. The water vapor in the Martian atmosphere is 75% less than on Earth's, but adequate to form big quantities of water ice beneath the surface [41]. The presence of these water ice quantities emerges the goal for the future human spaceflight exploration on Mars, and ways to in-situ utilize this specific space resource are already being studied [41]

The Martian surface is rather diverse, which also leads to big temperature variations in areas only a couple of meters away from each other. Martian winds reach extremely high speeds, while the dust of the soil is magnetic and thus shall stick to the surfaces of the spacecraft, scientific equipment or the spacesuits that will be used in human endeavors. This fact, along with the significant temperature variations which cause the material's contraction and expansion, create multiple challenges for the development of the required spacesuits.

NASA's Perseverance rover performed its first drive on the Martian surface on the 4th of May, 2021, capturing the following picture of the Martian landing site [2.25]:

(Fig. 2.27.: Martian Surface as captured from NASA's Perseverance Rover)

2.2.4. Extravehicular Activity (EVA) Safety Parameters

Having identified some important aspects of the hazardous space environment in which the Extravehicular Activities (EVAs) are performed, it is now easier to comprehend with the safety parameters and conditions that need to be met, in order for the activity to be safe for the crewmember, the scientific equipment and for the space mission at its wholeness. The fact that both the NASA Extravehicular Mobility Unit (EMU) and the Russian Orlan space suits, which were presented in Chapter 2, provide multiple restrictions to their users, regarding mobility, visibility, tactility, endurance and force application, makes it an even greater challenge for the space mission design engineers to compete with the potential environmental dangers.

The definition of an Extravehicular Activity (EVA) states that "it is any activity performed by a pressure suited crewmember in an unpressurized or space environment. This can be on the International Space Station, in the Space Shuttle payload bay, or even on the surface of the Moon or Mars" [35].

According to the reference Chapter 22 of the reference [35], the above mentioned information is presented. As it was stated before, since an extravehicular activity is performed in vacuum, the maximum temperature range that has been historically observed is -118 °C to +149 °C. As expected, a different thermal analysis shall be implemented for an EVA in the vacuum, than for an EVA on the lunar or the Martian surface. The spacesuit, the propulsion unit as well as the tools and the scientific equipment used in the EVA are all subjected to great thermal variations in the couple of hours the activity is performed, since different thermal

conditions are applied to them during the sun and the shadow. These variations not only cause malfunctions to the hardware and contraction/extraction to the structural materials, but they constitute a major danger if an astronaut comes in touch with corresponding hardware. NASA however has set the EVA requirement that any hardware used during an EVA, should maintain the temperature of its surface between -153 °C and +160 °C.

In addition, the presence of multiple space radiation sources and radiated electromagnetic emissions surrounding the crewmember's space suit while performing an EVA, is a great hazard for the astronaut's well-being as well as for the prosperity of the space mission. Radio frequency radiation and magnetic fields greater than 250 Gauss applied on the surface of the EMU, may cause damage to the ventilation system or the electronics and communications of the space suit, endangering the life of the astronaut.

The abundance of hazardous materials and chemical substances that drift around the vacuum or the planetary atmospheric environment, incur the risk of the astronaut carrying them on the spacesuit, when returning to the spacecraft's air lock. Even though the used space suit is being decontaminated right after the termination of the activity, the chances of the EVA crew being exposed to a contagious substance are still existing. It is really important to analyze the implications a chemical substance might have on the space suit, even from the design and development stages of the suit and hardware.

An astronaut performing an EVA may also encounter countless more hazards like laser radiation, electrical shocks, molten metal, potential entrapments, and emergency comebacks to the orbiter or explosions, but no further details shall be presented, since they are out of the scope of this chapter.

3. Methodology

3.1. Introduction to the Cold Gas Propulsion Systems

3.1.1. Basic Space Propulsion Concepts

A lot of things can be said about the field of "Space Propulsion", since the desire of the human kind to leave planet Earth and explore outer planets, starting from the Moon, always inflated its imagination. From written references of Ancient Greece satirists like Lucian of Samosata about ships thrown to the moon after being trapped in huge waterspouts, until the actual landing of the human kind on the lunar surface through the Apollo 11 mission, propulsion has always been our way of getting out of this planet. Nowadays, we have reached a point where the limiting factor that prevents us from following our inherent instincts and exploring what is out "there", is not the laws of physics applied to the universe, but the efficient management and distribution of the resources required [42].

In addition to space propulsion providing the necessary forces to orbit inside the atmosphere of Earth or even exceed it, many space applications are based on space propulsion systems to perform activities outside of the orbiters, in the vacuum of space or even in planetary surfaces. As it was mentioned in the previous chapters, propulsion units constitute an extra safety layer for astronauts during their Extravehicular Activities, in the hazardous case they become untethered from the spacecraft, as well as for scientific experiments and demonstrations outside of the orbiters. There are different functions a propulsion system can provide to its user, in order to implement the mission's corresponding objectives [42]:

- **Launch**: providing the necessary acceleration to a vehicle to send it into a designated orbit
- **Orbit insertion**: inserting the vehicle to the mission's orbit, after its launch to the designated orbit
- **Orbit maintenance and maneuvering**: the maintenance of the vehicle to the mission's orbit or its transport to a new designated orbit
- **Attitude Control**: providing the necessary torque to maintain the vehicle in the desired direction

A propulsion system is the primary mobility device of a spacecraft for orbit modifications and attitude control. One of the main factors, if not the main, for characterizing the cost and performance of a propulsion system is the change of velocity (Δv) it provides to the orbiter, in order to translate its center of mass. The three first functions of a propulsion system provide a Δv in the spacecraft, while the last one provides the

torque to rotate the spacecraft about its center of mass. The six main elements of a given propulsion system, can be seen in the following figure [3.1]:

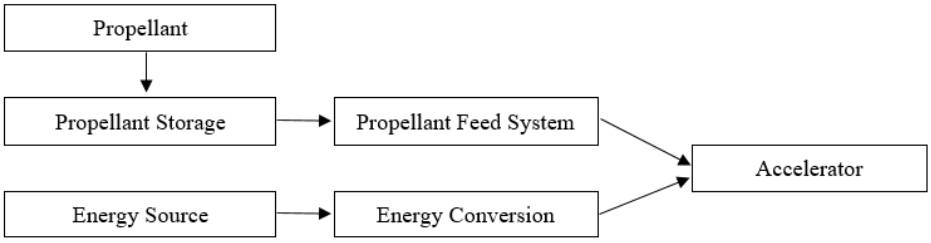

(Fig. 3.1.: Generic Block Diagram for a given propulsion system)

For the SAFER Nitrogen-Jet thrusters that will be described in this thesis, the above-mentioned elements can be specified as:

- **Propellant**: Gaseous Nitrogen (GN2)
- **Propellant storage**: four cylindrical tanks, each charged to 22407.96 kilopascals, hold a total of 1.4 kilograms of the propellant
- **Propellant feed system**: the way to get the gaseous propellant from the storage tanks to the accelerator
- **Energy source**: gas pressure (SAFER functions with a 28-volt battery pack)
- **Energy conversion**: pressure energy converts to thrust by allowing the gas to expand and move through the accelerator block by increasing the exhaust gas momentum
- **Accelerator**: thermodynamic accelerators force the gas to expand to utilize its pressure energy, thus pointing the propellant's mass particles to a designated direction and velocity, producing the thrust required.

In order to understand space propulsion, some basic concepts that characterize the performance of a propulsion system shall be introduced. The analysis of the performance of the Nitrogen-Jet thrusters used in Extravehicular Activities (EVAs) performed by astronauts during human-flight missions, requires the understanding of the process thrust is produced, the means to make this thrust efficient and auxiliary to the implementation of the mission's objectives and finally, the interaction between the thrust produced and the space suit. In the following subsections, those concepts shall be presented.

3.1.1.1. Thrust Equation

In the majority of the propulsion systems utilized in space applications, thrust derives from the exchange of momentum, when mass is expelled at a specific velocity [42]:

$$P_{mom} = mv \quad \text{(Eq. 3.1.)}$$

where P_{mom} is the momentum ($kg \cdot m \cdot s^{-1}$), m is the mass (kg) and v is the velocity ($m \cdot s^{-1}$) of the object.

According to the conservation of momentum, the amount of momentum, within some problem domain, shall remain constant. Momentum is neither created nor destroyed, but only changes through the appearance of applied forces, complying with Newton's Law of Motion. Thus, if for example a space suit's propulsion unit expels mass backward with a certain momentum, the forward momentum of the space suits shall increase equally [43]. By ejecting a small amount of propellant (dm) from the propulsion unit with an exhaust velocity (v_e), the change of the momentum of the unit over a period of time (dt), shall be [42]:

$$F_m = \frac{dP_{mom}}{dt} = \frac{dm}{dt} v_e = \dot{m} v_e \quad \text{(Eq. 3.2.)}$$

where F_m is the magnitude of the momentum thrust (N), $\dot{m}$ is the propellant mass flow rate ($kg \cdot s^{-1}$) and v_e is the exhaust velocity ($m \cdot s^{-1}$) of the propellant.

Thrust is a combination of the momentum thrust and the pressure thrust. The magnitude of the thrust can be obtained as:

$$F = \lambda[\dot{m} v_e + (p_e - p_a) A_e] \quad \text{(Eq. 3.3.)}$$

where, in addition to the previous parameters and assuming steady and one-dimensional flow through the nozzle, F is the magnitude of the thrust (N), λ is a nozzle coefficient accounting for different "real" effects and usually ranging between 0.85-0.98, p_e is the pressure at the exit of the nozzle (Pa), p_a is the ambient pressure (Pa) and A_e is the cross-sectional area at the exit of the nozzle (m^2). For space applications, p_a = 0 (Pa), since the pressure conditions experienced in space are that of the vacuum [42].

As seen in the thrust equation, a significantly important parameter for the magnitude of the thrust produced in a propulsion system is the geometry of the nozzle, expressed through the cross-sectional area at the exit of the nozzle. Nozzles are considered the expansion zones for the propellant and thus their geometry considerably affects the acceleration of the expelled fuel and the generation of high thrust. A very common type of nozzle used in space applications is the "Converging-Diverging" (CD) or "de Laval" nozzle, which

allows a greater amount of energy to be converted into kinetic energy, when the propellant is expelled through it. CD nozzles are usually referred to as supersonic nozzles, because the expelled propellant can reach Mach numbers higher than 1 [44].

3.1.1.2. Specific Impulse

Specific impulse (I_{sp}) is one of the most important performance parameters used to characterize a propulsion unit and it compares the amount of thrust produced from the unit with regards to the propellant mass flow rate. For example, in the Cold Gas Propulsion Systems (CGPS) which will be described below low specific impulse entails higher propellant mass, as seen from the definition of specific impulse (I_{sp}) [45]:

$$I_{sp} = \frac{F}{\dot{m} g_0} \qquad \text{(Eq. 3.4.)}$$

where F is the thrust produced (N), $\dot{m}$ is the propellant mass flow rate ($kg \cdot s^{-1}$) and g_0 is the gravitational acceleration equal to 9.80665 ($m \cdot s^{-2}$).

Different space applications require different amounts of specific impulse. In order to increase the specific impulse of a propulsion system, the temperature of the propellant shall be increased, or its molecular mass shall be decreased. Higher specific impulse means higher thrust produced for a particular propellant mass flow rate, which is desirable for space applications [42].

3.1.1.3. Effective Exhaust Velocity

The effective exhaust velocity (c) is the theoretical exhaust velocity that would exist in an equivalent nozzle producing the same thrust as the actual nozzle, but with the exit gases matching the ambient pressure. It defines the performance of the propulsion units and the spacecrafts utilizing them and can be defined as the product of the specific impulse and the gravitational acceleration at sea level [42]:

$$c = v_e + \frac{(p_e - p_a)A_e}{\dot{m}} \Rightarrow c = I_{sp} g_0 \qquad \text{(Eq. 3.5.)}$$

3.1.1.4. Velocity Change

The change in the velocity delta-v, of the spacecraft (or space suit, in this thesis) that the activation of a propulsion unit forces, can be obtained from the Tsiolkovsky Rocket Equation. The Tsiolkovsky Rocket Equation indicates the relationship between the change in the velocity of the spacecraft with the effective exhaust velocity of the propellant and the initial and final mass of the spacecraft. Considering no external forces such as drag and gravity applied on the space suit and integrating the equation between an initial time when the space suit mass is m_i and a final time when the space suit mass is m_f, the equation can be expressed as [46]:

$$\Delta v = c ln(\frac{m_i}{m_f}) \quad \text{(Eq. 3.6.)}$$

or alternatively, by introducing the mass m as the sum of the mass of the structure and the payload:

$$m = m_i e^{-\Delta v/c} \quad \text{(Eq. 3.7.)}$$

which corresponds to the final mass of the space suit with respect to its initial mass, the velocity change after the activation of the propulsion system and the effective exhaust velocity of the propellant at the exit of the nozzle. The mass of the propellant can now be calculated as:

$$m_p = m_0 - m = m_0(1 - e^{-\Delta v/c}) \quad \text{(Eq. 3.8.)}$$

From these equations it can be seen that by increasing the effective exhaust velocity of the propellant (c), the mass of the payload plus the mass of the structure (m) also increases, and the mass of the propellant (m_p) decreases. Since the velocity change is a really fast process, Δv can be considered as an impulse. Similar to the rockets, when studying the thrust produced during orbital maneuvers, only impulsive thrust is considered [46].

3.1.2. Fundamentals of the Cold Gas Propulsion Systems

As seen in section 2.1 “Extravehicular Activities (EVAs) Space Suits” of this thesis, a fully assembled space suit can be considered as an anthropomorphic, flexible, customized spacecraft, providing a wide range of survival means and protections to the astronauts. In specific aspects of a mission design and given the size, mass, volume and requirements, space suits can be treated in the same way small satellites which are launched into Earth orbit are.

In order to perform the necessary maneuvers, small satellites and space-suited astronauts use Cold Gas Propulsion Systems (CGPS) to control their attitude and orbit. As it can be seen from Table 3.1., cold/warm gas chemical propulsion technologies give a thrust ranging from 10 micronewton to 3 Newton and a specific impulse ranging from 30 to 110 seconds, data which comply with the information given in the presentation of the Simplified Aid for Extravehicular Activity Rescue (SAFER) propulsion unit, presented in section 2.1 "Extravehicular Activities (EVAs) Space Suits" of this thesis.

Cold Gas Propulsion Systems (CGPS), as a subcategory of the Chemical Propulsion Systems, have been researched and developed for many years and thus the R&D level in which they have reached is rather adequate, to satisfy multiple types of space missions. CGPS have been designed in simpler ways than other propulsion technologies and they are considered one of the most reliable systems for thrust generation, being used in different space applications [47]. They are able to provide the necessary spacecraft propulsion, with higher thrust to power rations than electric propulsion technologies, but lower specific impulse appropriate for accurate maneuvering and pointing [48].

The risk of an astronaut performing an Extravehicular Activity (EVA) becoming untethered and losing contact with the orbiter always exists during unpredictable activities like this. The insufficiency of the CGPS of the space suits to be used for large orbit correction maneuvers, in addition to the fact that a large spacecraft is hard to rendezvous with an untethered crewmember, makes it even more challenging for the engineers of the propulsion units of the space suits to ensure the safety of the crew member.

There are many different space applications which require the orbiter to maneuver and rendezvous with other orbiters, astronauts, meteoroids or modify the orbit maintained. Over the years, a wide increase in in-space propulsion devices for small spacecrafts has been observed. These technologies can be categorized as [48]:

- **Chemical**: chemical systems consisting of hydrazine-based systems, mono- or bipropellant systems, hybrids, cold/warm gas systems and solid propellants. They are mostly used when high thrust or sudden maneuvers are required to be performed.
- **Electric**: electrical propulsion devices include electrothermal, electrospray, gridded ion, Hall-effect, pulsed plasma and vacuum arc and ambipolar systems. Although they provide an order of magnitude greater total impulse than chemical systems, only recently the R&D costs have allowed electric propulsion devices to be used instead of chemical ones. Another significant difference in comparison with the function of the chemical systems is that electric propulsion systems require

hundreds or even thousands of hours of operation, while for a similar impulse, chemical systems require seconds or minutes.

- **Propellant-less**: propellant-less systems include solar sails, electrodynamic tethers and aerodynamic drag devices. The research and development level of these systems has not allowed them yet to operate in demonstrations other than the size of small-scale, although the ever increasing need to remove the orbited space debris may render these technologies effective.

A brief summary of the thrust range and the Specific Impulse (s) range of some significant propulsion technologies used in space applications, can be seen in the following table [48]:

Technology	Thrust Range	Specific Impulse Range [sec]
CHEMICAL PROPULSION TECHNOLOGIES		
Hydrazine Monopropellant	0.25 - 22 N	200 - 235
Other Mono- and Bipropellants	10 mN - 30 N	160 - 310
Hybrids	1 - 10 N	215 - 300
Cold / Warm Gas	10 μN - 3 N	30 - 110
Solid Motors	0.3 - 260 N	180 - 280
Propellant Management Devices	N/A	N/A
ELECTRIC PROPULSION TECHNOLOGIES		
Electrothermal	2 - 100 mN	50 - 185
Electrosprays	10 μN - 1 mN	250 - 5000
Gridded Ion	0.1 - 15 mN	1000 - 3500
Hall-Effect	1 - 60 mN	800 - 1900
Pulsed Plasma and Vacuum Arc Thrusters	1 - 600 μN	500 - 2400
Ambipolar	0.25 - 10 mN	500 - 1400
PROPELLANTLESS PROPULSION TECHNOLOGIES		
Solar Sails	TBD	N/A
Electrodynamic Tethers	TBD	N/A
Aerodynamic Drag	TBD	N/A

(Table 3.1.: Thrust and Specific Impulse (s) range of different propulsion technologies)

while, a diagram of the Thrust (mN) versus the Specific Impulse (s) of some of the above-mentioned technologies can be seen in the following figure from [3.2]:

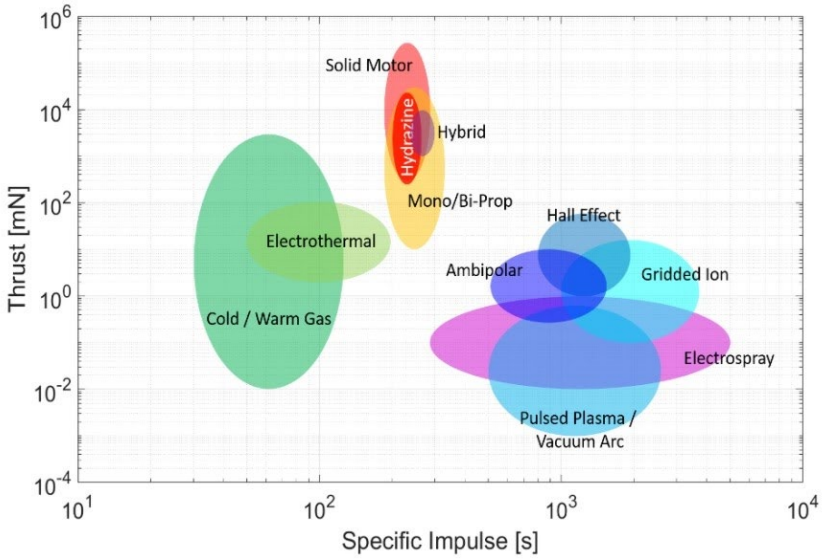

(Fig. 3.2.: Typical small spacecraft in-space propulsion trade space)

Regarding the Cold Gas Propulsion Systems (CGPS) used in space applications like the Extravehicular Activities (EVAs) performed by the astronaut crew members, a lot of similar requirements can be found with their utilization for the attitude control of small satellites [49]:

- high reliability and low system complexity, since no combustion processes take place
- high safety standards for the astronaut during the system's operation
- low velocity changes (Δv), low total impulses [50]
- no contamination of the space suit's external surfaces from the exhaust gases

In the following subsections, a brief introduction regarding the operation, propellant characteristics and the design process of a Cold Gas Propulsion System (CGPS) shall be presented, which will constitute the baseline for the in-depth analysis of the SAFER propulsion unit of the EMU space suits.

3.1.2.1. System Operation

As mentioned above, in order to produce the required thrust to perform the necessary maneuvers, the Cold Gas Propulsion System (CGPS) is based on the controlled ejection of a compressed liquid or a gaseous propellant without an oxidizer (like gaseous nitrogen, in the case of the SAFER propulsion unit). CGPS are considered simple to design and function, since no combustion processes are involved. They usually consist of two parts, a nozzle and an electromechanical valve, in addition to the propellant storage tank.

More specifically, CGPS is composed of the propellant storage tank(s), valves for filling the system and relieving excess pressure, feed line tubes and filters if needed for the implementation of the unit's objectives, a pressure regulator (not in the case of a blowdown system) and the thrusters and nozzles, controlled by the corresponding control valves [51].

Expanding through the nozzle, the cold gas accelerates to high velocities, producing the propulsive force in the cold gas thruster. The electromechanical valve, working on an "On/Off" mode, regulates the flow of the propellant gas through the nozzle and reduces the gas pressure [51], while the thruster usually consists of a cap, a cylindrical chamber and a convergent-divergent nozzle. When the thruster functions at constant pressure and the pressure of the valve is higher than the pressure inside the propellant's tank, thrust can be generated in more consistent levels. The cold gas thrusters can be operated in either a regulated or a blowdown mode, while the probability of the systems overheating is eliminated [49].

3.1.2.2. System Characteristics

The utilization of a CGPS in space applications entails lower mass of the system, as well as lower power requirements for the function of the system. However, a serious disadvantage of the Cold Gas Propulsion Systems is the low specific impulse, where for example, using gaseous nitrogen as propellant as in the case of the SAFER propulsion unit of the EMU spacesuits, the specific impulse is of the order of 68 seconds [49]. In addition, the thrust provided over a period of time decreases repetitively, since the propellant consumption reduces the pressure inside the storage tank and this last tank is directly proportional to the thrust produced [52]. A schematic of a Cold Gas Propulsion System can be seen below [3.3]:

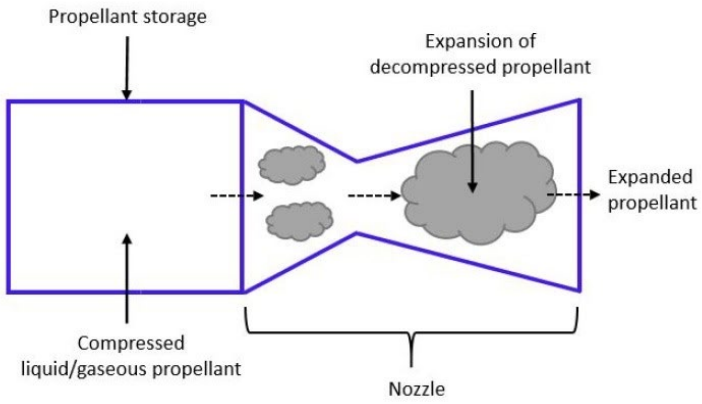

(Fig. 3.3.: Cold Gas Propulsion System schematic)

The specific impulse (I_{sp}) for a Cold Gas Propulsion System can be defined as [52]:

$$I_{sp} = \frac{\gamma c^*}{g_0}\sqrt{\frac{2}{\gamma-1}\left(\frac{2}{\gamma+1}\right)^{\frac{\gamma+1}{\gamma-1}}\left(1-\left(\frac{P_e}{P_c}\right)^{\frac{\gamma-1}{\gamma}}\right)} \quad \text{(Eq. 3.9.)}$$

where γ is the Poisson constant (the ratio of specific heats at constant pressure and constant volume), c^* is the characteristic velocity and P_e/P_c is the exit-to-chamber pressure ratio, which is related to the expanded propellant. It can be seen that the specific impulse is directly proportional to the characteristic velocity c^* and is highly affected by the exit-to-chamber ratio. Finally, the characteristic velocity depends on the molecular weight and the temperature of the propellant and it will be defined later in this chapter.

The exhaust velocity (v_e) for a Cold Gas Propulsion System can be defined as [53]:

$$v_e = \sqrt{\frac{2\gamma R_{N_2} T_c}{\gamma-1}\left(1-\left(\frac{P_e}{P_c}\right)^{\frac{\gamma-1}{\gamma}}\right)} \quad \text{(Eq. 3.10.)}$$

where in addition to the parameters found in the equation for the specific impulse of a CGPS, R_{N2} is the ideal gas constant for the gaseous nitrogen (N_2) and T_c is the temperature of the chamber, which also affects the final value of the exhaust velocity.

3.1.2.3. Propellant Characteristics

A very important decision that should be taken when designing or utilizing a Cold Gas Propulsion System (CGPS) for the implementation of a space mission, is the deliberate selection of the propellant that will be used. A number of factors should be taken into account when selecting the propellant. The propellant, either in a pressurized gas or in a saturated liquid form, is stored in high-pressure tanks and thrust is produced with the removal of it through the propulsion unit's nozzles. The gases used are usually noble, non-toxic, since for example in the propulsion units of the space suits, the primary "payload" affected by a potential dysfunction of the thruster, is the astronaut [47]. Furthermore, the selected propellant shall be non-reactive, so that no compatibility problems appear with the material and the exterior surface of the space suit (or the spacecrafts, in general), as well as it should be immediately available for the space agency and the corresponding crew members participating in the missions, in cases of emergency [51].

Gaseous nitrogen and helium are the most commonly used cold gas propellants, due to their high inertia (the ability to resist various types of gaseous or liquid chemical influences) and low molecular mass [51]. Using nitrogen as the main propellant has many advantages in comparison with other gas such as hydrogen and helium· It is easier to store because of its cryogenic characteristics and the probability of a gas leakage is lower [49]. Thus, gaseous nitrogen is most commonly selected for utilization in Cold Gas Propulsion Systems [51]

Finally, the selected propellant should have a high specific impulse to unit volume ratio, so that the propellant can be maintained on board unaltered for a longer period of time [52]. Many different propellants have been used in space applications with CGPS, the characteristics of which are given in the table shown below, for Standard Temperature and Pressure (STP) conditions [49], [54]:

Propellant	Specific Impulse (s)	Specific Heat Ratio	Density (kg/m^3)	Molecular Weight
Hydrogen	296	1.409	0.0899	2
Helium	179	1.667	0.1785	4
Nitrogen	80	1.4	1.2506	28
Argon	57	1.667	1.7837	39.9
Methane	114	1.299	0.717	16

(Table 3.2.: Cold Gas Propulsion Systems propellants characteristics)

Considering isentropic relations during the extraction of the pressurized gas from the tank through the nozzle, the temperature and density of the gas at different pressure points along a streamline can be calculated as [55]:

$$\frac{p}{p_t} = \left(\frac{\rho}{\rho_t}\right)^{\gamma} = \left(\frac{T}{T_t}\right)^{\frac{\gamma}{\gamma-1}} \qquad \text{(Eq. 3.11.)}$$

where regarding the gas parameters, p is the pressure, ρ is the density, T is the temperature and γ is the specific heat ratio, while the indicator t implies the throat characteristics. Using this equation, the pressure and the density of the gaseous nitrogen can be defined, using the tables of thermodynamics.

3.1.3. Design Process

The design of a Cold Gas Propulsion System (CGPS) requires an exceptional perception and understanding of the fundamentals of thermodynamics and fluid mechanics and dynamics. Before proceeding to the

selection of the proper gaseous fuel to implement successfully the mission's objectives, a mathematical analysis of the equations describing all the processes taking place in the thruster, shall be carried out.

The Cold Gas Propulsion System (CGPS) either comprises or lacks a pressure regulator. A typical system architecture of a CGPS consisting of a pressure regulator, can be seen in the following figure [3.4]:

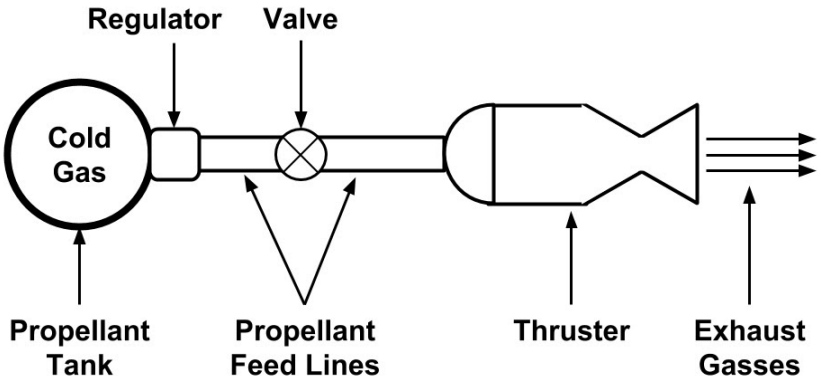

(Fig. 3.4.: Typical Cold Gas Propulsion System architecture)

The presence (or lack) of a pressure regulator affects the operation and performance of the CGPS and as a result, the determination of whether or not a pressure regulator shall be included in the system, shall be in accordance with the mission's objectives [49]:

In the case of an existing regulator, the pressure inside the storage tank (P_{tank}) remains constant during the function of the system. Thus, other parameters such as the outlet pressure of the thruster, as well as the output flow rate remain constant as well, which leads to a constant specific impulse (I_{sp}). The propulsion system continues working until Ptank becomes equal to the pressure of the chamber (Pc), yielding a remaining fuel called "propellant dead mass".

In case the CGPS lacks a regulator, Ptank is equal to Pc, due to the fact that the storage tank and the chamber are directly connected. The pressure of the tank (as well as the chamber pressure), the outlet pressure of the thruster, the output flow rate, the thrust produced and the specific impulse (I_{sp}) all reduce, while the propellant gas is extracted from the storage tank.

Finally, the total mass of the Cold Gas Propulsion System (m_{total}) consisting of the following components can be determined as [49]:

- $\mathbf{m_{tank}}$: the storage tank of the propellant
- $\mathbf{m_{prop}}$: the propellant mass

- **$m_{thruster}$**: the mass of the thruster
- **m_{access}**: the mass of other accessories

$$m_{total} = m_{tank} + m_{prop} + m_{thruster} + m_{access} \quad \text{(Eq. 3.12.)}$$

3.1.3.1. Theoretical Performance Prediction

An initial approach to the design of a CGPS requires the definition of a number of assumptions regarding the operation and the thermodynamic analysis of the propulsion unit. The assumptions that can be made when designing a CGPS are the following [42]:

- no losses appear in the feed lines, the valve or the pressure regulator
- no pressure or mass flow losses appear in the nozzle
- an isentropic process assumed for the flow from the pressure regulator to the nozzle exit
- the gaseous fuel and the feed lines are assumed to be in an isothermal state at a temperature of 25°C (or 298.15 K). By switching on and off the system successively (operating it intermittently), the pressure inside the storage tank slowly drops. On the one hand heat is transferred by the unit to the tank, while on the other hand assuming an isentropic state, the temperature inside the tank drops, as the pressure drops. Thus, an isothermal state can be assumed inside the storage tank.

In the gaseous state of matter, the following set of equations can be extracted, for the determination of the behavior of the Cold Gas Propulsion Systems (CGPS) [42]:

(acoustic velocity) $$a_0 = \sqrt{\gamma R T_0} \quad \text{(Eq. 3.13.)}$$

(characteristic velocity) $$c^* = \frac{a_0}{\gamma\left(\frac{2}{\gamma+1}\right)^{\frac{\gamma+1}{2\gamma-2}}} \quad \text{(Eq. 3.14.)}$$

The thrust equation, as described in section 3.1.1.1, can now be defined as [42]:

$$F = A_t p_c \gamma \left[\left(\frac{2}{\gamma-1}\right)\left(\frac{2}{\gamma+1}\right)^{\frac{\gamma+1}{\gamma-1}}\left(1-\left(\frac{p_e}{p_c}\right)^{\frac{\gamma-1}{\gamma}}\right)\right]^{\frac{1}{2}} + (p_e - p_a)A_e \quad \text{(Eq. 3.15.)}$$

where A_t is the cross-sectional area at the throat, A_e the cross-sectional area at the exit of the nozzle, p_e the pressure at the exit of the nozzle and p_c the pressure of the chamber. The parameter p_a has already been defined as the ambient pressure and has been set equal to zero for the vacuum (p_a=0).

To further simplify the complex analysis of a Cold Gas Propulsion System design process, the assumption of an infinite expansion ratio can be made, yielding a pressure at the exit of the nozzle equal to p_e=0. The following set of equations, described as the key performance parameters, can now be derived [42]:

(propellant mass flow rate) $$\dot{m} = \frac{A_t p_c}{c^*} \Rightarrow \dot{m} = \frac{F}{c^* \gamma}\left[\left(\frac{2}{\gamma-1}\right)\left(\frac{2}{\gamma+1}\right)^{\frac{\gamma+1}{\gamma-1}}\right]^{-\frac{1}{2}}$$ (Eq. 3.16.)

(thrust) $$F = \dot{m} c^* \gamma [\left(\frac{2}{\gamma-1}\right)\left(\frac{2}{\gamma+1}\right)^{\frac{\gamma+1}{\gamma-1}}]\text{^}\frac{1}{2}$$ (Eq. 3.17.)

(specific impulse) $$I_{sp} = \frac{F}{\dot{m} g_0} \Rightarrow I_{sp} = \frac{c^* \gamma}{g_0}\left[\left(\frac{2}{\gamma-1}\right)\left(\frac{2}{\gamma+1}\right)^{\frac{\gamma+1}{\gamma-1}}\right]^{\frac{1}{2}}$$ (Eq. 3.18.)

(total propellant mass) $$m_{prop} = \dot{m} \Delta t$$ (Eq. 3.19.)

(total propellant tank volume) $$V_p = \frac{m_{prop}\, RT}{p_c}$$ (Eq. 3.20.)

Two new parameters can now be introduced, to further proceed with the design process of a Cold Gas Propulsion System and the analysis of its performance [42]:

(expansion ratio) $$\varepsilon = \frac{A_e}{A_t} = \frac{1}{M_e}\left[\left(\frac{2}{\gamma+1}\right)\left(1 + \frac{\gamma-1}{2} M_e^2\right)\right]^{\frac{\gamma+1}{2\gamma-2}}$$ (Eq. 3.21.)

(pressure ratio) $$\frac{p_e}{p_c} = \left[1 + \frac{\gamma-1}{2} M_e^2\right]^{-\frac{\gamma}{\gamma-1}}$$ (Eq. 3.22.)

where M_e is the exhaust Mach number of the gases at the exit of the nozzle.

Finally, the geometric parameters for the determination of the dimensions of the thruster shall be introduced, with respect to the dimension of the throat [42]:

(throat cross-sectional area) $$A_t = \frac{\dot{m} c^*}{p_r}$$ (Eq. 3.23.)

(throat diameter) $$D_t = 2\sqrt{\frac{A_t}{\pi}}$$ (Eq. 3.24.)

where p_r is the specified regulator static pressure (if present in the Cold Gas Propulsion System), equal to the pressure of the chamber.

Numerous plots can now be extracted, regarding the operation and performance of the examined Cold Gas Propulsion System. For example, the "storage tank volume versus the pressure in the tank" plot, the "specific impulse versus the expansion ratio" and the "nozzle and orifice diameters versus the regulator pressure" plot, which determines the dimensions of the thruster.

3.1.3.2. True Performance Prediction

In order to estimate the "true" performance of a Cold Gas Propulsion System (CGPS), the assumptions presented above, that simplified the design process of the system should be eliminated and high-efficiency bell nozzle λ should be introduced (as seen in section 3.1.1.1, λ is a nozzle coefficient accounting for different "real" effects and usually ranging between 0.85-0.98 [42]).

Initially, the information regarding the isothermal performance and the sizing of the storage tank should be interpreted. By determining the characteristic velocity (c^*) and the Mach number at the exit of the nozzle (M_e) of the gaseous propellant used in the CGPS, the pressure ratio can be defined, taken as datum, that the chamber pressure (p_c) is equal to the specified regulator pressure (p_r).

The amount of thrust produced can now be calculated, using the (Eq. 3.15.) [42], multiplied by the high-efficiency bell nozzle λ [42]:

$$F = \lambda \left[A_t p_c \gamma \left[\left(\frac{2}{\gamma-1}\right)\left(\frac{2}{\gamma+1}\right)^{\frac{\gamma+1}{\gamma-1}}\left(1-\left(\frac{p_e}{p_c}\right)^{\frac{\gamma-1}{\gamma}}\right)\right]^{\frac{1}{2}} + (p_e - p_a)A_e\right] \qquad \text{(Eq. 3.25.)}$$

yielding the calculation of the propellant mass flow rate ($\dot{m}$) and the propellant mass (m_{prop}). As mentioned before, λ coefficient accounts for different "real" effects, such as the case where the exhaust gas does not exit the nozzle in a straight line. Thus, the high-efficiency bell nozzle λ coefficient depends on the geometry of the thruster's nozzle, allowing for taking into account the non-uniformities that may be present across the nozzle exit plane.

It should be noted however that, in contrast to the theoretical performance prediction of a Cold Gas Propulsion System (CGPS), the propellant mass (m_{prop}) estimated here does not include a leftover propellant mass (m_r), deriving from the tank pressure reducing to the pressure enforced by the pressure regulator [42].

The total propellant mass required for the operation of the CGPS can be defined as:

$$m_t = m_{prop} + m_r \quad \text{(Eq. 3.26.)}$$

thus, its calculation requires the estimation of the residual propellant mass (m_r), in addition to the volume of the propellant storage tank (V), by solving the following set of equations [42]:

$$p_r = m_r RT \quad \text{(Eq. 3.27.)}$$

$$p_{ti} = (m_r + m_{prop})RT \quad \text{(Eq. 3.28.)}$$

where p_r is the regulator pressure (equal to the chamber pressure) and p_{ti} the initial tank pressure, which is an input data to the design process. By solving this 2x2 system of equations for m_r and V, the total propellant mass can be determined.

As expected, since the assumption of ideal expansion no longer applies to the true performance prediction of the CGPS, the amount of thrust produced and, as a result, the specific impulse of the system are lower than their corresponding "theoretical" values [42].

Although the system before was examined in an isothermal state, it is also really interesting to examine the thrust as if it were continuous and in an isentropic state. Thus, thrust remains constant throughout the operation of the system, by assuming a calorically perfect gas, while the change in the temperature inside the storage tank modifies the mass flow rate of the propellant [42]. Different parameters such as the isentropic temperature, pressure and propellant mass in the tank, for the whole Δt of the operation of the system can now be comprehended. For example, the internal energy and its rate of change are defined as [42]:

(initial energy rate of change) $$\dot{U} = -\dot{m} c_p T_t \quad \text{(Eq. 3.29.)}$$

(internal energy) $$U = m_t c_p T_t \quad \text{(Eq. 3.30.)}$$

where T_t is the instantaneous temperature in the tank and c_p is the specific heat for a constant-pressure process (J/kgK). The transcript "t" on the mass and the temperature terms of these equations, refers to the corresponding instantaneous values of those terms at any time examined during the "blowdown". The mass flow rate of the propellant with respect to time, can now be defined as [42]:

$$\dot{m} = \frac{A_t p_r}{c^*} \quad \text{(Eq. 3.31.)}$$

where again A_t is the cross-sectional area at the throat, p_r is the regulator pressure (equal to the chamber pressure) and c^* is a function of the instantaneous pressure of the tank.

The history of the thruster performance of the Cold Gas Propulsion System (CGPS) can now be derived, by integrating (Eq. 3.28.) and (Eq. 3.30.). Through this analysis, the descending behaviors of the isentropic tank temperature, pressure and propellant mass in the tank versus the time of the system's operation are observed, as the propellant is rapidly expelled from the storage tank. Finally, the specific impulse also decreases as the system keeps operating, despite the constant pressure feed, due to the decrease in the isentropic temperature of the propellant gas [42].

3.2. Simplified Aid for Extravehicular Activity Rescue (SAFER) Propulsion Unit

3.2.1. Introduction to the SAFER Nitrogen-Jet Propulsion Unit

The Simplified Aid for Extravehicular Activity (EVA) Rescue (SAFER) is a backpack propulsion unit which was first tested on the STS-64 mission (September 1994), is considered part of the Government Furnished Equipment (GFE) and is provided by the National Aeronautics and Space Administration (NASA) to the crewmembers of different space missions, for supplementary use on the Extravehicular Mobility Unit (EMU) [56]. Although a brief introduction to the main characteristics of the SAFER propulsion unit was made in "Section 2.1. Extravehicular Activities (EVAs) Space Suits", the scope of this chapter is to present an in-depth analysis to the description of the system and provide the necessary scientific background to implement the analysis on the performance of the unit. The SAFER propulsion unit can be seen in the following figure [3.5]:

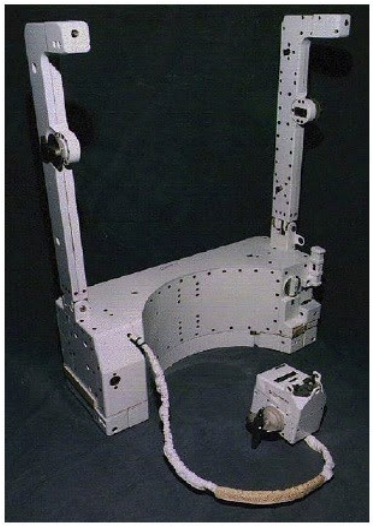

(Fig. 3.5.: Picture of the SAFER propulsion unit)

The SAFER backpack propulsion system is considered an optimum version of earlier the Manned Maneuvering Unit (MMU), which was also presented in "Section 2.1. Extravehicular Activities (EVAs) Space Suits". The MMU, and consequently the SAFER unit are considered applications of the category of "Cold Gas Thrusters" [57] and thus they will be examined by applying the same fundamentals, principles and mathematical equations that were presented in "Section 3.1. Introduction to the Cold Gas Propulsion Systems" of this thesis.

In comparison with MMU, although SAFER provides sufficient propellant to the crew member to perform the necessary self-rescue maneuvers, it lacks the propellant capacity and the systems redundancy the MMU provides to its user. After all, the two propulsion systems share an overall system concept, as well as similar general subsystem features like the HCM grip design and other features of the gaseous nitrogen propellant subsystem (recharge-port, quick disconnect and the pressure regulator/relief valve) [58]. The MMU has been used widely since 1984, since it is considered an appropriate propulsion unit for the implementation of different mission's objectives. However, its volume and as a result, the cost required to carry the unit during space missions, highlight the need for a lighter propulsive system, but equally effective while performing EVAs. These two parameters, in addition to the self-rescue and attitude hold capabilities that the SAFER unit backpack provides, resulted in its utilization during space missions up to the present [59].

During the Space Shuttle Mission STS-64 in September 1994, the pre-production model of the SAFER unit was first tested during flight. In the 6.9 hours test flight, the mission crew was able to check the performance, flying qualities and the systems of the unit, in addition to evaluate its operational utility. It was found that the unit was able to provide the amount of thrust required to perform a self-rescue maneuver, since the control and the stabilization the unit offered were satisfactory and achieved the self-rescue requirements [14].

As stated before, the function and operation of the SAFER nitrogen-jet propulsion unit is based on the fundamental principles of the Cold Gas Propulsion Systems. The compressed gaseous nitrogen (GN2) propellant is expanded through the nozzles of the system, producing the required thrust for the implementation of the Extravehicular Activity's objectives.

3.2.1.1. SAFER Flight Unit Description

The SAFER flight unit is a small, lightweight, functionally independent from the Extravehicular Mobility Unit (EMU), 24 jet-thrusters propulsion unit that is utilized by the Extravehicular Activity (EVA) crew members, to perform self-rescue maneuvers in the vacuum of space or rendezvous with the orbiters. The unit is attached to the underside of the Primary Life Support Subsystem (PLSS) of the EMU, without adding any movement restrictions to the crew member wearing it [56]. The stowage and deployment of the SAFER propulsion unit, can be seen in the following figure [3.5]:

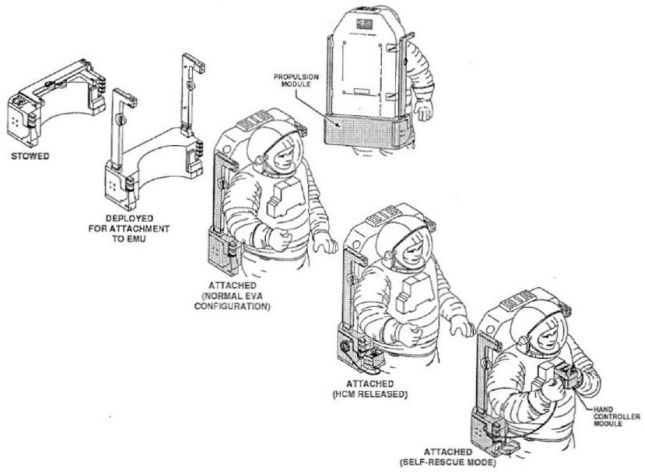

(Fig. 3.6.: SAFER propulsion unit deployment and stowage)

As it was mentioned in the previous chapters, SAFER provides its users with 6-degrees-of-freedom movement, controlling the activation of the thrusters and the mobility of the space suit using a single Hand Controller Module (HCM). The usage of the HCM is very simple: when the activation of the SAFER is necessary, the EVA astronaut deploys the HCM while holding it on the left hand and turns on the power switch, firing a pyrotechnic device which pressurizes the propulsion system. In case the astronaut needs both hands to perform the self-rescue maneuver or implement any other Extravehicular Activity requiring the activation of the SAFER propulsion unit, a fastening strap located in the back of the HCM allows the attachment of the hand controller to the astronaut's EMU Display and Controls Module (DCM). The HCM used for the control of the SAFER unit, can be seen in the following figure [3.6]:

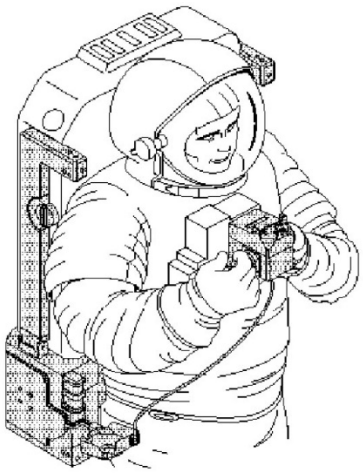

(Fig. 3.7.: Hand Controller Module attached to the SAFER unit)

When not used, the unit is folded and stored in the spacecraft during the whole launch, on-orbit and landing process. The SAFER unit consists of four hardware components: the propulsion module, the Hand Controller, the Hand Controller Module Hardmount and the Intravehicular Activity (IVA) replaceable Battery Pack [56]. A representation of the unit can be seen in the following figure [3.6]:

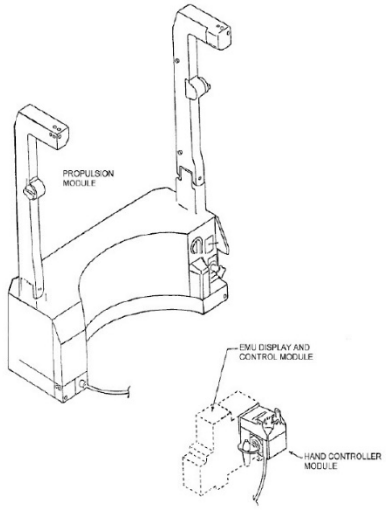

(Fig. 3.8.: Representation of the SAFER unit components - IVA battery pack excluded)

However, since this thesis focuses on the analysis of the performance of the propulsion unit, only the first component shall be presented.

3.2.1.2. SAFER Propulsion Module Characteristics

One of the most important performance characteristics of any given propulsion system, as presented in the previous chapters, is the minimum total delta velocity (Δv) it is able to provide. The SAFER propulsion unit provides the user with a minimum Δv of 3.05 meters per second nitrogen charge, during ground processing [56] and with an acceleration of 0.061 meters per square seconds (0.2 ft./sec^2) [14]. However, the total delta velocity required to perform a self-rescue maneuver significantly depends on the orbital effects applied on the system Astronaut/Extravehicular Mobility Unit (EMU)/ SAFER unit system [59].

From the comparative table of the three propulsion units presented in “Section 2.1. Extravehicular Activities (EVAs) Space Suits”, an overview of the performance and technical characteristics of the SAFER propulsion unit can be seen below:

	Simplified Aid for EVA Rescue (SAFER)
First EVA used	STS-64 mission
Number of Propellant Tanks	4
Propellant	Gaseous N2 (GN2)
Propellant Pressure (kPa)	22407.96
Propellant Mass (kg)	1.4
Unit Mass (kg) (No propellant)	38.56
Number of Jets / Nozzles	24
Thrust / nozzle (kg)	0.4
Velocity Change ΔV (m/s)	3.05
Degrees of freedom	6
Automatic Attitude Hold (AAH)	Yes
Shape	Fit over PLSS backpack

(Table 3.3.: SAFER propulsion unit characteristics)

The propulsion module comprises the main volume of the SAFER unit and consists of three subsystems: Propulsion, Structures & Mechanisms and the Avionics. The propulsion subsystem schematic can be seen in the following figure [3.6]:

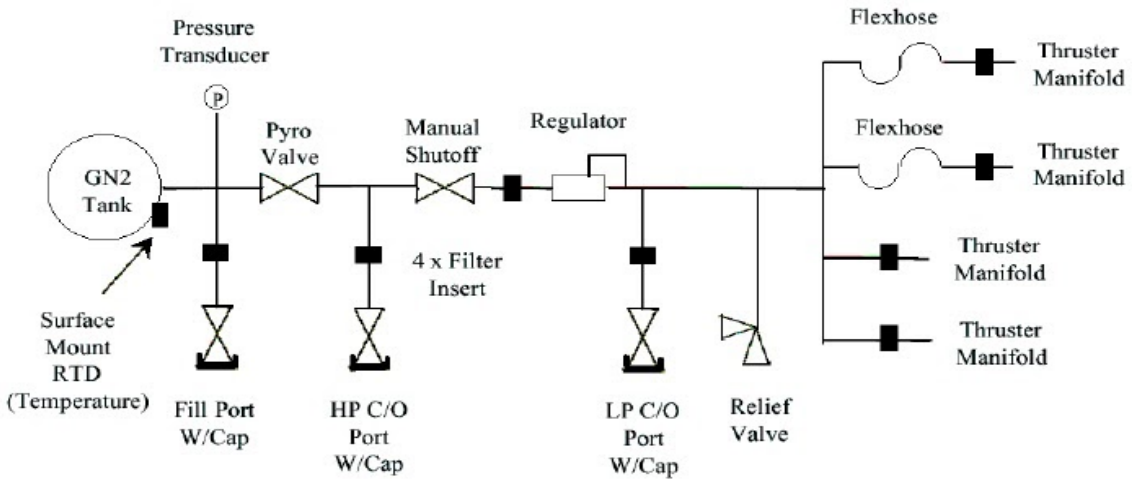

(Fig. 3.9.: SAFER propulsion subsystem schematic)

As it can be seen, the propulsion subsystem basically consists of a propellant storage tank, a pressure regulator and the thruster manifolds and its operation is based on the fundamentals of the Cold Gas Propulsion Systems, presented in "Section 3.1. Introduction to the Cold Gas Propulsion Systems". The description of the SAFER propulsion subsystem components will be presented forthwith [56]:

- The Cylindrical Pressure Vessel or a Propellant Storage Tank supplies the propulsion subsystem with the gaseous nitrogen (GN2) which is used as propellant. There are 4 stainless steel pressure vessels in the subsystem, each with a limited life of 100 cycles to the maximum design pressure, which is set to 68947.57 kilopascals (10000 psig) at 93.3°C (200°F). The factor of safety on burst has been determined in 2 and the nominal ground load is approximately 55158.06 kilopascals (8000 psig) at 26.67°C (80°F). Each pressure vessel is charged to 22407.96 kilopascals (3250 psig) and holds a total of 1.4 kilograms of the propellant [13]. It should be noted that the performance of the thruster is reduced, as the propellant storage tank empties [60].
- The Surface Mount Resistance Temperature Detector (RTD) is located on the exterior surface of the propellant tank, to measure and determine the temperature of the gaseous nitrogen propellant supply. The measurement obtained is then utilized as an input data for the avionics subsystem.
- The Pressure Transducer is responsible for monitoring the pressure inside the propellant storage tank. The main function of the pressure transducer is to convert the pressure measured into an analog electrical signal [61], within the range of 0 and the maximum design pressure (68947.57 kilopascals).
- The Pyrotechnic Isolation Valve (Pyro Valve) is located after the pressure transducer and provides the system with long-term protection from any potential leakages of the gaseous nitrogen propellant supply. The pyro valve has been designed to handle pressures up to 68947.57 kilopascals (10000 psig), with a minimum burst pressure of 137895.15 kilopascals (20000 psig). “Burst pressure” can be defined as the pressure that a pressure vessel (like the cylindrical pressure vessels storing the propellant of the unit) can withstand, before bursting [62].
- In SAFER’s unit pyro valve, the initiator used is the NASA Standard Initiator (NSI), which translates an electrical stimulus into a pyrotechnic action (the “first fire”). NSI produces the flame and the hot particles which either ignite other powders or initiate the pressure impulses and thus the propulsion procedure [63].
- The Manual Shutoff Valve (Manual Isolation Valve) is manually operated by the astronaut and it separates the high-pressure system (propellant storage tank, pressure transducer, pyro valve and the two high-pressure fill/test ports) from the low-pressure system (pressure regulator, low pressure fill/test port, relief valve and the thruster manifolds). The Manual Shutoff Valve allows pressure isolation between the two systems and flow through either of the two directions (either left or right of the valve). The valve has been designed allowing a burst pressure of 358527.38 kilopascals (52000 psig).

- The Pressure Regulator is located after the "Manual Shutoff" valve and is responsible for the regulation of the propellant tank pressure, before the propellant flows in the thruster manifolds. The pressure regulator is a major component of a Cold Gas Propulsion System. It is set to the nominal pressure of 148.37 kilopascals (215 psig) and regulates down the operational pressure of the system to +172.37/-103.42 kilopascals (+25/-15 psig). The design and dimensioning of the pressure regulator is based on the capability of it to support the propellant flow to the four thrusters of the SAFER propulsion unit, to an inlet pressure of approximately 6894.76 kilopascals (1000 psig).
- The high-pressure system consists of two high pressure fill/test ports, the "Fill Port W/Cap" and the "HP C/O Port W/Cap", while the low-pressure system consists of one low pressure fill/test port, the "LP C/O Port W/Cap". The three fill/test ports are used to recharge the propellant pressure vessel, while on ground servicing, they provide a regulator or relief valve checkout. The three ports are sealed with their corresponding pressure caps, which are only installed or removed during ground operations of the propulsion unit. These pressure caps are used to ensure that no pressure is left in the ports when they are being removed. Finally, before the Extravehicular Activity initiates, they are lockwired so that they are not being accidentally removed during the activity, risking the crew member's life.
- The Relief Valve is located after the pressure regulator, and is responsible for protecting the low-pressure system in the case of a failed-open or a regulator that appears to leak. The sizing of the relief valve is based on the maintenance of the downstream pressure to values below 2757.9 kilopascals (400 psig).
- The Thruster Integral Module (Thruster Cluster) consists of 24 fixed-position nozzles that translates into six similar thrusters' blocks located at the four corners of the SAFER propulsion unit. Each one of these thruster integral modules consists of an electrically operated solenoid valve and electrical connector accommodating the wires from the valves, for each of the six thrusters. In order to allow a better control of the maneuvering capability of the propulsion unit, the twenty four thrusters are located about the center of mass of the Astronaut/Extravehicular Mobility Unit (EMU)/ SAFER unit system. As shown before, with the activation of the SAFER unit through the Hand Controller Module (HCM), electrical power is transmitted to the solenoid valves of each thruster, producing propulsion by expanding the gaseous nitrogen (GN2) propellant through the conical nozzle of each thruster. Each thruster has the capability to produce a nominal vacuum thrust of 3.584 ± 0.3584 Newton [56] (or 0.8 ± 0.08 lbf. In the vacuum of space, the acceleration of a

free-falling object remains constant and equal to the gravitational acceleration g0 which is 9.80665 meters per square second at sea level on the Earth [64]. Thus, the conversion of pound forces to Newton is implemented through the formula 1 lbf = 0.45359237 kg × 9.80665 m/s² = 4.448 N). Finally, the flex hoses connecting the thruster manifolds with the rest of the unit are located in the hinge joints of the tower assemblies and have a minimum burst pressure rating of 11031.61 kilopascals (1600 psig).

To sum up the operation of the Cold Gas Propulsion System (CGPS) like the SAFER propulsion unit, the stored gaseous nitrogen (GN2) propellant passes through the regulator valve and is directed to the four thruster manifolds, each consisting of six electric-solenoid thruster valves. The avionics software of the unit translates the EVA crew member's commands and opens the valves, where the gaseous nitrogen is then released and expanded through the nozzle, producing the required thrust [65].

The structures and mechanisms of the SAFER propulsion module can be seen in the following figure [3.6]:

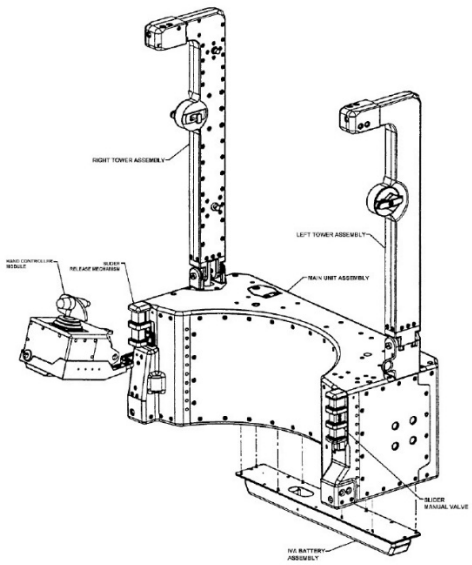

(Fig. 3.10.: SAFER top assembly layout)

As it can be seen in the figure above, the unit consists of two tower assemblies. The Right and Left Tower Assembly of the unit store most of the necessary components of the propulsion unit, such as lines and fittings, filters, valve cable assemblies, the two latches used to attach the SAFER to the EMU Primary Life Support Subsystem (PLSS) and finally the thrusters. The hinges at the joints provide the routing of the propellant, the electrical power and the signal to the thrusters, while the hinges of the tower allow the two towers to rotate, in order to reduce the volume of the propulsion unit [56].

Regarding the Hand Control Module (HCM), it is located in the HCM stowage compartment in the right hand end of the propulsion module. In case self-rescue maneuvers are required to be performed, the astronaut lifts up the actuation lever and the HCM is released, ready for use.

Finally, the SAFER battery assembly supplies the Power Supply Assembly with power and provides the required voltage to the electronic compartments of the propulsion module, such as the Control Electronics Assembly (CEA), the Valve Driver Assembly (VDA) providing the control of the 24 thrusters, the Hand Controlled Module (HCM) and the Inertial Reference Unit (IRU). Without getting into further details regarding every element consisting the SAFER product at its wholeness (although some elements have been and will be described in this chapter), the detailed breakdown structure of the "product", can be seen in the following figure [3.5]:

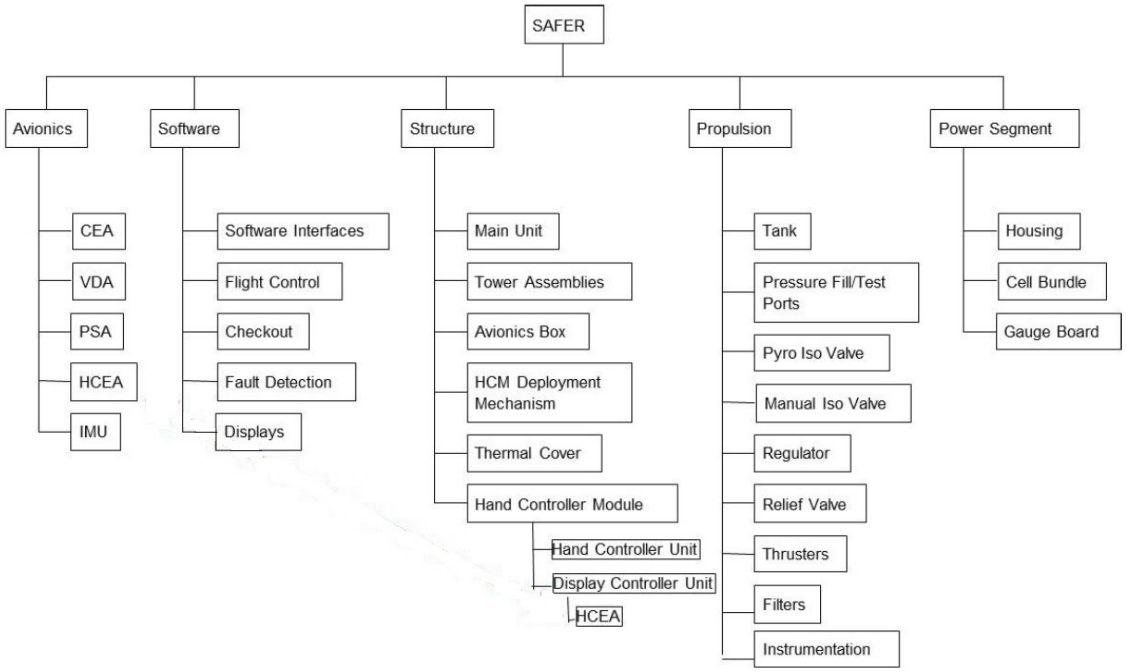

(Fig. 3.11.: SAFER Detailed Product Breakdown Structure)

3.2.2. Maneuvering Control and Fault Detection Functions

The Maneuvering Control and the Fault Detection of the SAFER propulsion unit, are the two primary functions of the avionics software. The maneuvering control consists of the commanded accelerations and the Automatic Attitude Hold (AAH) actions, while the fault detection supports every operation regarding

the inflight procedures, the pre-EVA and the ground checkouts [58]. The two functions of the avionics software controlling the SAFER unit shall be briefly described below.

3.2.2.1. Maneuvering Control Software

The Maneuvering Control Software is responsible for the control and command of the commanded accelerations based on the 6 degrees of freedom that the SAFER propulsion unit allows, as well as the Automatic Attitude Hold (AAH) control. The commanded accelerations are categorized in rotational and translational accelerations. The commands regarding the translation of the propulsion unit are along a single translational axis where X is regarded as the first axis, Y as the second and Z as the third [58].

When two commands, one rotational and one translational, are given at the same time by the Hand Controller Module utilized by the EVA crew member, the rotational one precedes the translational. In the case where commands given by the crew member are "conflicting", the thrusters receive no input signals from the avionics software. The single acceleration command sent by the software chooses the thruster firings to implement the commanded signal. Finally, a maximum of four thrusters can be activated at the same time, in other words the avionics software shall provide accelerations with a maximum of four simultaneous thruster firing commands [58].

As mentioned above, SAFER consists of 24 thrusters using gaseous nitrogen (GN2) as propellant. The avionics subsystem provides the thruster valves with commands to open, causing the thruster to fire in response and initiate the propulsion force generation. The six degrees of freedom provided by the SAFER unit to the EVA crew member for the maneuvering control are the following: ± X, ± Y, ± Z, ± roll, ± pitch and ± yaw [58]. Thus, the astronaut has the ability to fly up and down, left and right, forward and backward, in addition to perform roll, pitch and yaw rotations [60]

A very important function the avionics software of the SAFER propulsion unit (as well as the Manned Maneuvering Unit) provides to the EVA crew member, in contrast to the Hand-Held Maneuvering Unit, is the Automatic Attitude Hold (AAH) function. The Automatic Attitude Hold functions as an autopilot system and can be activated for a limited period of time, to keep the astronaut at the same orientation and free the hands for work. The function is controlled through the Hand Controller Module: a single-click of the pushbutton located on the top of the module initiates the function, while a double-click terminates it,

for all three rotational axes. Lastly, an automatic rotational deceleration is provided with the activation of the AAH function, until all the rotational axes are near zero.

More specifically, a three-axis fiber optic gyroscope evaluates the rotational velocities in the roll, pitch and yaw, in order to stabilize the attitude of the EVA crew member. The signals of the gyroscope are then translated into commands to the thrusters of the SAFER unit via its control software, yielding a thrust production that neutralizes the rotations. The Automatic Attitude Hold function can thus be considered one of the most important and innovative functions of the SAFER propulsion unit [60].

3.2.2.2. Fault Detection Function

The second subsystem of the avionics software is the "Fault Detection Subsystem". The fault detection subsystem consists of four different testing functions: a self-test, an activation test, a monitoring function and a ground checkout function. It is responsible for the estimation of the parameters and the messages that are being sent to the Hand Controller Module (HCM) LCD screen and as a result to the EVA crewmember, as well as for the management of the display interface. A brief introduction to the four testing functions shall be presented below [58]:

- The self-test is implemented without using any propellant or equipment outside of the SAFER unit and it tests the overall function of the unit. In order to perform the self-test, the EVA crew member goes through a list of particular tests to be checked: a "Thruster" test, a "Hand Controller Controls and Display" test and a "Rate Sensor Function" test. In case one of the tests fails, a message is displayed to the astronaut.
- The activation test is implemented using a very small amount of propellant, also utilizes no extra equipment outside of the SAFER unit and it checks the functionality of the unit in operational mode. By commanding 20 millisecond thruster pulses in both translational and rotational axes and having thrusters firing in the opposite direction, so no net acceleration is produced, the astronaut can check the function of the pressure regulator of the propulsion unit.
- The monitoring function can be regarded as a continuous fault check of the subsystems comprising the SAFER propulsion unit. The monitoring function implements a variety of tests like monitoring of leakages, checks on the battery voltage and the temperature of the battery pack as well as checks of the pressure and temperature of the rank and the regulator. The results and the information regarding them are all available for the astronaut to check and act accordingly.

- The ground checkout function receives requests for data or tests regarding the avionics software from the ground support equipment and processes those commands.

3.2.3. Extravehicular Activity (EVA) Self-Rescue

During an Extravehicular Activity (EVA) performed by an astronaut crew member, there are many different scenarios where the activation of the SAFER propulsion unit might be life-saving. Researchers in the Weightless Environment Training Facility (WETF) of the NASA Johnson Space Center have actually estimated the possibility of an EVA crew member becoming untethered from the orbiter as once every 1000 EVA hours [66]. Thus, it is of great importance to examine and understand the self-rescuing techniques and capabilities the usage of a propulsion unit provides to the astronauts performing EVAs.

According to the EVA protocol, in the beginning of an Extravehicular Activity, the EMU spacesuits are double tethered to the orbiter. That means that in order for an EVA crew member to become untethered, two failures would have to occur, which was the basis for the decision to not include system redundancy in the SAFER propulsion unit. This decision, although provided a smaller-sized and practical device, made the unit's operation "vulnerable" to a single failure that would render it useless. That is why the 16.76 meters (55 feet) long tether was replaced with a new, 25.91 meters (85 feet) safety tether, to restore the system's redundancy [60].

However, different parameters should also be taken into consideration, regarding the capability of the SAFER propulsion unit to perform the required EVA inspections on the outer sites of the space station that appear to have dysfunctions [60]:

- the duration of the flight performed using the SAFER propulsion unit. Although the inspection of the station's sites requires a great amount of time to be implemented, due to the different sites and the measurements and evaluations that have to be performed in each site, the SAFER hardware was designed and certified to operate for thirteen minutes minimum, during rescue operations
- the operational life of the three-axis fiber optic gyroscope used for the Automatic Attitude Hold (AAH) function. Even though the operational life of every component of the SAFER unit has been determined based on its endurance in the worst-case extreme temperatures, the gyroscope has been found to overheat and fail after forty-five minutes of powered operation.

- the human factor, present in every Extravehicular Activity performed. There is a difference in approaching the two different scenarios of performing a self-rescue maneuver and using the SAFER unit to perform the necessary inspections of the station's sites. In the first case, after training sessions performed in the Virtual Reality (VR) Laboratory at the Johnson Space Center it was found that based on the experience of the EVA crew member, the amount of propellant consumed and the time required for the rescue varied. However, the total amount of the propellant can be consumed during a rescue operation. In the second case, the amount of the inspection tasks the crew member has to implement during the Extravehicular Activity, in addition to the actions required in each inspection (fly away from the robotic arm, evaluate the depth of the damage, return to the robotic arm or proceed to the second inspection site) oblige the astronaut to considerate the amount of propellant consumed during each task.

Below, a brief introduction to the characteristics of a self-rescue action will be presented.

3.2.3.1. SAFER Self-Rescue Details

As in every development process, the SAFER propulsion unit should fulfill some requirements. The general requirements that characterize the SAFER propulsion unit are [14]:

- minimal cost and weight
- astronaut rescues shall take place within 4.5 minutes from the separation
- no interferences with the normal tasks that are performed during the EVAs

An important factor when examining the rescue of an untethered EVA crewmember, is the rate of separation of the astronaut from the station. Again, researchers in the Precision Air-Bearing Floor (PABF) of the NASA Johnson Space Center, as well as during KC-135 flights in zero-gravity parabolas, examining four test subjects of different sizes, estimated the following results for practical use [59]:

- **separation speed**: 0.762 meters per second (2.5 fps)
- **pitch rate**: 55 degrees per second
- **roll and yaw rates**: 20 degrees per second

The necessity of carrying SAFER along with the Primary Life Support Subsystem (PLSS) backpack when becoming untethered from the orbiter is manifested, if the three rescue options available for an untethered astronaut are presented [59]:

- **1st option**: the astronaut immediately uses an equipment device with the shape of a "shepherd's crook", to not flow away from the orbiter
- **2nd option**: the astronaut is rescued by a standing-by astronaut who uses a Manned Maneuvering Unit (MMU) and is responsible for monitoring and supervising the implementation of the Extravehicular Activity (EVA).
- **3rd option**: the astronaut uses a self-rescue propulsive system

The first option can be considered "unrealistic" in multiple different situations, since it requires extremely quick reflexes and near-optimal response by the endangered astronaut. The second option can also be characterized as "unrealistic": the reaction time of the rescuer to rendezvous with the "floating" crew member is the most critical factor, in addition to the constant availability of both the rescuer crew member monitoring the EVA and the MMU that shall be used. More specifically, even if it takes 10 minutes for the rescuer to reach and activate the MMU, the rendezvous with the endangered astronaut shall occur thousands of feet away from the orbiter [67]. That leads to the third option as the most appropriate in the case of an untethered crew member during an EVA and therefore, space agencies work in the direction of implementing and upgrading the Simplified Aid for EVA Rescue (SAFER) propulsion unit [59].

Another factor of great importance for the self-rescue of the EVA crew member, is the amount of light surrounding the astronaut. Depending on the position in which the Extravehicular Activity is being performed, the visual clues available to the astronaut vary· for example, during a dark night pass, the separated crew member cannot see anything but the lights of the space station. In this case, the activation of the SAFER Automatic Attitude Hold (AAH) is necessary to stabilize the applied rotation [14].

As stated before, there are different cases in which an EVA astronaut can become untethered from the station. One of them is during an Extravehicular Activity for the inspection of the thermal protection system and surfaces of the orbiter. The main hazard for the usage of SAFER in such an activity, lies in the moment the crew member reaches its hand to evaluate and measure the damage in the external of the orbiter, and is pushed back and away from the orbiter, if the force applied is strong enough. Although researchers in the Virtual Reality (VR) Laboratory at the Johnson Space Center have managed to simulate different parameters such as the propellant consumption, the orbital dynamics and the flight control, a scenario like

the one mentioned before might differentiate the propellant consumed in order to maintain the control of the flight. That is the reason why different techniques and improvements were implemented not only during the astronaut training, but also in the SAFER propulsion module [60].

4. Results & Discussion

4.1. Performance Analysis

In this chapter, the results of the performance analysis of the Simplified Aid for Extravehicular Activity Rescue (SAFER) propulsion unit will be presented, based on the equations obtained from the fundamentals of the Cold Gas Propulsion Systems (CGPS). The computational package that will be utilized for this analysis will be Matlab R2018a, while the code implemented shall be presented in the "Annex" section, at the end of this thesis.

Initially, the input data characterizing the problem shall be presented. Then, after solving all the necessary equations, as presented in the section "3.1. Introduction to the Cold Gas Propulsion Systems", the propellant mass flow rate of the SAFER propulsion unit will be calculated, which shall yield the calculation of a number of basic space propulsion concepts, like the specific impulse and the thrust produced by the unit's thrusters.

Having calculated these parameters, a verification between the calculated values and the values obtained by the bibliography shall be performed, to obtain the percentage difference. The performance analysis shall verify that all the calculations performed in the computational package of Matlab coincide with the reference values of the propulsion unit, as well as with the reference values obtained by the presented theory of the Cold Gas Propulsion Systems.

4.1.1. Input Data

The input data used for the implementation of the performance analysis of the Simplified Aid for Extravehicular Activity Rescue (SAFER) propulsion unit can be categorized in three categories:

1. Propellant gas and environmental characteristics
2. Thruster and propellant characteristics
3. System masses characteristics

The input data can be seen in the following table, as extracted by the presented theory of this thesis, in addition to supplementary bibliographical references, used for the determination of a number of parameters:

Parameter	Value	Unit	Parameter description	Reference
Propellant gas and environmental characteristics				
P_a	0	Pa	Ambient pressure	[42]
g_0	9.80665	ms^{-2}	Gravitational acceleration	Sec. 3.1.1.2.
R	8.3145	$JK^{-1}mol^{-1}$	Ideal gas constant	Sec. 2.2.2.3.
MWN_2	0.028014	$kgmol^{-1}$	Molecular weight of gaseous nitrogen	Sec. 3.1.2.3.
RN_2	R/MWN_2	$JK^{-1}kg^{-1}$	Individual gas constant of nitrogen	Sec. 3.1.2.3.
gamma (γ)	1.40	-	Specific heat ratio of nitrogen	Sec. 3.1.2.3.
$viscN_2$	$15.95 \cdot 10^6$	sPa	Dynamic viscosity of nitrogen	[68]
Thruster and propellant characteristics				
A_{ratio}	100	-	Exit area to throat area ratio	[69]
T_c	311	K	Chamber temperature (26.85°C)	[69]
P_c	1482372	Pa	Chamber pressure = Regulator pressure	Sec. 3.2.1.2.
dv_{min}	3.05	ms^{-1}	Minimum velocity change (ground process.)	Sec. 2.1.2.3.
m_p	5.6	kg	Total propellant mass (4 tanks x 1.4 kg each)	Sec. 2.1.2.3.
lamda (λ)	0.95	-	Bell nozzle coefficient	Sec. 3.1.1.1.
F_{act}	4.448	N	Thrust produced per nozzle	Sec. 3.2.1.2.
System masses characteristics				
m_{astro}	70	kg	Mass of the EVA crew member	-
m_{emu}	124.6	kg	Mass of the EMU space suit (SAFER incl.)	Sec. 2.1.1.1.
m_i	$m_{astro} + m_{emu}$	kg	Initial mass of the system	-
m_f	$m_i - m_p$	kg	Final mass of the system	-

(Table 4.1.: Input data of the SAFER propulsion unit)

4.1.2. Performance calculations

The performance analysis of the SAFER propulsion unit shall be made on the assumption that the gases involved during the activation of the thrusters behave ideally. It is also assumed that the 4 propellant storage tanks comprising the SAFER unit, are connected to the Cold Gas Propulsion System (CGPS) through one tube, thus the tanks providing the propellant to the thrusters behave as one. The schematic of

the propulsion subsystem, as seen in (Fig. 3.9.), characteristically depicts the GN_2 tank as part of the subsystem. The equations are developed in the code "*Thesis1.m*", which is presented in the "Annex".

4.1.2.1. Thruster performance characteristics

The first step for the performance analysis of the nitrogen-jet thrusters of the SAFER propulsion unit, was the calculation of the Mach number at the exit of the nozzles. The function "*mbar_from_Mach.m*", as presented in the "Annex" of this thesis, was developed for the calculation of the M_e (Mach number at the exit of the nozzles), which will be a fundamental parameter for this analysis.

Then, regarding the characteristics of the thrusters' performance, the following set of equations was utilized:

(vacuum thrust coefficient) $$C_F = \left(\frac{2}{\gamma+1}\right)^{\frac{\gamma+1}{2(\gamma-1)}} \frac{\gamma M_e + 1/M_e}{\sqrt{1+\frac{\gamma-1}{2}M_e^2}} \quad \text{(Eq. 4.1.)}$$

(characteristic velocity) $$c^* = \frac{\sqrt{RN_2T_c}}{\bar{m}(M_t=1,\gamma)} \quad \text{(Eq. 4.2.)}$$

(pressure at the exit of the nozzle) $$P_e = P_c\left[1+\frac{\gamma-1}{2}M_e^2\right]^{-\frac{\gamma}{\gamma-1}} \quad \text{(Eq. 4.3.)}$$

(exhaust velocity) $$v_e = \sqrt{\frac{2\gamma RN_2T_c}{\gamma-1}\left(1-\left(\frac{P_e}{P_c}\right)^{\frac{\gamma-1}{\gamma}}\right)} \quad \text{(Eq. 4.4.)}$$

(specific impulse) $$I_{sp} = \frac{c^*C_F}{g_0} \quad \text{(Eq. 4.5.)}$$

(effective exhaust velocity) $$c = I_{sp}g_0 \quad \text{(Eq. 4.6.)}$$

(Tsiolkovsky equation, total velocity change) $$dv_{tsiol} = c\ln\left(\frac{m_i}{m_f}\right) \quad \text{(Eq. 4.7.)}$$

(theoretical thrust with nozzle coefficient) $$F_{theor} = \frac{F_{act}}{lamda} \quad \text{(Eq. 4.8.)}$$

4.1.2.2. Nozzle throat characteristics

In order to calculate the propellant mass flow rate ($\dot{m}$), a method as suggested in [70] shall be implemented. This method calculates the pressure, temperature, density of the propellant gaseous nitrogen and the velocity at the throat of the nozzle and then approaches the calculation of the propellant mass flow rate, through the iteration method of "Trial and Error" for the parameters of the diameter and the cross-sectional area of the throat, in addition to the calculation of the discharge coefficient (c_d).

First, the following set of equations shall be solved:

(throat pressure) $$P_{thr} = P_c \left(\frac{2}{\gamma+1}\right)^{\frac{\gamma}{\gamma-1}}$$ (Eq. 4.9.)

(throat temperature) $$T_{thr} = 2\frac{T_c}{(1+\gamma)}$$ (Eq. 4.10)

(gaseous nitrogen throat density) $$rho_{thr} = \frac{P_{thr}}{RN_2 T_{thr}}$$ (Eq. 4.11.)

(throat velocity) $$v_{thr} = \sqrt{\gamma RN_2 T_{thr}}$$ (Eq. 4.12.)

The system is matched iteratively to establish the mass flow rate, hence determining the performance of all system components. The iteration method of "Trial and Error" is implemented, starting from a discharge coefficient of $c_d = 1$, performing 4 iterations. The set of equations solved in the iteration method is the following:

(propellant mass flow) $$\dot{m} = \frac{F_{theor}}{c_d c}$$ (Eq. 4.13.)

(throat cross-sectional area) $$A_{thr} = \frac{\dot{m}}{v_{thr} rho_{thr}}$$ (Eq. 4.14.)

(throat diameter) $$D_{thr} = 2\sqrt{\frac{A_{thr}}{\pi}}$$ (Eq. 4.15.)

(Reynolds number at throat) $$Re_{thr} = \frac{rho_{thr} v_{thr} D_{thr}}{visc_{N2}}$$ (Eq. 4.16.)

(discharge coefficient) $$c_d = 0.8825 + 0.0079 \log(Re_{thr})$$ (Eq. 4.17.)

4.1.2.3. Propellant tanks

The calculation of the propellant mass flow rate ($\dot{m}$) is crucial for the implementation of the performance analysis of a propulsion unit. Now, the propellant tank's characteristics can be calculated:

(total time to empty the propellant tanks) $$dt = \frac{m_p}{\dot{m}}$$ (Eq. 4.18.)

(total propellant tank volume) $$V_p = \frac{m_p R N_2 T_c}{P_c}$$ (Eq. 4.19)

4.1.2.4. Nozzle dimensioning and geometry

Now that the dimensions of the throat have been defined, using the iteration method of "Trial and Error", the dimensions of the exit of the nozzle can be calculated, for an assumed exit to throat area ratio of $A_{ratio} = 100$. The equations that shall be solved are the following:

(exit cross-sectional area) $$A_e = A_{thr} A_{ratio}$$ (Eq. 4.20.)

(exit diameter) $$D_e = 2\sqrt{\frac{A_e}{\pi}}$$ (Eq. 4.21.)

4.1.3. Performance analysis results

The solution of the equations presented above using the computational package of Matlab R2018a, yields the results, as seen in the following table:

Parameter	**Value**	**Unit**	**Parameter description**
Thruster performance			
M_e	6.9363	-	Mach number at the exit of the nozzle
C_F	1.7948	-	Vacuum thrust coefficient
c^*	443.7010	ms^{-1}	Characteristic velocity
P_e	379.4673	Pa	Pressure at the exit of the nozzle
v_e	765.0506	ms^{-1}	Exhaust velocity
I_{sp}	79.1717	s	Specific impulse
c	776.4087	ms^{-1}	Effective exhaust velocity

dv_{tsiol}	22.6705	ms^{-1}	Tsiolkovsky equation, total velocity change
F_{theor}	4.6821	N	Theoretical thrust produced (λ included)
m_i	194.6	kg	Initial mass of the system
Nozzle throat			
P_{thr}	783110	Pa	Pressure at the throat of the nozzle
T_{thr}	259.1667	K	Temperature at the throat of the nozzle
rho_{thr}	10.1808	kgm^{-3}	Gaseous nitrogen throat density
v_{thr}	328.1588	ms^{-1}	Throat velocity
A_{thr}	$1.8369 \cdot 10^{-6}$	m^2	Throat cross-sectional area
d_{thr}	0.0015	m	Throat diameter
Re_{thr}	320330	-	Reynolds number at the throat of the nozzle
c_d	0.9826	-	Discharge coefficient
$\dot{m}$	0.0061	kgs^{-1}	Propellant mass flow rate
Propellant tanks			
dt	912.5061	s	Total time to empty the propellant tanks
V_p	0.3487	m^3	Total propellant tank volume
Nozzle dimensioning and geometry			
A_e	$1.8369 \cdot 10^{-4}$	m^2	Exit cross-sectional area
d_e	0.0153	m	Exit diameter
Calculated thrust			
F_{calc}	4.448	N	Thrust calculated

(Table 4.2.: Performance analysis results)

The thrust (Fcalc) was calculated based on the equation:

(thrust) $$F_{calc} = \lambda c_d(\dot{m}v_e + (P_e - P_a)A_e)$$ (Eq. 4.22.)

4.1.4. Performance analysis discussion

Based on the results produced, it appears that they coincide with the theory presented for the Cold Gas Propulsion Systems (CGPS) and the characteristics of the Simplified Aid for Extravehicular Activity Rescue (SAFER) propulsion unit. More specifically:

- The Mach number at the exit of the nozzle was found to be $M_e = 6.9363$, which is a rather logical value is for a Mach number at the exit of a "Converging-Diverging" CD or "de Laval" nozzle, utilized in a Cold Gas Propulsion System (CGPS).
- The characteristic velocity, exhaust velocity and effective exhaust velocity were calculated as $c^* = 443.7010$ (ms^{-1}), $v_e = 765.0506$ (ms^{-1}) and $c = 776.4087$ (ms^{-1}) respectively. These values are also normal for a Cold Gas Propulsion System (CGPS) consuming gaseous nitrogen as propellant.
- Specific impulse was found to be $I_{sp} = 79.1717$ (s). As it was presented before in (Table 3.1.), the typical values of the specific impulse for a Cold Gas Propulsion System (CGPS) have been determined to range from 30-110 (s). Characteristically, as shown in (Table 3.2.), a typical value for a CGPS using gaseous nitrogen has been calculated to be 80 (s). The percentage difference of the theoretical and calculated value of the specific impulse is set to be 1.0354%, which is acceptable.
- The total velocity change provided by the thrusters of the SAFER propulsion unit, was calculated using the Tsiolkovsky equation as $dv_{tsiol} = 22.6705$ (ms^{-1}). In (Section 2.1.2.3.), it was stated that the minimum total velocity change that SAFER unit can provide during ground processing is $dv_{min} = 3.05$ (ms^{-1}). Thus, the result is acceptable.
- Based on the calculations of the nozzle's throat, the propellant mass flow rate was determined as $\dot{m} = 0.0061$ (kgs^{-1}) or 6.1 (gs^{-1}). This value is adequate for a Cold Gas Propulsion System (CGPS) producing that small amount of thrust.
- Finally, the thrust calculated using (Eq. 4.22.) coincides with the thrust presented in (Section 3.2.1.2.), regarding the thrusters of the SAFER propulsion unit. The difference between the two values was evaluated at 0.00000018523%, and is most probably due to the accuracy of the computational package. This value produced highlights the integrity of the results and verifies the accuracy of the code developed during this thesis.

4.2. Orbital Dynamics and Astronaut Repositioning

In this section, the orbital dynamics applying to the Extravehicular Activity (EVA) crew member floating in space and performing a self-rescue maneuver will be examined. The calculation of the thrust produced was a major parameter for the determination of this maneuver, since the activation of the Simplified Aid for Extravehicular Activity Rescue (SAFER) propulsion unit, offers this exact capability to the crew member.

Before proceeding to the orbital dynamics analysis and the determination of the mission's optimal parameters, two assumptions shall be made. Firstly, it is assumed that the position of the EVA crew member corresponds to a circular orbit and a motion on the equatorial plane. Then, it is also assumed that the orbiter (ISS, etc.) performs the exact same circular orbit as the EVA crew member, during the activity taking place outside of it.

Initially, the input data for the implementation of the orbital dynamics analysis shall be presented and inserted to the corresponding code, as found in the "Annex" of this thesis. Consequently, the Clohessy-Wiltshire equations describing the relative motion of a body towards one another shall be introduced and resolved, both with a numerical and analytical approach. Taking into account the thrust produced during the activation of the SAFER propulsion unit, a simple case study of the return of the astronaut to the orbiter will be presented.

4.2.1. Input Data

The input data used for the implementation of the orbital dynamics analysis of the Simplified Aid for Extravehicular Activity Rescue (SAFER) propulsion unit can be categorized in two categories:

1. Orbital parameters
2. Performance analysis input data

The input data can be seen in the following table, as obtained from the performance analysis of the SAFER propulsion unit, in addition to supplementary bibliographical references:

Parameter	Value	Unit	Parameter description	Reference
Orbital parameters				
RT	6371000	m	Radius of Earth	[72]
h	400000	m	Altitude of the International Space Station (ISS)	-
r	RT+h	m	Distance of ISS from Earth's center of mass	-
mu	$3.986 \cdot 10^{14}$	m^3s^{-2}	Earth's standard gravitational parameter	[72]
g_0	9.80665	ms^{-2}	Gravitational acceleration	Sec. 3.1.1.2.
Performance analysis input data				
m_0	194.6	kg	Initial mass of the system (m_i)	Sec. 4.1.3.
I_{sp}	79.1717	s	Specific impulse	Sec. 4.1.3.
Thr	4.448	N	Thrust produced from SAFER activation (F_{calc})	Sec. 4.1.3.
dt	912.5061	s	Total time to empty the propellant tanks	Sec. 4.1.3.

(Table 4.3.: Input data for the orbital dynamics analysis)

4.2.2. Orbital dynamics calculations

One of the most challenging aspects one has to encounter when analyzing the orbital dynamics and on-orbit proximity operations, is the relativity of the motions. As stated above, the scope of the SAFER propulsion unit is the performance of a rendezvous maneuver that will rescue the untethered EVA crew member. During a rendezvous maneuver, the two free-falling orbiting vehicles (in this case the spacecraft and the EVA astronaut) observe each other's movements in a non-inertial frame of reference. Thus, in order to comprehend the relative velocity and acceleration of the bodies, the transformation of these parameters into an inertial frame is required. In any other case, the true thrust produced by the two vehicles cannot be distinguished from the fictitious "inertial forces" [71]

A rendezvous maneuver "consists" of two vehicles, a passive, non-maneuvering which in this case is the orbiter and an active vehicle that performs the necessary maneuvers to approach the orbiter, which in this case, is the untethered EVA crew member. Probably the most important parameter to take into consideration in this analysis, is the angular rate (ω, omega), which is described by Hill's equations.

The initialization calculations for the implementation of the orbital dynamics analysis as developed in the code "*a_repositioning_main.m*" presented in the "Annex", can be seen below:

(circular velocity) $$V_{sc} = \sqrt{mur}$$ (Eq. 4.23.)

(angular rate) $$\omega = V_{sc}/r$$ (Eq. 4.24.)

(propellant mass flow) $$\dot{m} = \frac{Thr}{Ispg_0}$$ (Eq. 4.25.)

Using a Local Vertical/Local Horizontal coordinate system, Hill's equations are obtained as [59]:

$$\ddot{x} = 2\omega\dot{z}$$ (Eq. 4.26.)

$$\ddot{y} = -\omega^2 y$$ (Eq. 4.27.)

$$\ddot{z} = 3\omega z^2 - 2\omega\dot{x}$$ (Eq. 4.28.)

where the x-axis has the same direction with the velocity vector ($\vec{v}$) of the reference body, the y-axis is along the orbit normal and the z-axis is along the negative local vertical ($\vec{r}$). The closed-form solutions of the equations presented are known as Clohessy-Wiltshire (CW) equations. Clohessy-Wiltshire equations constitute the core of the preliminary studies of the self-rescue problem and are used to straightforward determine the motion of the body given its initial velocity [59]:

$$x(t) = [-2\dot{z_0}\cos(\omega t) + (4\dot{x_0} - 6\omega z_0)\sin(\omega t) - (3\dot{x_0} - 6\omega z_0)\omega t + (2\dot{z_0} + \omega x_0)]/\omega$$ (Eq. 4.29.)

$$y(t) = [\omega y_0\cos(\omega t) + \dot{y_0}\sin(\omega t)]/\omega$$ (Eq. 4.30.)

$$z(t) = [(2\dot{x_0} - 3\omega z_0)\cos(\omega t) + \dot{z_0}\sin(\omega t) - (2\dot{x_0} - 4\omega z_0)]/\omega$$ (Eq. 4.31.)

where $[x_0, y_0, z_0]$ is the initial relative position of the body and $[\dot{x_0}, \dot{y_0}, \dot{z_0}]$ its initial relative velocity. By differentiating the above-mentioned equations, the closed-form equations which describe the velocity of the body can be obtained. It can be seen that during the operation of the SAFER propulsion unit, the physical vectors like the angular velocity and the acceleration change continuously with respect to the time [65].

It should be noted that a safety factor of 0.20 will be used as "maneuvering time", which yields the 1/5 of the total time to empty the propellant tanks ($dt = 912.5061$ (s)). Thus, it is assumed that the thruster has the capability of being activated for almost the 1/5 of the total time required to empty the propellant tanks. That time has been calculated to be 183 (s), but the value of 180 (s) will be eventually used.

4.2.2.1. Numerical solution

The function "*Fsyst.m*", as presented in the "Annex" of this thesis, was developed for the numerical resolution of the Clohessy-Wiltshire (CW) equations.

By inserting a value of $Thr = 4.448$ (N) the activation of the SAFER's nitrogen-jet thrusters can be taken into account, while by inserting a value of $Thr = 0$ (N), the orbital dynamics of the free-floating body of the EVA crew member can be presented.

The function "*Fsyst.m*" will now be implemented, for the following set of initial conditions:

Parameter	**Value**	**Unit**	**Parameter description**
x_0	30	m	Initial relative position in x-axis
y_0	30	m	Initial relative position in y-axis
z_0	30	m	Initial relative position in z-axis
$\dot{x_0}$	0.762	ms^{-1}	Initial relative velocity in x-axis $\dot{x_0} = v_x$
$\dot{y_0}$	0.762	ms^{-1}	Initial relative velocity in y-axis $\dot{y_0} = v_y$
$\dot{z_0}$	0.762	ms^{-1}	Initial relative velocity in z-axis $\dot{z_0} = v_z$

(Table 4.4.: Initial conditions of numerical solution)

It should be noted that the initial relative velocity $[\dot{x_0}, \dot{y_0}, \dot{z_0}]$ = [0.762, 0.762, 0.762] (ms^{-1}) was obtained from the information regarding the separation speed of the astronaut from the orbiter, as presented in "Section 3.2.3.1.".

The numerical resolution of the Clohessy-Wiltshire for a duration of 180 (s) and without taking into account the thrust produced, yields the following 3-D plot of the free floating astronaut:

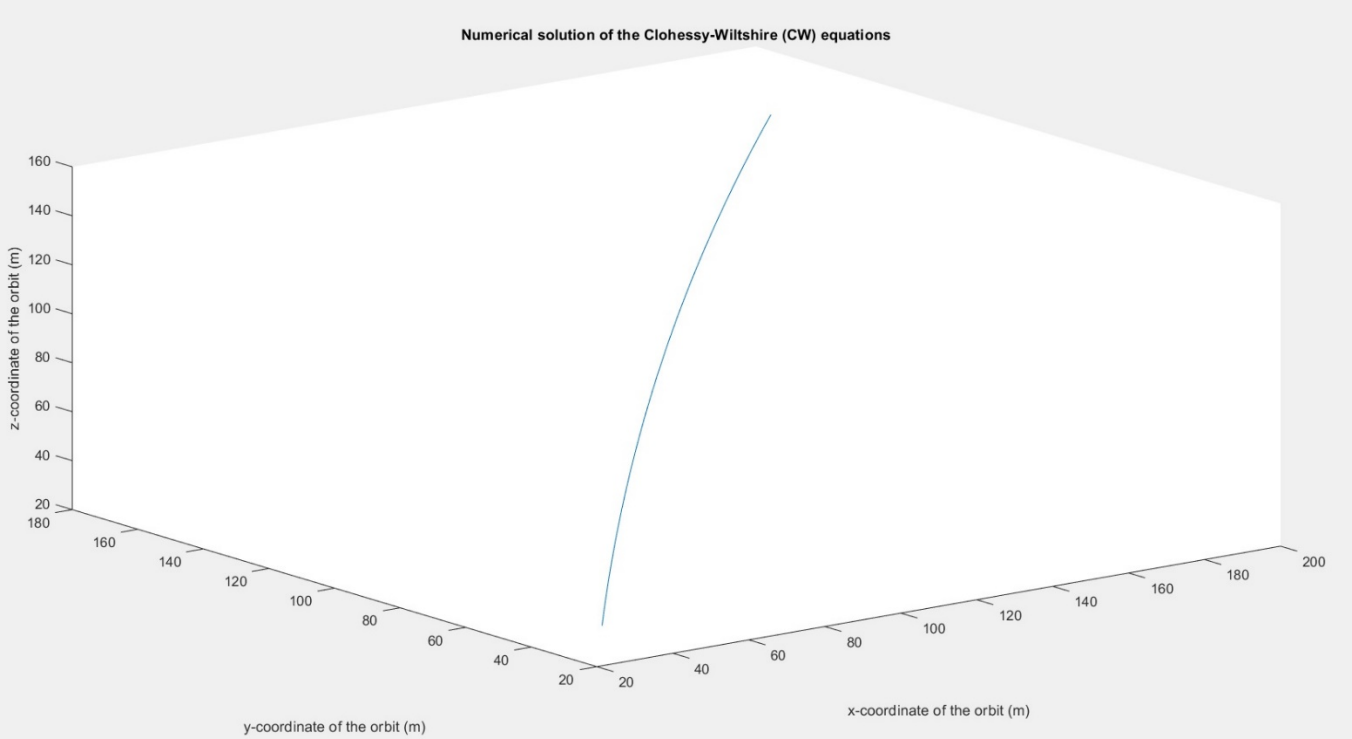

(Fig. 4.1.: Numerical solution of the Clohessy-Wiltshire (CW) equations)

As described above, the Clohessy-Wiltshire equations straightforwardly determine the motion of a body (EVA crew member) relative to another body (ISS, etc.). Thus, and since it is assumed that the astronaut becomes untethered 30 meters away in both 3 axes from the ISS ($[x_0, y_0, z_0]$ = [30m, 30m, 30m]), the origin of the 3D plot is the orbiter.

4.2.2.2. Analytical solution

Now, the analytical solution of the Clohessy-Wiltshire (CW) equations shall be performed. The analytical solution is implemented inside the body of the "*a_repositioning_main.m*" code, and is an iteration process from $t = 1$ (s) to $t = 180$ (s). The analytical solution will use the following set of initial conditions, same as the numerical solution:

Parameter	**Value**	**Unit**	**Parameter description**
x_0	30	m	Initial relative position in x-axis
y_0	30	m	Initial relative position in y-axis
z_0	30	m	Initial relative position in z-axis

$\dot{x}_0$	0.762	ms^{-1}	Initial relative velocity in x-axis $\dot{x}_0 = v_x$
$\dot{y}_0$	0.762	ms^{-1}	Initial relative velocity in y-axis $\dot{y}_0 = v_y$
$\dot{z}_0$	0.762	ms^{-1}	Initial relative velocity in z-axis $\dot{z}_0 = v_z$

(Table 4.5.: Initial conditions of analytical solution)

Again, in this case the thrust produced will not be taken into account and thus, the following plot describes the motion of the free floating body of the EVA crew member:

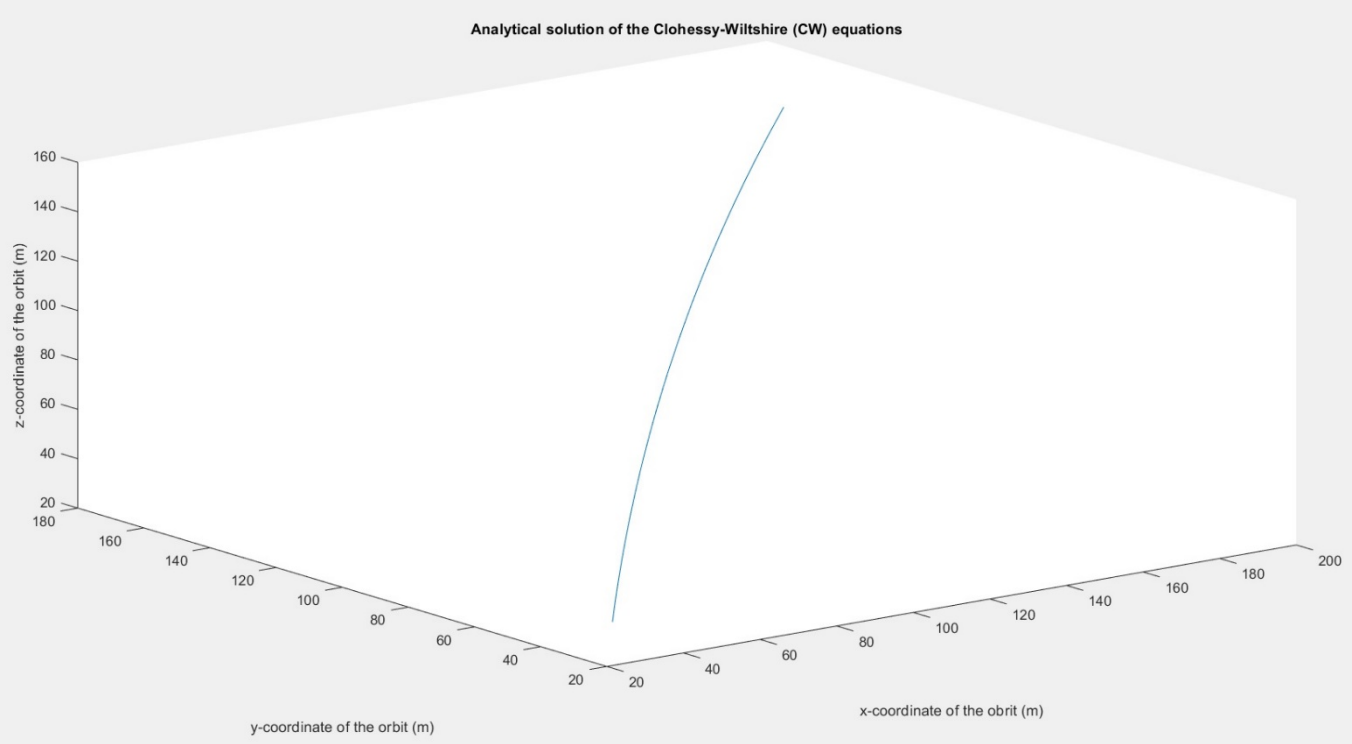

(Fig. 4.2.: Analytical solution of the Clohessy-Wiltshire (CW) equations)

Again, it is assumed that the astronaut becomes untethered 30 meters away in both 3 axes from the ISS ($[x_0, y_0, z_0]$ = [30m, 30m, 30m]), the origin of the 3D plot is the orbiter.

4.2.2.3. Verification of the two solutions

In order to verify that the two plots extracted are correct, a verification of the two solutions shall be performed. The numerical and analytical solution of the Clohessy-Wiltshire equations should coincide, to assure that the results are accurate. In the following figure, the two solutions of the straightforward motion of the free floating EVA crew member, relative to the orbiter (ISS, etc.) can be seen:

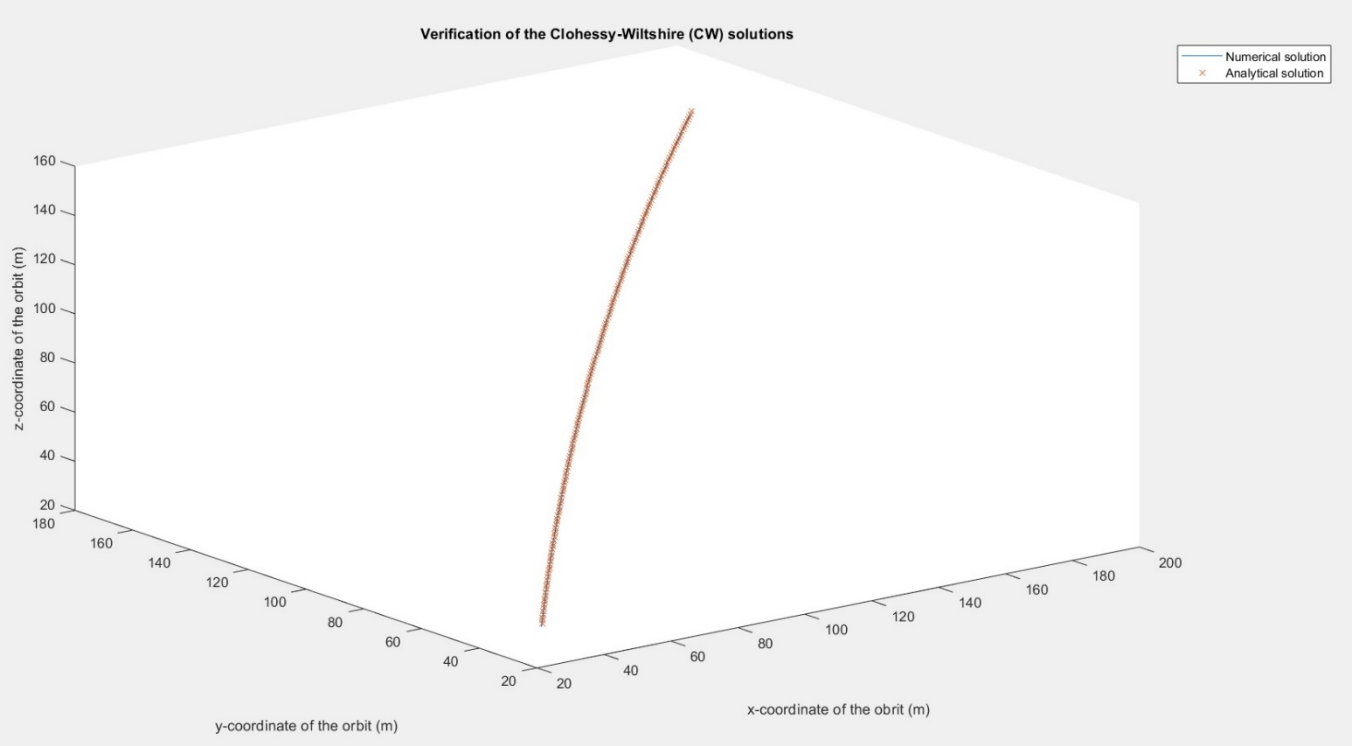

(Fig. 4.3.: Verification of the two Clohessy-Wiltshire (CW) solutions)

As it can be seen from the figure presented above, the two solutions of the Clohessy-Wiltshire (CW) equations coincide. Without diving into more case studies regarding the initial relative position and velocity of the free floating EVA crew member, it should be noted that the two solutions coincide for any set of initial conditions, no matter how far from the orbiter the motion of the body begins, or what the initial relative velocity of the astronaut is, when he/she becomes untethered.

4.2.3. Self-rescue maneuver

Now, by inserting a value of $Thr = 4.448$ (N) the activation of the SAFER's nitrogen-jet thrusters can be taken into account. Again, the Clohessy-Wiltshire equations will be numerically resolved, considering the relative motion (of the EVA crew member) with respect to the spacecraft, assuming this last has an exact circular motion. The reference frame that will be used will rotate according to the angular velocity of the spacecraft, so that the z-axis always points towards the center of the Earth, and also the gradient of the inertial centrifugal force on the astronaut is accounted for.

Since thrust is taken into consideration in this case study, the first thing function "*Fsyst.m*" calculates is the final mass of the system (astronaut/EMU/SAFER) at any given moment, by reducing the amount of propellant consumed at each second from the initial mass of the system:

$$m = m_0 - \dot{m}t \qquad \text{(Eq. 4.32.)}$$

Two correction factors will be inserted in the orbital dynamics analysis, for the determination of the self-rescue maneuver and the return (indicated by the negative signs) of the astronaut to the spacecraft:

- u1: proportional to the position vector $\vec{\mathbf{r}} = [x, y, z]$ of the astronaut with respect to the spacecraft, which is the origin of coordinates, with a negative sign.
- u2: proportional to the relative velocity vector $\vec{\mathbf{v}} = [\dot{x}, \dot{y}, \dot{z}]$, with respect to the spacecraft, with a negative sign.

In addition, to coefficients (k_1 and k_2) were introduced and adjusted, in order to give a smooth return of the EVA crew member to the spacecraft in 180 seconds, given an initial relative position to the orbiter of $[x_0, y_0, z_0] = [30\text{m}, 30\text{m}, 30\text{m}]$.

The two coefficients (k_1 and k_2) were calculated based on the method of "Trial and Error", where for each set of values, the distance of the astronaut from the orbiter was observed and adjusted, to approach the orbiter as close as possible. The values used for the two coefficients were determined as $[k_1, k_2] = [0.1, 2]$.

The maneuver performed by the astronaut, in order to return from a relative position of $[x_0, y_0, z_0] = [30\text{m}, 30\text{m}, 30\text{m}]$ back to the orbiter, can be seen in the following figure:

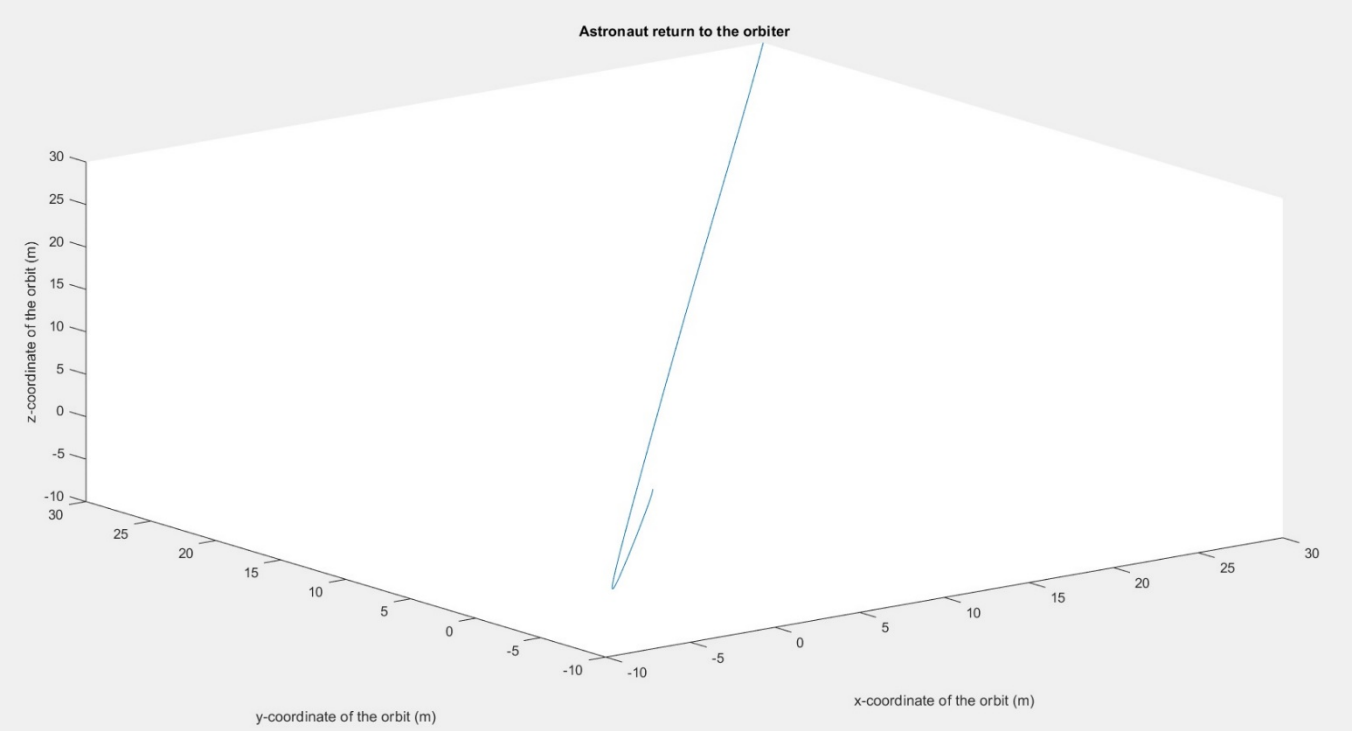

(Fig. 4.4.: Astronaut return back to the orbiter)

As obtained from the extracted results, the astronaut eventually approaches the orbiter in a relative position of $[x, y, z] = [1.244\text{m}, 1.0405\text{m}, 0.8094\text{m}]$ and with a relative velocity of $[\dot{x}, \dot{y}, \dot{z}] = [-0.0056, -0.004, 0.0049]$ (ms^{-1}). Thus, the return of the astronaut in the orbiter, activating the nitrogen-jet thrusters of the SAFER propulsion unit can be implemented.

The goal of this orbital dynamics analysis is not the optimization of the control law for the return of the EVA crew member that performs the self-rescue maneuver, but to show that the performance of this maneuver is actually feasible.

5. Conclusions

5.1. Summary

The conclusions of this thesis can be summed up in two main categories: the performance analysis of the Simplified Aid for Extravehicular Activity Rescue (SAFER) propulsion unit and the orbital dynamics analysis of the free floating EVA crew member and whether or not, a safe return to the orbiter is feasible.

Initially, the performance analysis implemented on the propulsion unit indicated that the results produced verified the characteristics of the unit available in bibliographical references. The SAFER propulsion unit, utilizing nitrogen-jet thrusters was studied based on the fundamentals of the Cold Gas Propulsion Systems, yielding a produced specific impulse 1.0354% lower than the corresponding reference value for nitrogen Cold Gas Propulsion Systems. In addition, the calculated thrust was found to be 0.00000018523% different than the corresponding reference value for the thrust produced, difference which may appear due to the accuracy of the computational package. Thus, the performance analysis can be characterized as successful and accurate, since the results match the reference values obtained by the available bibliography.

Then, regarding the orbital dynamics analysis, two case studies were examined: the motion of the free floating EVA crew member, without taking into account the activation of the nitrogen-jet thrusters of the SAFER propulsion unit, and the return of the crew member to the spacecraft, through the activation of the thrusters. The straightforward determination of the motion of the untethered EVA crew member was approached in both a numerical and analytical solution of the Clohessy-Wiltshire (CW) equations, yielding the same results, fact that verifies the accuracy of the two solutions. Finally, in order to present the feasibility of a self-rescue maneuver and the return of the astronaut back to the orbiter, the thrust was taking into account in the Clohessy-Wiltshire equations, changing the acceleration terms of the Hill's equations and verifying that a return to the spacecraft is indeed possible.

5.2. Recommendations for Future Work

The goal of this project were to present the performance analysis of the SAFER nitrogen-jet thrusters and to analyze the fundamentals of the orbital dynamics applied on an EVA crew member during the space activity in the vacuum of space. However, there is a number of recommendations for future projects to deal with, in order to acquire a wider perspective of the SAFER propulsion unit utilized for the performance of self-rescue maneuver.

Initially, a Computational Fluid Dynamics (CFD) analysis can be implemented on the nozzles of the nitrogen-jet thrusters, in order to fully understand the fluid dynamics of the thrusters. Also, a thermodynamics analysis of the thrusters could be performed, taking into account the characteristics of the gaseous nitrogen propellant and the geometric characteristics of the thrusters. The lack of available bibliography regarding these two aspects was observed during the implementation of this thesis and thus these recommendations are strongly suggested.

Then, in addition to the Simplified Aid for Extravehicular Activity Rescue (SAFER) propulsion unit, the performance, orbital dynamics, computational fluid dynamics and thermodynamics analyses could also be implemented regarding the Manned Maneuvering Unit (MMU), also utilized during Extravehicular Activities (EVAs), but not to perform self-rescue maneuvers. The information available regarding the MMU is greater, and thus a wider analysis on the function and performance of the propulsion unit would produce rather interesting results.

Since this analysis does not take into account the dynamics of the Extravehicular Mobility Unit (EMU) space suit, but studies the mass system (astronaut/EMU/SAFER) as a rigid body, the orbital dynamics applied on the astronaut would be more complicated. During the implementation of this thesis very limited bibliographical references were found regarding the dynamics of the Extravehicular Mobility Unit, with one characteristically found on [73].

Finally, there are multiple case scenarios regarding the performance of a self-rescue maneuver. For example, by taking into account the pitch, yaw and roll rates of the EVA crew member, the separation rate and the drift times, a more detailed analysis on the orbital dynamics of the free floating body of the astronaut can be implemented. An introduction to different case studies regarding the self-rescue maneuvers can be found in the bibliographic reference [59].

Bibliography

[1] Vogt, G. L. (1998). Suited for Spacewalking: A Teacher's Guide with Activities for Technology Education, Mathematics, and Science, pp 19.

[2] Clark, P. E. (2010). Revolution in field science: Apollo approach to inaccessible surface exploration. Earth, Moon, and Planets, 106(2-4), 133-157.

[3] Brady, A. L., Kobs Nawotniak, S. E., Hughes, S. S., Payler, S. J., Stevens, A. H., Cockell, C. S., ... & Lim, D. S. (2019). Strategic planning insights for future science-driven extravehicular activity on Mars. Astrobiology, 19(3), 347-368.

[4] Lutz, C. C., Stutesman, H. L., Carson, M. A., & Mcbarron, J. W. (1975). Apollo experience report: Development of the extravehicular mobility unit.

[5] What Is the International Space Station? NASA. (2020). Retrieved 2 March 2021, from: https://www.nasa.gov/audience/forstudents/5-8/features/nasa-knows/what-is-the-iss-58.html.

[6] Extravehicular Mobility Unit. Nasa.gov. (2012). Retrieved 4 March 2021, from: https://www.nasa.gov/centers/johnson/pdf/728896main_Extravehicular%20Mobility%20Unit%20Fact%20Sheet.pdf.

[7] Rose, D. (1998). International space station familiarization. In User Manual for International Space Station ISS FAM C 21109, pp 11-3, 11-6.

[8] Abramov, I. P., Glazov, G. M., & Svertshek, V. I. (2002). Long-term operation of "Orlan" space suits in the "Mir" orbiting station: Experience obtained and its application. Acta astronautica, 51(1-9), 133-143.

[9] Machell, R. M. (Ed.). (1967). Summary of Gemini extravehicular activity (Vol. 149). Scientific and Technical Information Division, Office of Technology Utilization, National Aeronautics and Space Administration.

[10] Maneuvering Unit, Hand-Held, White, Gemini 4 | National Air and Space Museum. Airandspace.si.edu. Retrieved 7 March 2021, from: https://airandspace.si.edu/collection-objects/maneuvering-unit-hand-held-white-gemini-4/nasm_A19670211000.

[11] Bonhams: GEMINI ASTRONAUT MANEUVERING UNIT (AMU) MODEL.. Bonhams.com. Retrieved 4 March 2021, from: https://www.bonhams.com/auctions/17778/lot/1084/?category=list.

[12] Lenda, J. A. (1978). Manned maneuvering unit: User's guide.

[13] Becker, J. Spaceflight mission report: STS-64. Spacefacts.de. Retrieved 9 March 2021, from: http://www.spacefacts.de/mission/english/sts-64.htm.

[14] Meade, C. J. (1995, September). First Flight Test Results of the Simplified Aid for EVA Rescue (SAFER) Propulsion Unit. In Symposium Proceedings-Society of Experimental Test Pilots (pp. 315-336). THE SOCIETY OF EXPERIMENTAL TEST PILOTS.

[15] Dutton, J. (1997). Extravehicular activity hardware for international space station. Journal of Aerospace Engineering, 10(2), 91-93.

[16] This Month in NASA History: Astronauts Make First Untethered Spacewalk | APPEL Knowledge Services. Appel.nasa.gov. (2020). Retrieved 8 March 2021, from: https://appel.nasa.gov/2020/02/06/this-month-in-nasa-history-astronauts-make-first-untethered-spacewalk.

[17] STS-64. Science.ksc.nasa.gov. Retrieved 9 March 2021, from: https://science.ksc.nasa.gov/shuttle/missions/sts-64/mission-sts-64.html.

[18] Plaque, Astronaut Wings. National Air and Space Museum. Retrieved 15 March 2021, from: https://airandspace.si.edu/collection-objects/plaque-astronaut-wings/nasm_A19760084000

[19] Earth's Atmosphere | UCAR Center for Science Education. Scied.ucar.edu. (2015). Retrieved 15 March 2021, from: https://scied.ucar.edu/learning-zone/atmosphere/earths-atmosphere

[20] Newman, D. J. (2002). Interactive aerospace engineering and design. New York, NY 10020. McGraw-Hill Companies, Chapter 2, 22.

[21] Earth's Atmospheric Layers. NASA. (2017). Retrieved 16 March 2021, from: https://www.nasa.gov/mission_pages/sunearth/science/atmosphere-layers2.html

[22] Layers of Earth's Atmosphere | UCAR Center for Science Education. Scied.ucar.edu. (2015). Retrieved 16 March 2021, from: https://scied.ucar.edu/learning-zone/atmosphere/layers-earths-atmosphere

[23] International Space Station - Wikipedia. En.wikipedia.org. Retrieved 16 March 2021, from: https://en.wikipedia.org/wiki/International_Space_Station

[24] The Thermosphere | UCAR Center for Science Education. Scied.ucar.edu. (2008). Retrieved 16 March 2021, from: https://scied.ucar.edu/learning-zone/atmosphere/thermosphere

[25] Solomon, S., & Roble, R. (2015). Thermosphere. Encyclopedia of Atmospheric Sciences, 402-408. https://doi.org/10.1016/b978-0-12-382225-3.00408-4

[26] Mesopause. En.wikipedia.org. Retrieved 17 March 2021, from: https://en.wikipedia.org/wiki/Mesopause

[27] The Solar Cycle | NOAA SciJinks – All About Weather. Scijinks.gov. Retrieved 17 March 2021, from: https://scijinks.gov/solar-cycle/

[28] Singh, P. R., Tiwari, C. M., & Saxena, A. K. (2016). Variations in Solar Cycles 22, 23 & 24 and Their Effect on Earth's Climate. International Journal of Astronomy and Astrophysics, 6(1), 8-13.

[29] Bhowmik, P., & Nandy, D. (2018). Prediction of the strength and timing of sunspot cycle 25 reveal decadal-scale space environmental conditions. Nature Communications, 9(1), 1-10.

[30] Why Space Radiation Matters. NASA. (2019). Retrieved 25 March 2021, from: https://www.nasa.gov/analogs/nsrl/why-space-radiation-matters

[31] Rishbeth, H., Fuller-Rowell, T. J., & Rees, D. (1987). Diffusive equilibrium and vertical motion in the thermosphere during a severe magnetic storm: a computational study. Planetary and space science, 35(9), 1157-1165.

[32] What Is Microgravity? NASA. (2017). Retrieved 25 March 2021, from: https://www.nasa.gov/audience/forstudents/5-8/features/nasa-knows/what-is-microgravity-58.html

[33] ISS: International Space Station. The European Space Agency (ESA). Retrieved 25 March 2021, from: https://www.esa.int/Science_Exploration/Human_and_Robotic_Exploration/International_Space_Station/ISS_International_Space_Station

[34] Explainer: What is microgravity? Phys.org. (2016). Retrieved 29 March 2021, from: https://phys.org/news/2016-04-microgravity.html

[35] Griffith, G., & Goka, T. (2009). The Space Environment: Natural and Induced. In Safety Design for Space Systems (Ch. 2, 22). Butterworth-Heinemann.

[36] Apollo 17. NASA. (2011). Retrieved 30 March 2021, from: https://www.nasa.gov/mission_pages/apollo/missions/apollo17.html

[37] Artemis Plan - NASA's Lunar Exploration Program Overview. Nasa.gov. (2020). Retrieved 1 April 2021, from: https://www.nasa.gov/sites/default/files/atoms/files/artemis_plan-20200921.pdf

[38] Roncoli, R. B. (2005). Lunar constants and models document, JPL D-32296. Jet Propulsion Laboratory, California Institute of Technology.

[39] Heiken, G. H., Vaniman, D. T., & French, B. M. (1991). Lunar Sourcebook, a user's guide to the Moon.

[40] What is a 'launch window'? Esa.int. Retrieved 1 April 2021, from: http://www.esa.int/Science_Exploration/Space_Science/What_is_a_launch_window.

[41] Schaeffer, R., "The extravehicular activity web project," MIT, term project for 16.423, Aerospace Physiology and Life Support Systems, Prof. Newman, fall, 1998.

[42] Larson, W. J., Henry, G. N., & Humble, R. W. (Eds.). (1995). Space propulsion analysis and design. McGraw-Hill. pp. 9, 139-146.

[43] "Conservation of Momentum", Grc.nasa.gov. (2015). Retrieved 15 April 2021, from: https://www.grc.nasa.gov/www/k-12/airplane/conmo.html.

[44] Sutton, G. P., & Biblarz, O. (2001). Rocket propulsion elements. John Wiley & Sons. pp. 58

[45] Specific Impulse, Grc.nasa.gov. Retrieved 16 April 2021, from: https://www.grc.nasa.gov/www/k-12/airplane/specimp.html

[46] Peraire J, Windall S. Lecture L14 - Variable Mass Systems: The Rocket Equation. Ocw.mit.edu. (2008). Retrieved 18 April 2021, from: https://ocw.mit.edu/courses/aeronautics-and-astronautics/16-07-dynamics-fall-2009/lecture-notes/MIT16_07F09_Lec14.pdf

[47] Liénart, T., Pfaab, K., Vidal, J., Galéra, S., & Koppel, C. (2014). Fluidic simulations and tests of space mechanical pressure regulators. In Space Propulsion Conference.

[48] 4.0 In-Space Propulsion. NASA. (2020). Retrieved 16 April 2021, from: https://www.nasa.gov/smallsat-institute/sst-soa-2020/in-space-propulsion

[49] Fatehi, M., Nosratollahi, M., Adami, A., & reza Argand, M. (2015). Multidisciplinary Design of Space Blowdown Cold Gas Propulsion System without Pressure Regulator by Genetic Algorithms. Cumhuriyet Üniversitesi Fen-Edebiyat Fakültesi Fen Bilimleri Dergisi, 36(3), 2363-2370.

[50] Hashem, A. A. (2004, October). Design and testing of a cold gas system. In 4th International Spacecraft Propulsion Conference (Vol. 555), pp 86.

[51] Nothnagel, S. L. (2011). Development of a cold gas propulsion system for the talaris hopper (Doctoral dissertation, Massachusetts Institute of Technology).

[52] Tummala, A. R., & Dutta, A. (2017). An overview of cube-satellite propulsion technologies and trends. Aerospace, 4(4), 58.

[53] Anis, A. (2012). Cold gas propulsion system-an ideal choice for remote sensing small satellites. Remote sensing-advanced techniques and platforms, pp. 31.

[54] Gases - Densities. Engineeringtoolbox.com. (2003). Retrieved 26 April 2021, from: https://www.engineeringtoolbox.com/gas-density-d_158.html

[55] Isentropic Flow Equations. Grc.nasa.gov. Retrieved 26 April 2021, from: https://www.grc.nasa.gov/www/k-12/airplane/isentrop.html

[56] UTC Aerospace Systems. (2017). NASA Extravehicular Mobility Unit (EMU) LSS/SSA Data Book [EBook] (pp. B-1, B-10). Retrieved 3 May 2021, from: https://www.lpi.usra.edu/lunar/constellation/NASA-EMU-Data-Book-JSC-E-DAA-TN55224.pdf

[57] Cold gas thruster - Wikipedia. En.wikipedia.org. Retrieved 3 May 2021, from: https://en.wikipedia.org/wiki/Cold_gas_thruster

[58] Kelly, J. C. (1997). Formal Methods Specification and Analysis Guidebook for the Verification of Software and Computer Systems Volume II: A Practitioner's Companion.

[59] Williams, T., & Baughman, D. (1994, May). Self-rescue strategies for EVA crewmembers equipped with the SAFER backpack. In NASA Conference Publication (pp. 357-357). NASA.

[60] Scoville, Z., & Rajula, S. (2005). SAFER inspection of space shuttle thermal protection system. In Space 2005 (p. 6722).

[61] How does a pressure transmitter work? Beginner's guide to pressure transmitters. Measure & Control Solutions. (2019). Retrieved 5 May 2021, from: https://www.drurylandetheatre.com/how-does-a-pressure-transmitter-work/#001

[62] Burst Pressure – What It Is and Why It's So Important. Corrosion Materials. (2015). Retrieved 5 May 2021, from: https://corrosionmaterials.com/burst-pressure-what-it-is-and-why-its-so-important/

[63] Hohmann, C. (2000). Propellant for the NASA standard initiator. National Aeronautics and Space Administration, Lyndon B. Johnson Space Center.

[64] Free Falling Object Motion. Grc.nasa.gov. Retrieved 5 May 2021, from: https://www.grc.nasa.gov/www/k-12/airplane/mofall.html

[65] Wen, J., Zhang, J., Gao, L., & Li, X. (2014). Modeling and Simulation of Simplified Aid for EVA Rescue Using Virtual Prototype Technology. The Open Automation and Control Systems Journal, 6(1).

[66] Brody, A. R., Jacoby, R., & Ellis, S. R. (1991). Man overboard-What next? [Simulation of retrieval of astronaut after accidental separation from space station].

[67] Fowler, W. T., & Neff, J. M. (1991). Minimum-fuel rescue trajectories for the Extravehicular Excursion Unit. Journal of the Astronautical Sciences, Vol. 39, 1991, pp. 21-45.

[68] Nitrogen - Dynamic and Kinematic Viscosity. Retrieved 10 May 2021, from: https://www.engineeringtoolbox.com/nitrogen-N2-dynamic-kinematic-viscosity-temperature-pressure-d_2067.html

[69] Lizandra Dalmases, O. J. (2020). Module 2 – Lecture 2: Cold-Gas Systems [Power Point slides]. Retrieved from UPC Universitat Politècnica de Catalunya, 220334 Space Propulsion

[70] Hashem, A. (2004). Design and Testing of a Cold Gas System. In Proceedings of the 4th International Spacecraft Propulsion Conference (ESA SP-555). Chia Laguna (Cagliari), Sardinia, Italy. Retrieved 15 May 2021, from: http://articles.adsabs.harvard.edu//full/2004ESASP.555E..86H/0000086.001.html.

[71] Curtis, H. (2005). Orbital Mechanics for Engineering Students (1st ed., p. 315). Elsevier Butterworth-Heinemann.

[72] Williams, D. Earth Fact Sheet. Nssdc.gsfc.nasa.gov. Retrieved 10 May 2021, from: https://nssdc.gsfc.nasa.gov/planetary/factsheet/earthfact.html.

[73] Rahn, D. B. (1997). A dynamic model of the extravehicular mobility unit (EMU): human performance issues during EVA (Doctoral dissertation, Massachusetts Institute of Technology).

Bibliography (Images)

[2.1] Mercury Spacesuit Image Gallery. National Aeronautics and Space Administration (NASA). Retrieved 9 March 2021, from: https://www.nasa.gov/sites/default/files/541802main_el-1996-00089-600t.jpg

[2.2] Space History Photo: Ed White First American Spacewalker. Space.com. (2014). Retrieved 9 March 2021, from: https://www.space.com/25990-ed-white-first-american-spacewalker.html

[2.3] Apollo 16, Astronaut John Young. National Air and Space Museum. Retrieved 9 March 2021, from: https://airandspace.si.edu/multimedia-gallery/gpn-2000-001131hjpg

[2.4] Jordan, N. C., Saleh, J. H., & Newman, D. J. (2006). The extravehicular mobility unit: A review of environment, requirements, and design changes in the US spacesuit. Acta Astronautica, 59(12), 1135-1145.

[2.5]. Orlan-M. Russianspaceweb.com. Retrieved 10 March 2021, from: http://www.russianspaceweb.com/images/spacecraft/manned/space_stations/iss/orlan_mks/top_1.jpg

[2.6] Abramov, I. P., Glazov, G. M., & Svertshek, V. I. (2002). Long-term operation of "Orlan" space suits in the "Mir" orbiting station: Experience obtained and its application. Acta astronautica, 51(1-9), 133-143.

[2.7] File:HHMU.jpg - Wikimedia Commons. Commons.wikimedia.org. Retrieved 10 March 2021, from: https://commons.wikimedia.org/wiki/File:HHMU.jpg

[2.8] Astronaut Maneuvering Unit, Gemini, Mock-up. National Air and Space Museum. Retrieved 10 March 2021, from: https://airandspace.si.edu/collection-objects/astronaut-maneuvering-unit-gemini-mock-up/nasm_A19731450000

[2.9] Lenda, J. A. (1978). Manned maneuvering unit: User's guide.

[2.10] Manned Maneuvering Unit (MMU) displays. Collectspace.com. Retrieved 11 March 2021, from: http://www.collectspace.com/ubb/Forum41/HTML/000047.html

[2.11] How do astronaut jetpacks work? Quora.com Retrieved 11 March 2021, from: https://www.quora.com/How-do-astronaut-jetpacks-work

[2.12] Vogt, G. L. (1998). Suited for Spacewalking: A Teacher's Guide with Activities for Technology Education, Mathematics, and Science.

[2.13] STS-41-B crew.jpg. Commons.wikimedia.org. n.d. Retrieved 11 March 2021, from: https://commons.wikimedia.org/wiki/File:STS-41-B_crew.jpg

[2.14] NASA Celebrates 50 Years of Spacewalking. NASA. (2017). Retrieved 11 March 2021, from: https://www.nasa.gov/image-feature/nasa-celebrates-50-years-of-spacewalking

[2.15] File:Sts-64 crew.jpg. Commons.wikimedia.org. Retrieved 11 March 2021, from:

https://commons.wikimedia.org/wiki/File:Sts-64_crew.jpg

[2.16] Astronaut Tests SAFER Backpack. NASA. (2017). Retrieved 11 March 2021, from: https://www.nasa.gov/multimedia/imagegallery/image_feature_2120.html

[2.17] Earth's Atmosphere | UCAR Center for Science Education. Scied.ucar.edu. (2015). Retrieved 15 March 2021, from: https://scied.ucar.edu/learning-zone/atmosphere/earths-atmosphere

[2.18] Earth's Atmospheric Layers. NASA. (2017). Retrieved 16 March 2021, from: https://www.nasa.gov/mission_pages/sunearth/science/atmosphere-layers2.html

[2.19] NASA, EOS Science Steering Committee Report, vol. 2, From Pattern to Process: The Strategy of the Earth Observing System. National Aeronautics and Space Administration, Washington, appeared as Fig.1.1 in Fundamentals of Space Life Sciences, S. E. Churchill, ed., vol. 1, p. 4, Krieger Publishing Company, Malabar, FL, 1997.

[2.20] Solomon, S., & Roble, R. (2015). Thermosphere. Encyclopedia of Atmospheric Sciences, 402-408. https://doi.org/10.1016/b978-0-12-382225-3.00408-4

[2.21] NASA - Sources of Ionizing Radiation in Interplanetary Space. Nasa.gov. Retrieved 1 April 2021, from: https://www.nasa.gov/mission_pages/msl/multimedia/pia16938.html

[2.22] Space travel, long-term exposure to microgravity causes a 'leaky' gut in astronauts: Study-Technology News, Firstpost. Tech2. (2019). Retrieved 1 April 2021, from: https://www.firstpost.com/tech/science/space-travel-long-term-exposure-to-microgravity-cause-a-leaky-gut-in-astronauts-study-7710591.html

[2.23] ARES | Orbital Debris Program Office | Photo Gallery. Orbitaldebris.jsc.nasa.gov. Retrieved 1 April 2021, from: https://orbitaldebris.jsc.nasa.gov/photo-gallery/

[2.24] Apollo Lunar Surface Journal. Hq.nasa.gov. Retrieved 2 April 2021, from: https://www.hq.nasa.gov/alsj/.

[2.25] NASA's Perseverance Drives on Mars' Terrain for First Time. NASA. (2021). Retrieved 2 April 2021, from: https://www.nasa.gov/press-release/nasa-s-perseverance-drives-on-mars-terrain-for-first-time.

[3.1] Larson, W. J., Henry, G. N., & Humble, R. W. (Eds.). (1995). Space propulsion analysis and design. McGraw-Hill.

[3.2] 4.0 In-Space Propulsion. NASA. (2020). Retrieved 16 April 2021, from: https://www.nasa.gov/smallsat-institute/sst-soa-2020/in-space-propulsion

[3.3] Tummala, A. R., & Dutta, A. (2017). An overview of cube-satellite propulsion technologies and trends. Aerospace, 4(4), 58.

[3.4] Everything about rocket engines. Space 'n' Science. Spaceandscience.fr. Retrieved 16 April 2021, from: https://spaceandscience.fr/en/blog/rocket-engines

[3.5] Williams, A. G., Anderson, H. A., & Pierce, G. J. (2016). Integrating MBSE into ongoing projects: requirements validation and test planning for the ISS SAFER. In AIAA SPACE 2016 (p. 5313).

[3.6] UTC Aerospace Systems. (2017). NASA Extravehicular Mobility Unit (EMU) LSS/SSA Data Book [EBook] (pp. B-1, B-10). Retrieved 3 May 2021, from: https://www.lpi.usra.edu/lunar/constellation/NASA-EMU-Data-Book-JSC-E-DAA-TN55224.pdf